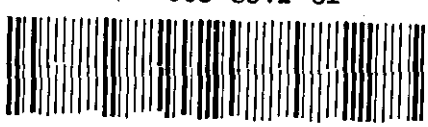

A STUDY OF SOME QUINOXALINE AND HALO-PYRIDINE COMPLEXES OF TRANSITION-METALS.

by D.E.Billing, M.A.

A thesis submitted for the degree of Doctor of Philosophy of Loughborough University of Technology.

November, 1967.

Supervised by Dr.A.E.Underhill.

PART 1

Chapters I - VI

Introduction and Investigation of the Halo-pyridine Complexes.

Acknowledgments.

I am deeply grateful to Dr.A.E.Underhill for his exceptional interest, encouragement and guidance throughout the course of this work. I am also indebted to my family for help in many ways.

The work would not have been possible without a research scholarship awarded by the Loughborough University of Technology, or the facilities given to me by its Department of Chemistry. I readily acknowledge both.

D.E.Billing.

Publications.

The following papers have been published on the work described in this thesis:

1) "Transition - metal Quinoxaline Complexes. Part II. Copper (I) Derivatives." By D.E.Billing and A.E.Underhill. Journal of the Chemical Society, 1965, 6639.

2) "Calculations of the Racah Parameter B for Nickel (II) and Cobalt (II) Compounds." By A.E.Underhill and D.E.Billing. Nature, 1966, 210, 834.

3) "Transition - metal Quinoxaline Complexes. Part III. Copper (II) Derivatives with Substituted Quinoxalines." By D.E.Billing, A.E.Underhill, D.M.Adams and D.M.Morris. Journal of the Chemical Society, Section A, 1966, 902.

The following papers have been accepted for publication in Section A of the Journal of the Chemical Society:

4) "Complexes of Cobalt (II) and Nickel (II) Halides with some Halo-pyridines." By D.E.Billing and A.E.Underhill.

5) "Transition - metal Quinoxaline Complexes. Part IV. Cobalt (II) Derivatives." By D.E.Billing and A.E.Underhill.

6) "Transition - metal Quinoxaline Complexes. Part V. Nickel (II) Derivatives." By D.E.Billing, A.E.Underhill and G.M.Smart.

Summary.

The preparations and properties of fifty-three new complexes of Cobalt (II), Nickel (II), Copper (II) and Copper (I) halides and nitrates are described. The ligands used were 3-Bromopyridine, 4-Chloropyridine, 1:2:4-Triazole, Quinoxaline, 2-Methylquinoxaline, 2:3-Dimethylquinoxaline, 2:3-Diphenylquinoxaline and Phenazine.

The electronic reflectance spectra of these complexes have been measured, and the spin-allowed transitions assigned. The calculated ligand-field parameters are compared with those of related complexes, and the value of such calculations assessed. The spectra, along with confirmatory magnetic and infrared data are used to elucidate the stereochemistries of the complexes.

The Copper (I) complexes of the quinoxalines have linear structures, involving bidentate amine molecules. In the absence of substantial steric hindrance, high ligand basicity and high anion polarisability the other complexes are found to exhibit polymeric, octahedral structures similar to that of α-$CoCl_2py_2$. The influence of these effects is, generally, to impose four-coordinate stereochemistry upon the complexes.

The change, from octahedral $CuCl_2Q$ and $CuCl_2Mq_2$ to square-planar $CuCl_2Dmq$ and $CuCl_2Dpq_2$, shows the effect of a progressive increase of steric hindrance. A similar progression is found for the series of Copper (II) complexes with Triazole, pyridine, 2-Chloropyridine, 2-Methylpyridine, 2-Bromopyridine and Phenazine. Steric factors also lead to the tetrahedral structures of the Cobalt (II) complexes with 2-Chloropyridine, 2-Bromopyridine, 2:3-Dimethylquinoxaline,

and the bis-quinoxaline species.

The tetrahedral structures of $CoI_2(3Brpy)_2$, $CoBr_2Q$ and $CoBr_2Mq$, and the square-planar structures of NiI_2Q_2, NiI_2Mq_2 and NiI_2Dmq_2 are in contrast to the octahedral structures of the corresponding chlorides. This is considered to result from the high polarisabilities of the bromide and iodide ions. The octahedral structures of $CoBr_2(3Brpy)_2$ and $CoBr_2(4Clpy)_2$, compared with the tetrahedral structure of $CoBr_2py_2$, are due to the lower basicities of the halopyridines compared with pyridine.

Variations of thermal stabilities, infrared spectra, charge-transfer bands and ligand-field parameters are discussed in terms of metal-ligand π-bonding.

Some studies of the thermal decompositions of the quinoxaline complexes are reported.

Contents.

Abbreviations.

a) Abbreviations used for ligands.

A	: Acridine.
acac	: Acetylacetone.
ATc	: Anhydrotetracyline.
B	: Benzimidazole.
Bdn	: 1:3-diaminobutane.
Bipy	: 2,2 -Bipyridine.
Bpz	: Bipyrazinyl.
Brpy	: Bromopyridine.
Cl-py	: Chloropyridine.
CN-py	: Cyanopyridine.
DAAAP	: 2-[β-(Diethyl-amino)-ethyl] -pyridine.
Dithizone	: Diphenylthiocarbazide.
DMAAP	: 2-[β-(Dimethyl-amino)-ethyl] -pyridine.
Dmepy	: Dimethylpyridine.
DMeQuin	: Dimethyl Quinoline.
Dmp	: Dimethylpyrazine.
Dmq	: 2:3-Dimethylquinoxaline.
Dpa	: di-2-pyridylamine.
DPNO	: Dimethylpyridine-N-oxide.
Dpq	: 2:3-Diphenylquinoxaline.
DTc	: Dedimethylaminotetracyline.
En	: Ethylenediamine.
Enta	: Ethylenediaminetetraacetate.
Etpy	: Ethylpyridine.

IQuin : Iso-quinoline.

L : Lutidine (=Dimethylpyridine), or any ligand.

M : Any metal.

MeB : Methylbenzimidazole.

MeBT : Methylbenzothiazole.

MeIQuin : Methyliso-quinoline.

Mepy : Methylpyridine.

MeQuin : Methylquinoline (= Quinaldine).

Mp : Methylpyrazine.

Mq : 2-Methylquinoxaline.

NH_2-py : Aminopyridine.

N-MeSalim : N-Methyl Salicylaldimine.

NO_2-py : Nitropyridine.

NO_2-Quin : Nitroquinoline.

Ox : Oxalate.

P : Phenazine.

PAAP : 2-[β-(Phenyl-amino)-ethyl] -pyridine.

PAH : 2-pyridinealhydrazone.

paphy : pyridine-2-aldehyde-2-pyridylhydrazone.

pc : Phthalocyanine.

Phen, Phenan : 1:10-Phenanthroline.

φacac : 3-Phenylacetylacetone.

φcoo : Benzoate.

φpy : Phenyl-pyridine.

pic : Picoline (= Methylpyridine).

PMH	: 4,4'-diethoxycarbonyl-3,3',5,5',-Tetramethyldi-pyrromethene.
Prpy	: Propylpyridine.
py	: Pyridine.
pyH	: Pyridinium.
pyz	: Pyrazine.
Q	: Quinoxaline.
QHCl	: Quinoxalinium monochloride.
Quin	: Quinoline.
Sal	: Salicylaldehyde.
Salim	: Salicylaldimine.
T	: 1:2:4-Triazole.
Tc	: Tetracyline.
Tetren	: Tetraethylenepentamine.
Th	: Thiourea.
TMepy	: Trimethylpyridine.
TMp	: Tetramethylpyrazine.
Tol	: Toluidine.
TPNO	: Trimethylpyridine-N-oxide.
Tren	: Tris(amino ethyl) amine.
Vpy	: Vinylpyridine.
X	: Any halide.
Xyl	: Xylidine.

b) Abbreviations used in describing spectra.

kK : kilokaiser ($\hat{=}$ 1000 cm^{-1}).

vs : Very strong.

s : Strong.

ms : Medium strong.

m : Medium intensity.

mw : Medium weak.

w : Weak.

vw : Very weak.

b : Broad.

vb : Very broad.

sh : Shoulder.

ush : Unresolved shoulder.

Captions for Diagrams.

Figure 1.1 - Crystal Field Splitting Diagram for the Lowest atomic D term of Octahedral d^1 and d^6 ions, and Tetrahedral d^4 and d^9 ions. (E = Energy scale)

a) Field-Free Energy Level.

b) Addition of Spherically Symmetric Part of Perturbation.

c) Splitting caused by Cubic Part of Potential.

Figure 1.2 - Crystal Field Splitting Diagram for the Lowest atomic D term of Octahedral d^4 and d^9 ions, and Tetrahedral d^1 and d^6 ions.

a) Field-Free Energy Level.

b) Addition of Spherically Symmetric Part of Perturbation.

c) Splitting caused by Cubic Part of Potential.

d) Further Splitting caused by a small Tetragonal Elongation.

~~e) Alternative Further Splitting caused by a Tetragonal Compression.~~

e) Effect of increasing the Tetragonal Elongation.

f) Additional effect of descent to Rhombic Symmetry.

Figure 1.3 -Crystal Field Splitting Diagram for the High-Spin atomic F and P terms of Octahedral d^2 and d^7 ions, and Tetrahedral d^3 and d^8 ions.

a) Field-Free atomic terms.

b) Addition of Spherically Symmetric Part of a weak Perturbation.

c) Splitting caused by the Cubic Part of Potential.

d) Further effect of the Interaction between States of the same symmetry.

Figure 2.1 a) The left-hand part of the diagram corresponds to octahedral d^3 and d^8 ions, and tetrahedral d^2 and d^7 ions.

b) The right-hand part of the diagram corresponds to octahedral d^2 and d^7 ions, and tetrahedral d^3 and d^8 ions.

Figure 3.0 -Formulae of some heteroaromatic amines.

a) Pyridine. b) Quinoline.

c) 1:2:4-Triazole. d) Phenazine.

Figure 3.1 -Structure of $CuCl_2py_2$.

Figure 3.2 -Structure of α-$CoCl_2py_2$ viewed from above the plane of the $CoCl_2$ chains.

Figure 3.3 -Proposed structure of $CuCl_2Quin_2$. The amine molecules are probably twisted out of the plane of the $CuCl_2N_2$ chromophore.

Figure 3.4 -Proposed structure of $CoBr_2py_2$.

Figure 3.5 -Structure of $CuCl_2$(Triazole).

Figure 3.6 -Structure of a possible CuX_2L_2 polymer based on a cis- arrangement of long Cu-X bonds. The structure is viewed from above the planes of the CuX_2 chains. The amine rings (L) are shown in profile (as C.....C).

Figure 3.7 -Demonstration of misorientation of orbitals for metal-nitrogen π-bonding.

a) Metal d_{yz} orbital has wrong parity to bond with nitrogen p-orbital.

b) Metal d_{xy} and d_{xz} orbitals (shown in profile) are misplaced relative to the nitrogen p-orbital.

Figure 8.2 -Thermogravimetric decomposition curves for CuI complexes of quinoxalines. (Wr = weight remaining).

a) CuI. b) Cu_2I_2Q.

c) Cu_2I_2Dmq. d) Cu_2I_2Mq.

Figure 8.3 -Thermogravimetric decomposition curves for the Copper (I) complexes of Dimethylquinoxaline.

a) Cu_2Cl_2Dmq. b) Cu_2Br_2Dmq. c) Cu_2I_2Dmq.

Figure 9.1 -Diffuse Reflectance Spectra of the Copper (II) Complexes of Quinoxalines.

a) $CuCl_2Q$. b) $CuCl_2Dpq_2$.

c) $CuCl_2Dmq$. d) $CuCl_2Mq_2$.

Figure 9.2 -Far-Infrared Spectra (cm^{-1}) of the Complexes of Copper (II) halides with Dimethylquinoxaline.

(M = absorption of the "Melinex" beam splitter;
P = absorption of the Polythene cell.)

a) $CuCl_2Dmq$. b) $CuBr_2Dmq$. c) Dmq.

Figure 9.3 -T.G.A. curves for the complexes of Copper (II) Chloride with quinoxalines.

a) $CuCl_2Q$. b) $CuCl_2Mq_2$. c) $CuCl_2Dmq$.

d) $CuCl_2Dpq_2$. e) $CuCl_2\ 2H_2O$ (for comparison).

Figure 9.4 -Origins of steric hindrance in possible five-coordinate $CuCl_2Dpq_2$.

a) Hindrance between chlorine and the 8-hydrogen atom.

b) Hindrance between chlorine and the 2-phenyl group.

CHAPTER I

AN INTRODUCTION TO THE STUDY OF CO-ORDINATION COMPOUNDS OF THE TRANSITION ELEMENTS

General

A renaissance transformed inorganic chemistry during the 1950's. At this time the importance of theoretical work, in the 1930's, (by Bethe[1], Van Vleck[2-10] and other physicists[11-15]) was realised by chemists and applied to simple systems, such as the Transition-Metal hydrates[16,17].

The present importance of the compounds of the Transition-Metals to the understanding of chemical bonding arose because their electronic spectra and paramagnetism were related[18-31] to the theories of electronic structure. In addition, instruments (such as electron spin resonance spectrometers[32]) developed immediately after the war made the study of these properties much easier. Further, this theoretical insight was accompanied by a renewed interest in the chemical properties of these compounds in connection with industrial[33-35] and biochemical[36-39] catalysis, and with solid-state electronic devices[40].

The theories developed by the physicists dealt most successfully with the interaction between a metal ion and its immediate environment. Knowledge of the structure of this 'co-ordination sphere' thus became desirable, and was provided by the increased availability[41-43] of crystal

structure determinations in the 1950's. The maximum amount of information was obtained by examining the properties of complexes of known crystal structure in the solid state; particularly the anisotropy of single crystals [18,21,44-47].

However, early spectrophotometers were not adapted for solid state studies and much preliminary work was therefore performed with solutions [23,24]. With the more recent availability of recording spectrometers capable of measuring electronic spectra by means of diffuse reflectance (D.R.S.) [48-50], fundamental studies in the solid state were made considerably easier. Such reflectance spectra aided studies of polymers which dissociated in solution. Many such co-ordination polymers [51-54] have recently become of interest because of their potentially useful thermal and mechanical properties.

Understanding of co-ordination compounds, or 'complexes', thus became based on electronic theory and known crystal structure. It also became evident that magnetic and electronic properties were sensitive to the sterochemistry of the co-ordination species. [55-57] Measurements of such properties promised stereochemical information while by-passing lengthy, single crystal, X-ray diffraction studies. This promise has not been fulfilled and only a full structure analysis

can resolve ambiguities in the interpretation of spectral and magnetic data.

However, some information may be all that is required to understand trends within a series of complexes, and this can often be provided by studies of electronic spectra and paramagnetic susceptibility.[58-60] Supplementary evidence is now available from the vibrational spectrum of the co-ordination cluster or 'chromophore', and in favourable cases from the paramagnetic resonance absorption spectrum (E.S.R.).[45,46,61,62] A few elements can also be studied by means of the recoilless γ-resonance (Mössbauer Spectrum)[63-70] or by nuclear magnetic resonance (N.M.R.)[71-73]. Conformations of the molecules, or 'ligands', attached to the central metal ion can be studied by means of NMR, and with techniques, which depend on optical activity, such as optical rotatory dispersion or circular dichroism[74-77].

Theoretical studies have also been made on the relative stabilities of complexes. Thermal stabilities of the solids have been examined by means of Thermogravimetric Analysis (T.G.A.)[78-82] and Differential Thermal Analysis (D.T.A.)[83-85]. These results have been correlated with more extensive studies of solution equilibria[86-88].

A study of the infrared (I.R.) spectra, due to ligand molecules, can sometimes provide information on whether these are co-ordinated[89,90].

The work to be reported here is of the type outlined above, where a collection of physical techniques are used to obtain information on the stereochemistries of several series of solid complexes, often co-ordination polymers.

The elements of the theories available for the interpretation of such measurements will now be outlined. It is convenient to begin with the results of a quantum mechanical treatment of isolated Transition-Metal ions.

Atomic Spectroscopic States [18,91,92]

The Transition-Metals have electronic configurations in which a d-shell is incomplete. An electronic configuration possesses angular momentum due to the spin of the electrons ($s=\pm\frac{1}{2}$ each) and due to their orbital motion ($l = 2$ for each d- electron). The quantum numbers S ($= |\underline{S}| = |\Sigma \underline{s}|$) and L ($= |\underline{L}| = |\Sigma \underline{l}|$), (which specify the total spin and orbital momentum of a configuration) are often the most important quantum mechanical properties of a system. Such a situation is called the "LS", or "Russell-Saunders", coupling scheme.

There is only one way of arranging a single electron (or a single positive hole resulting from a d^9 configuration) in the degenerate d-orbitals. Both d^1 and d^9 therefore have $L=l=2$ and $S=s=\frac{1}{2}$. These

configurations are denoted as ^2D 'terms'. Here the superscript is the 'spin' multiplicity' (2S+1) and the letter (D) refers to the value of L(S,P,D,F correspond respectively to L=0,1,2,3). More than one term can arise for other configurations, because the vector additions of l and s can be performed in several ways. However, not all the combinations of l and s are permitted by the Pauli exclusion principle. A d^2 ion, for example, gives rise to ^1G, ^1D, ^1S, ^3F and ^3P terms while ^2G, ^2D, ^2H, ^2F, ^2P, ^4F and ^4P terms arise for d^3.

Under the action of interelectronic repulsion forces, these terms possess different energies, and transitions between them can be measured in atomic emission or absorption spectra. Such measurements allow the energy orders of the terms to be derived; thus for d^2:

$$^3F < ^1D < ^3P < ^1G < ^1S$$

and for d^3:

$$^4F < ^4P < ^2H = ^2P < ^2G < ^2F < ^2D$$

The ground state term was always found by Hund to be that of largest L value amongst those of highest spin multiplicity.

The term energies may be derived by solving the quantum mechanical secular equations, if certain integrals involving the atomic wavefunctions

can be evaluated. Generally this has proved difficult or impossible for such heavy atoms, and the energies are therefore expressed in terms of parameters A, B and C introduced by Racah[93-95]. These are functions of the repulsions between electrons in the various orbitals. Thus, for example, the 'triplet' term energies of d^2 are given by:

$$E(^3F) = A-8B; \quad E(^3P) = A + 7B;$$

while the 'quartet' terms of d^3 have energies:

$$E(^4F) = 3A-15B; \quad E(^4P) = 3A.$$

In both cases a transition from the ground state to the excited state of the same multiplicity results in the absorption of energy 15B. Only such transitions are 'spin-allowed' since a quantum mechanical selection rule forbids transitions between terms of unequal spin multiplicity. All further discussion will therefore be devoted to spin-allowed absorption bands. Table 1.1 gives experimental[19,21,23] values of B for some ions. No such transitions are possible for isolated d^1 or d^9 ions because of the presence of only one term.

d^6, d^7 and d^8 ions may be considered to have 4,3 and 2 positive holes respectively. The repulsions between positive holes will have the same consequences as between electrons, and hence the term energies

TABLE 1.1

Values of the Racah B parameter and the spin-orbit coupling constant, measured for field-free transition-metal ions. Units are kilo Kaisers (kK).

Ion	B	λ
V^{2+}	0.757	0.056
V^{3+}	0.851	0.105
Cr^{3+}	0.918	0.091
Mn^{4+}	1.064	0.138
Co^{2+}	0.971	-0.170
Ni^{2+}	1.041	-0.315
Cu^{2+}	-	-0.830

of d^6, d^7 and d^8 configurations can be expressed by the same equations which obtain for d^4, d^3 and d^2 ions. It appears that the half-filled d-shell has a special stability, similar to that of empty and filled shells. Thus addition of electrons to d^5 can be compared, in this respect, with addition to d^0. So in some respects d^6, d^7, d^8 and d^9 ions are similar to d^1, d^2, d^3 and d^4 configurations. For example, although many terms arise from d^4 and d^6, the ground state is the only quintet term and being ^5D may be compared with the single ^2D term arising from d^1 and d^9.

18-21,23

Crystal Field Theory

So far only isolated ions have been considered. These have only been observed in the gas phase, since in condensed phases neighbouring ligands are close enough to interact. In a complex, to a first approximation, an ion may be considered to be subjected to an electrostatic potential field due to point charges, or to point dipoles, attributable to ligands. Such an assumption, of a purely electrostatic interaction, is the 'crystal field' approximation. Corrections or more sophisticated theories are necessary to understand the effect of covalency.

The two commonest environments for a metal ion have octahedral and tetrahedral symmetry. Since the octahedron may be considered to be derived from a cube by placing six ligands at the face-centres, and the

tetrahedron by placing four ligands at alternate corners, both symmetries are said to give rise to 'cubic' crystal fields.

96-98

Symmetry

The operations generated by the symmetry elements of molecular co-ordination polyhedra have been found to conform to the requirements of mathematical groups, in this case called 'point' groups. Thus the cis-square coplanar MA_2B_2 species only has a diad axis (C_2) and two planes (σ_v, σ_v') containing it, and is said to belong to the C_{2v} point group. The traces of the matrices which describe the operation of all symmetry elements on a set of basis functions (such as the d-orbital wavefunctions) are said to form a 'representation' (Γ) of the group. Thus, in the C_{2v} point group, the dyz orbital forms a basis for the representation $\{1 \quad -1 \quad -1 \quad 1\}$. These numbers are unit matrices which express the operation respectively of the identity (E), $C_2(z)$, $\sigma_v(xz)$ and $\sigma'_v(yz)$ symmetry elements on the dyz wavefunction. The d_{yz} orbital is then said to 'transform' like the B_2 representation in C_{2v} symmetry. This 'B_2' symbol denotes, following Mulliken, that the character for the E operation is 1 (hence: 'A' or 'B'); that the character for the highest rotation operation (C_2) is -1 (hence: 'B'); and that the character for the σ_v operation is -1 (hence the subscript '2').

The character tables[96] for point groups, such as those for octahedral (O_h) and tetrahedral (T_d) symmetry, are a list of the representations which are not reducible to the sum of others. In O_h symmetry the representation based on the wavefunction of a P atomic term transforms as T_{1g}, (a 'T' representation has 3 for the E-character, while an 'E' representation has 2 for E; 'g' refers to a +1 character for the inversion operation, while 'u' refers to a -1 character in this case) but that based on an F term is reducible to ($A_{2g} + T_{1g} + T_{2g}$) and a D term splits giving ($E_g + T_{2g}$).

If cartesian vectors for each point in the co-ordination polyhedron are used as basis functions, the derived representations describe the symmetry properties of the molecular vibrations. Hence group theory may be used to treat not only electronic properties but also vibrational spectra[96,99,100].

Ions in Weak Octahedral Crystal Fields[18-20]

The electrostatic potential in an octahedral field can be expressed as the sum of two parts: $V = V_r + V_o$. V_r is large ($\backsim 10^4$ cm^{-1}) and corresponds to the replacement of the six ligands by a spherically symmetric field. Its effect is to raise all the energies of all free ion terms by an equal amount. V_o is smaller ($\backsim 10^3 cm^{-1}$)

and spherically asymmetric. This has the effect of splitting the orbitally degenerate free ion terms into 'states', which transform as the irreducible components of the term representation in the O_h group. The splitting of P, D and F terms has been given in the preceeding section.

The energies of these states may be expressed relative to their parent D and F terms by a single parameter:

$$Dq = 5\mu_L\overline{r^4}/6a^6 \qquad \ldots\ldots\ldots\ldots\ldots\ldots\ldots\ldots\ldots\ldots 1.1$$

which characterises V_o. Here 'μ_L' is the ligand point dipole moment, 'a' the metal-ligand internuclear distance and 'r' the distance of a d-electron from the metal nucleus. Thus for d': $E(^2E_g) = 6Dq$; $E(^2T_{2g}) = -4Dq$ relative to an energy $(E(^2D) + V_r)$. For d^9 the hole formalism may be used but V_o is reversed in sign, giving:

$$E(^2Eg) = -6Dq; \qquad E(^2T_{2g}) = 4Dq$$

relative to the equivalent origin.

Table 1.2 gives the energies of the component states of ^2D, ^5D, ^3F and ^4F terms for d^1, d^2, d^3, d^4, d^6, d^7, d^8 and d^9 configurations while $E(T_{2g}(P)) = (E(P) + V_r)$ in all cases. This table shows that the energies of the states derived from P, D and F terms in O_h fields are identical for d^2 and d^7 and again for d^3 and d^8, for d^1 and d^6 and for d^4 and d^9. This is one of the consequences of the stability of d^5 which has already

TABLE 1.2

Energies of the component states of ^2D, ^5D, ^3F and ^4F terms for d^n configurations in cubic crystalline fields. The energies are measured relative to the parent atomic term, after the addition of the spherically symmetric part of the potential. Units are Dq_o or Dq_t as appropriate.

Configuration	Symmetry	E	Energies of the states: T_2	T_1	A_2
d^n: n = 1,6	O_h	6	-4		
n = 4,9	T_d				
n = 1,6	T_d	-6	4		
n = 4,9	O_h				
n = 2,7	O_h		2	-6	12
n = 3,8	T_d				
n = 2,7	T_d		-2	6	-12
n = 3,8	O_h				

been mentioned. Only four energy level diagrams are therefore necessary to describe the spin-allowed transitions of all the d^n configurations except d^0 and d^{10}, which give no terms and d^5, which has a ^6S non degenerate ground state but no other sextet states. These diagrams are shown in figures 1.1C, 1.2C, 1.3C and 1.4C (Captions for the figures are listed at the beginning of this work). Further inspection shows that two pairs (1.1C. and 1.2C; 1.3C and 1.4C) are identical except for an inversion of the F or D term splittings (ie. of the sign of Dq).

Table 1.2 also illustrates a general rule that the baricentre of a term is unaltered when the latter splits. Thus p states arise and the i'th has energy q_i (relative to the original term with the addition of V_r) and orbital degeneracy r_i then $\sum_1^p r_i q_i = 0$.

Weak tetrahedral crystal fields [18-20]

Qualitatively, four negative charges at alternate cube corners are equivalent to six positive charges at the face centres of a cube. Thus, a d^n ion in a tetrahedral field will have the same term splitting pattern as an octahedral d^n ion except for a reversal of the sign of Dq. Moreover it has been shown that for the same cation and ligands at the same internuclear distance $Dq_t \backsim (-4/q)Dq_o$ (where 't' and 'o' subscripts

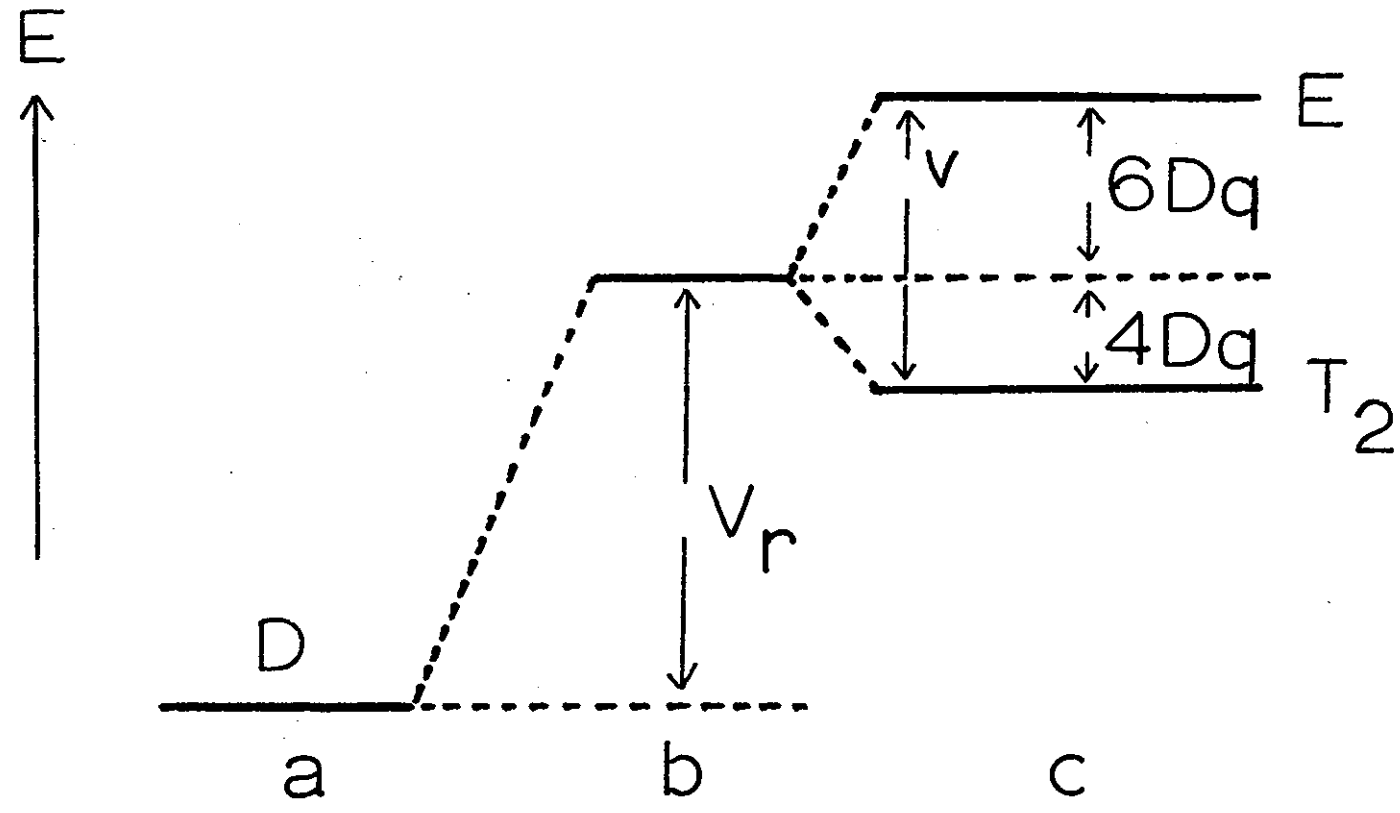

Figure 1.1

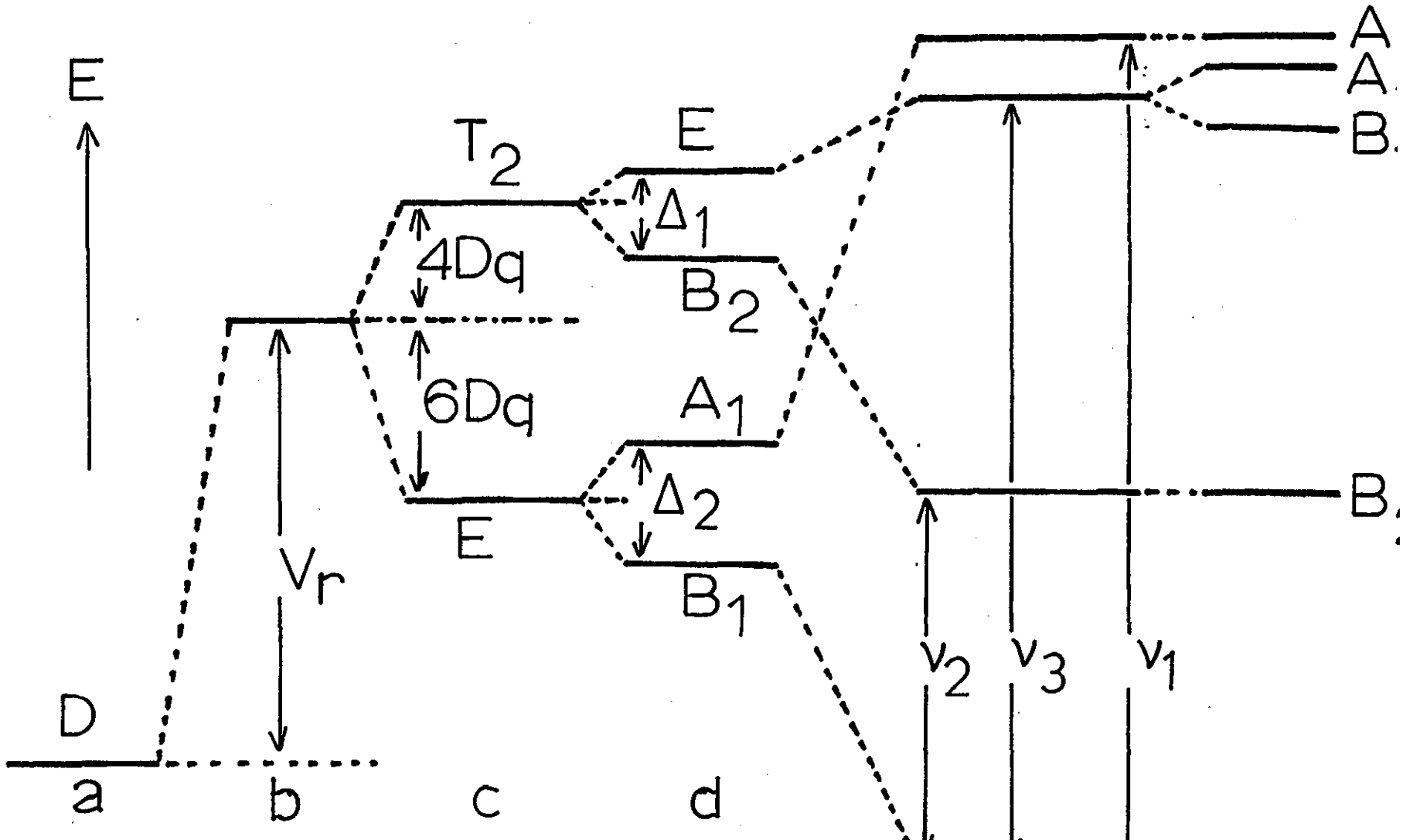

Figure 1.2

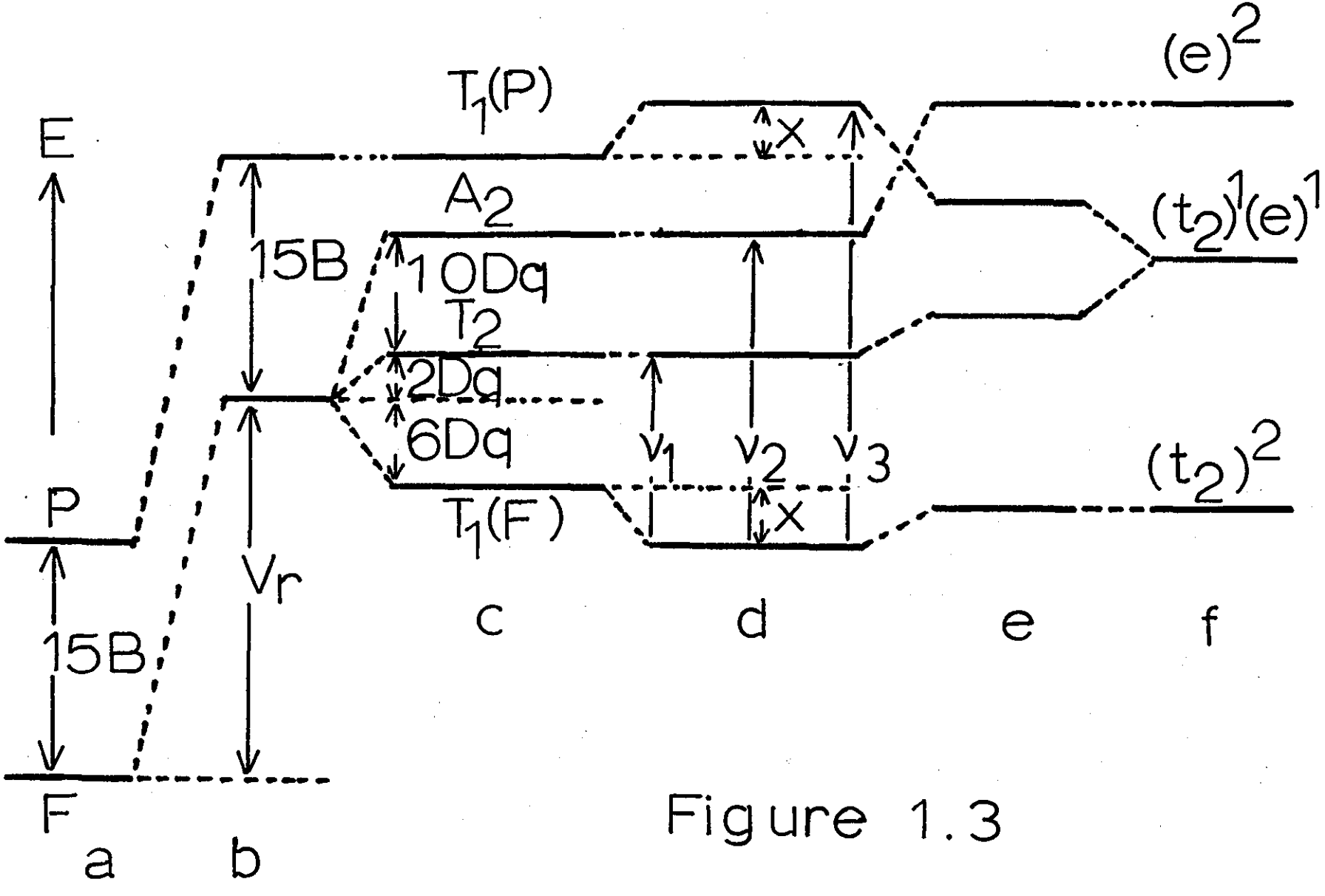
E
P
F
15B
15B
Vr
a
b
T1(P)
A2
T2
T1(F)
10Dq
2Dq
6Dq
X
X
ν1
ν2
ν3
c
d
e
f
(e)2
(t2)1(e)1
(t2)2

Figure 1.3

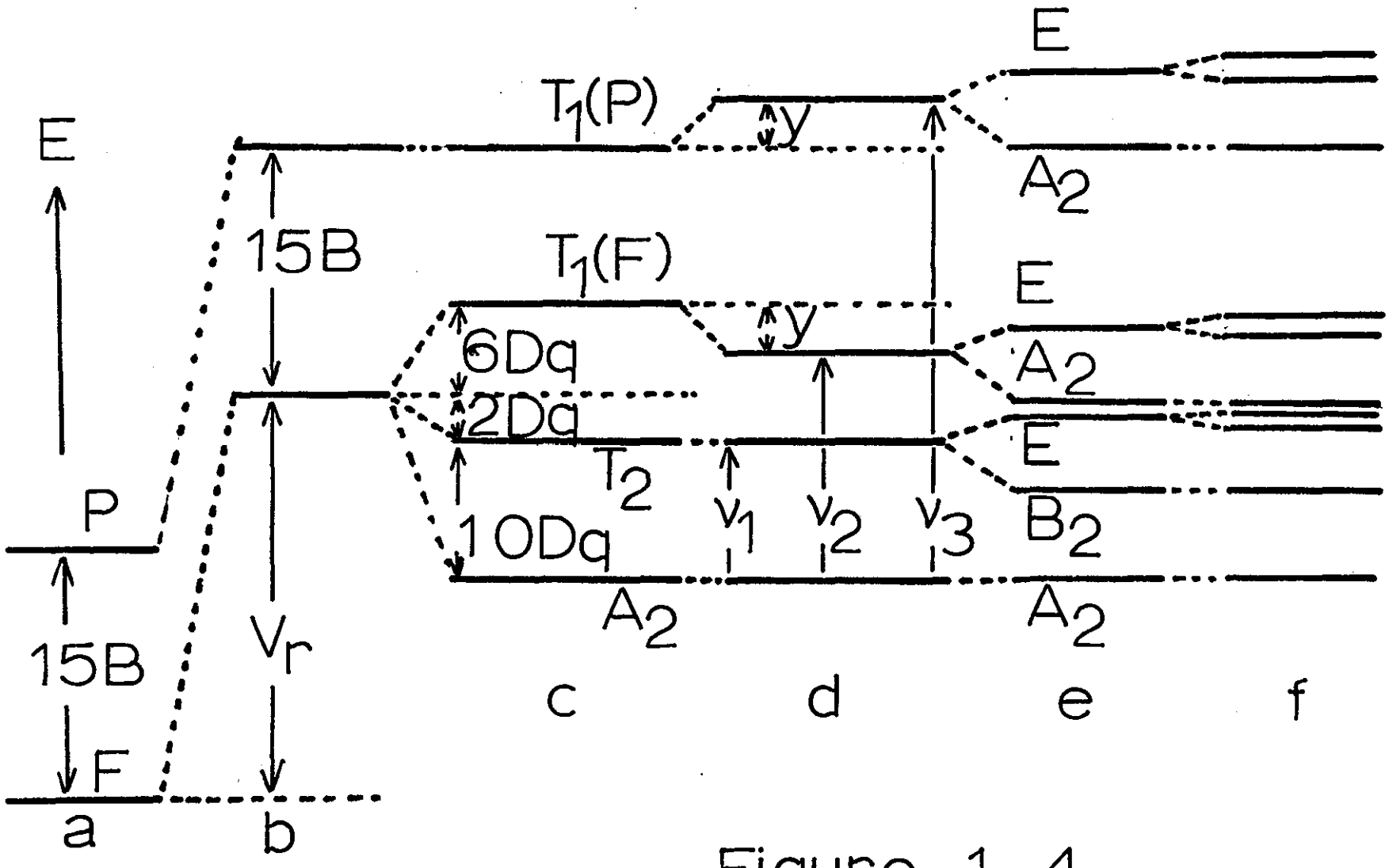
E
15B
P
15B
F
a
b
$T_1(P)$
$T_1(F)$
6Dq
2Dq
T_2
10Dq
A_2
V_r
y
y
ν_1
ν_2
ν_3
E
A_2
E
A_2
E
B_2
A_2
c
d
e
f

Figure 1.4

refer to tetrahedral and octahedral symmetry).

Thus d^3 and d^8 tetrahedral ions share the same energy diagram ("case a"; see figure 1.3) as octahedral d^2 and d^7 ions; while tetrahedral d^2 and d^7 species share the d^3 and d^8 octahedral diagram ("case b"; see figure 1.4). Similar relations exist for d^1, d^4, d^6 and d^9 configurations (see figures1.1 and 1.2). In later chapters the magnitude of Dq is measured, its sign being taken into account by using the correct diagram.

Hence in weak cubic fields one electronic absorption transition at a frequency $\nu = 10Dq$ is expected for d^1, d^4, d^6 and d^9 configurations but three spin-allowed transitions (ν_1, ν_2, ν_3) for d^2, d^3, d^7 and d^8 ions where:

In case (a):

$$\begin{cases} \nu_1 = E(T_2)-E(T_1(F)) & =8Dq \\ \nu_2 = E(A_2)-E(T_1(F)) & =18Dq \\ \nu_3 = E(T_1(P))-E(T_1(F)) & =15B + 6Dq \end{cases}$$

and in case (b):

$$\begin{cases} \nu_1 = E(T_2)-E(A_2) = & 10Dq \\ \nu_2 = E(T_1(F))-E(A_2) & =18Dq \\ \nu_3 = E(T_1(P))-E(A_2) & =15B + 12Dq \end{cases}$$

18-20

Ions in strong Cubic Fields

Weak fields such as those discussed above are defined as producing energy changes which are small compared with the separations between terms of the same multiplicity; ie Dq $\ll$B.

When the ligands produce larger fields it is helpful to consider first the effect of this potential on the one-electron orbitals. These are split by 10Dq, as in the d^1 case above, into a triply degenerate set t_{2g} and a doubly degenerate set e_g; the lower case letters emphasising the one-electron nature. The other d^n configurations may then be developed by distributing electrons into these orbitals, subject to the Pauli exclusion principle. Thus d^2 gives rise to three configuration $(t_{2g})^2$, $(t_{2g})^1$ $(e_g)^1$ and $(e_g)^2$. In the weak field case these arrangements differ little in energy. However for larger Dq the lower levels (t_{2g} in O_h fields; e in T_d fields) are preferentially occupied and the configurations differ considerably in energy. Electron exchange energy, between pairs of electrons with parallel spins, is a stabilising factor, and this inhibits unnecessary spin-pairing. Thus in d^4, d^5, d^6 and d^7 configurations in octahedral fields, the preferential occupation of the t_{2g} orbitals competes with the consequent loss of exchange energy. Thus a d^7 ion can have a high-spin $(t_{2g})^5(eg)^2$ configuration giving rise to quartet states ($2S+1=2.3.\frac{1}{2}+1=4$) or a low-spin $(t_{2g})^6(e_g)^1$ configuration

with doublet states. The ground state of a d^7 ion will thus be of quartet multiplicity at low fields but a doublet at high fields.

In very strong fields, the splitting produced by Dq is more important than interelectronic repulsion energies, and it is more appropriate to consider that states originate from the one-electron orbital configurations rather than from the atomic terms. The energies of these strong-field configurations may be expressed in terms of Dq only. For d^7 these energies relative to the atomic ^4F term are in O_h fields:

$$E(t_{2g}^5 e_g^2) = -8Dq; \quad E(t_{2g}^4 e_g^3) = 2Dq; \quad E(t_{2g}^3 e_g^4) = 12Dq$$

while for d^8 ions in O_h fields they are:

$$E(t_{2g}^6 e_g^2) = -12Dq; \quad E(t_{2g}^5 e_g^3) = -2Dq; \quad E(t_{2g}^4 e_g^4) = 8Dq.$$

As for weak fields, these two splitting patterns cover all the d^2, d^3, d^7 and d^8 systems in cubic fields. The low-spin energies are not given by this treatment, and are not considered here, since it is the high-spin configurations which correlate with the weak-field states, as Dq is reduced and interelectronic repulsions become more important.

Group theory identifies the components of each configuration by

decomposing its direct product. Thus the d^2 configuration $(t_{2g})^1(e_g)^1$ has a direct product: $t_{2g} \times e_g = (t_{1g} + t_{2g})$ (in the O_h group). In terms of spectroscopic states the $(t_{2g})^1(e_g)^1$ configuration therefore splits into $({}^3T_{1g} + {}^3T_{2g})$. Similarly $(t_{2g})^2$ transforms as $3 \times {}^3T_{1g}$, and $(e_g)^2$ as $2 \times {}^3A_{2g}$. The same states ${}^3T_{1g}$, ${}^3T_{2g}$, ${}^3T_{1g}$ and ${}^3A_{2g}$ are thus found near the strong and the weak field limits. The energies of the ${}^3T_{2g}$ and ${}^3A_{2g}$ states have, in fact, identical expressions at both limits:

$$E({}^3T_{2g}) = 2Dq \; ; \quad E({}^3A_{2g}) = 12Dq.$$

The energies of the components of the ${}^2D$ and ${}^5D$ terms of d^1, d^4, d^6 and d^9 ions are also identical at both limits.

Intermediate Fields for Triplet and Quartet States [18-20,23]

In most complexes, the crystal field strength is intermediate between the limits considered above, and Dq is comparable to B.. Since a one-to-one correspondence exists between the high-spin states at high and low field, the intermediate region may be approached from either extreme. In a graph (such as fig. 1.5) of state energy against crystal field strength, the T_{2g} and A_{2g} states of d^2, d^3, d^7 and d^8 ions and the E_g and T_{2g} states of d^1, d^4, d^6 and d^9 ions are connected by straight lines. However, curves must be drawn for the two T_{1g} states, since it

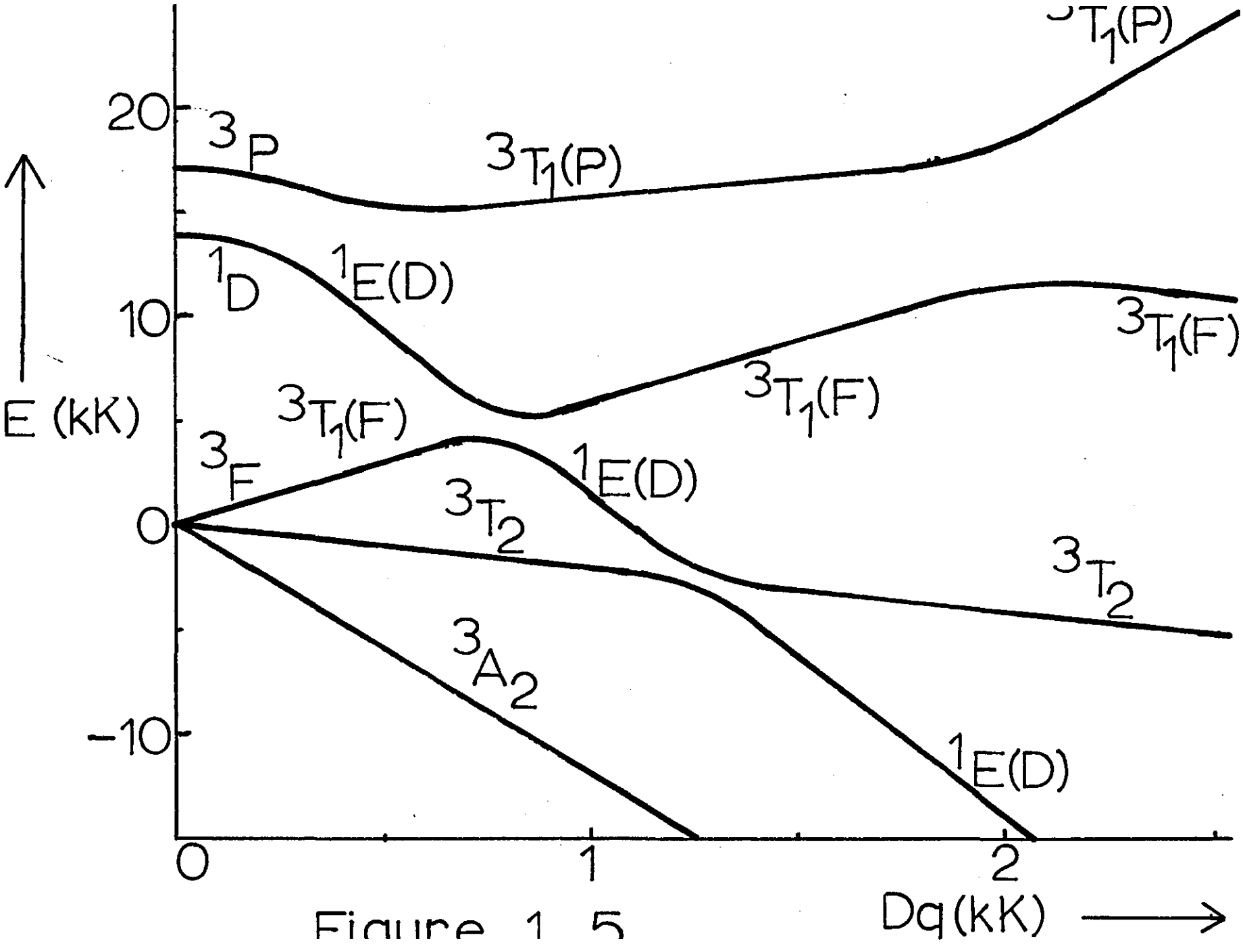
$^3T_1(P)$
20
^3P
$^3T_1(P)$
^1D
$^1E(D)$
10
$^3T_1(F)$
$^3T_1(F)$
E (kK)
$^3T_1(F)$
^3F
$^1E(D)$
$^3T_2$
0
$^3T_2$
$^3A_2$
$^1E(D)$
-10
0
1
2
Dq(kK) ⟶

Figure 1.5

has been found that states of the same symmetry interact. These graphs are called 'Orgel' diagrams.

This interaction is an inverse function of the energy difference between the states and is important at intermediate fields where the states are energetically similar. The interaction results in a 'repulsion' between the levels, the higher $T_1(P)$ being raised by energy increment x (say!) and the lower $T_1(F)$ being lowered by decrement which may be assumed equal to x. As figures 1.3d and 1.4d show, this further perturbation modifies the expressions for the spin-allowed frequencies:

For case (a):
$$\left.\begin{aligned} \nu_1 &= 8Dq + x \\ \nu_2 &= 18Dq + x \\ \nu_3 &= 15B + 6Dq + 2x \end{aligned}\right\} \quad .. \quad .. \quad .. \quad .. \quad .. \quad .. \quad 1.2$$

giving an elimination of x, the 'diagonal sum' rules:

$$\left.\begin{aligned} \nu_2 - \nu_1 &= 10Dq \\ \nu_3 - 2\nu_1 &= 15B - 10Dq \\ \nu_3 - 2\nu_2 &= 15B - 30Dq \end{aligned}\right\} \quad .. \quad .. \quad .. \quad .. \quad .. \quad .. \quad 1.3$$

and hence:

$$\left.\begin{aligned} Dq &= (1/10)(\nu_2 - \nu_1) \\ B &= (1/15)(\nu_3 + \nu_2 - 3\nu_1) \end{aligned}\right\} \quad .. \quad .. \quad .. \quad .. \quad .. \qquad 1.4$$

while for case (b):

$$\left.\begin{aligned} \nu_1 &= 10Dq \\ \nu_2 &= 18Dq - y \\ \nu_3 &= 15B + 12Dq + y \end{aligned}\right\} \quad .. \quad .. \quad .. \quad .. \quad .. \qquad 1.5$$

or:

$$\left.\begin{aligned} Dq &= \nu_1/10 \\ B &= (1/15)(\nu_3 + \nu_2 - 3\nu_1) \end{aligned}\right\} \quad .. \quad .. \quad .. \quad .. \quad .. \qquad 1.6$$

The form of this interaction between the T_{1g} states has been evaluated and the secular equations derived from a weak-field basis are [23]:

for case (a):
$$\begin{vmatrix} 15B-E & 4Dq \\ 4Dq & -6Dq-E \end{vmatrix} = 0 \quad .. \quad .. \quad .. \quad .. \quad .. \qquad 1.7$$

and for case (b):
$$\begin{vmatrix} 15B-E & -4Dq \\ -4Dq & 6Dq-E \end{vmatrix} = 0 \quad .. \quad .. \quad .. \quad .. \quad .. \qquad 1.8$$

while a strong-field basis gives expressions [23] which may be shown by expansion to be identical:

for case (a):

$$\begin{vmatrix} -8Dq + 3B - E & 6B \\ 6B & 2Dq + 12B - E \end{vmatrix} = 0 \qquad \ldots\ldots\ldots\ldots \quad 1.9$$

and for case (b):

$$\begin{vmatrix} 8Dq + 3B - E & 6B \\ 6B & -2Dq + 12B - E \end{vmatrix} = 0 \qquad \ldots\ldots\ldots\ldots \quad 1.10$$

Here, the two solutions for E are the energies of the T_1 states after interaction, relative to the atomic ^3F or ^4F term. Further, here as elsewhere, all case (b) equations are related to their case (a) analogues by a reversal of the sign of Dq.

These equations allow the energies of the states of highest multiplicity to be plotted as functions of Dq, if some value is assumed for B. Figure 1.5 shows the example of the Ni^{2+} ion.

The Jahn-Teller Theorem [18,101]

An ion such as Cu^{2+} in a regular octahedral crystal field has an E_g ground state which is thus orbitally degenerate. However, Jahn and Teller showed [102] that a complex, in a state with orbital degeneracy, is unstable with respect to distortions which remove that degeneracy. The

crystal field in the case of the Cu^{2+} ion must therefore lose its regular symmetry.

Qualitatively this can be seen as the result of an asymmetrical electron distribution. In an O_h field the $(t_{2g})^6(e_g)^3$ configuration has a hole in the e_g subshell. If the hole is in the $d_{x^2-y^2}$ orbital, ligands in the xy-plane will experience less repulsion by the d-electrons than those along the z-axis. Hence the xy-ligands may approach closer than the z-axis ligands, to give an elongated, tetragonally, distorted environment of D_{4h} symmetry. Quantitative calculations have shown this stereochemistry to be more favourable than the alternative compressed D_{4h} species, resulting from a d_{z^2} hole. Such distortions have been revealed[103] by many crystal structure determinations[42].

Similar arguments show that any complex having subshells, which are not empty, filled, or half-filled, should be subject to distortions. However, since in O_h symmetry the t_{2g} orbitals interact less with the ligands than do the e_g orbitals, smaller distortions are expected for asymmetric t_{2g} subshells.

Such a tetragonal distortion for an E_g ground state may be seen to be effective since, in the resulting D_{4h} symmetry, the ground state is non-degenerate (A or B). A trigonal distortion would not be effective

since an E state is still lowest in the D_3 group. Effective distortions always have the form of one of the 'normal' vibration modes of the molecule; These being the fundamental vibrations which are mutually independent ("orthogonal").

It has further been shown[104] than an effective distortion must transform as one of the non-totally-symmetric components of the ground state direct product. Thus, $(E_g)^2 = (2A_{1g} + E_g)$ and since A_{1g} is totally symmetric, only an E_g mode can be effective for an octahedral d^9 ion. Either of the components of this doubly degenerate E_g mode can produce the required distorition. One vibration leads as exprected to a compressed or an elongated D_{4h} stereochemistry, but the rhombic (D_{2h}) symmetry resulting from the other component is also found in many crystal structures.

Other sterochemistries should also distort for similar reasons. Thus the $(Cu(en)_3)^{2+}$ cation should distort to lift the ground state E degeneracy in the D_3 point group. A suitable distortion may be shown to involve two chelate rings contracting, and one expanding.

Ions in Non-Cubic Fields[18-20,105-108]

The energy levels of a trigonal bipyramidal complex must be calculated[109-111] ab initio; but most other common stereochemistries, such as square-pyramidal, may be treated by a descent of symmetry from a

cubic species. Thus, for example, the tetragonal crystal field predicted from the Jahn-Teller theorem for a d^9 ion may be treated using a potential $V = V_r + V_o + V_t$ (where V_t is the tetragonal part of the total perturbation).

In the D_{4h} group the E_g state transforms as $(A_{1g} + B_{1g})$ and the T_{2g} state as $(E_g + B_{2g})$. Thus a splitting of both octahedral energy levels is predicted. It may be deduced that the ground state is $^2B_{1g}$ in the elongated environment but $^2A_{1g}$ in the compressed species, as illustrated in figure 1.2d. Three optical transitions are thus expected in either case.

If Δ_1 and Δ_2 characterise the T_{2g} and E_{cg} splittings and the baricentre rule applies to these, then for the elongated case:

$$\left.\begin{aligned} \nu_1 &= \Delta_2 \\ \nu_2 &= 10Dq - (2/3)\Delta_1 + (1/2)\Delta_2 \\ \nu_3 &= 10Dq + (1/3)\Delta_1 + (1/2)\Delta_2 \end{aligned}\right\} \quad .. \quad .. \quad .. \quad .. \qquad 1.11$$

Ballhausen has used[18] radial integrals D_s and D_t to describe these splittings, where $\Delta_1 = 3D_s - 5D_t$ and $\Delta_2 = 4D_s + 5D_t$. A further splitting (Δ_3) of the remaining degeneracy (E_g) results from a rhombic distortion (D_{2h}).

A square coplanar structure can often be considered as the limiting case of such an elongation, when the axial ligands are too remote to influence the energy levels (fig.1.2c).

The T_{2g} state of d^2, d^3, d^7 and d^8 configurations also splits, in tetragonal fields as above, while A_{2g} is unsplit and T_{1g} transforms as $(A_{2g} + E_g)$. (See figure 1.4e).

For d^8 complexes in square coplanar fields, the $d_{x^2-y^2}$ orbital becomes less stable[112] than all the rest because the distribution of ligands on the x- and y- axes repels electrons in this orbital most. The resulting destabilisation of $d_{x^2-y^2}$ is often greater than the spin-pairing energy and hence diamagnetic complexes may be formed. The ground state has been found[113] to be of the $^1A_{1g}$ type. In this case, only singlet-singlet transitions will be spin-allowed in the absorption spectrum.

Spin Orbit Coupling[18,19]

The interaction between the magnetic dipole due to the spin of an electron and that due to its orbital momentum has so far been ignored in this discussion. In the Russell-Saunders scheme the interelectronic repulsion energy has been taken as greater than that due to such 'spin-orbit' coupling. The coupling energy is characterised by the spin-orbit

coupling parameter ξ for a single electron or $\lambda = \pm \xi / 2S$ for multi-electron terms. It results in splitting of the LS terms into levels characterised by their total angular momentum $J = |\underline{J}| = |\underline{L} + \underline{S}|$. The atomic terms thus retain their (2J+1)-fold degeneracy only when $\lambda \backsim 0$, and otherwise are denoted $^{2S+1}L_J$.

Table 1.1 shows[19] λ to be smaller for dipositive ions of the 3d period (0.1 - 0.8 kK) than for those of the 4d(0.4-1.8kK) or 5d(1.5-5.0kK) periods. Spin-orbit coupling has thus often been ignored in spectral treatments[114-117] of first row transition ions, though more complete calculations are sometimes available[118-120]. In heavier transition-elements spin-orbit coupling must be included, and in the octinides the Russell-Saunders scheme must be abandoned in favour of a "j-j" scheme, in which ξ is more important than B.

If calculations are corrected to include spin-orbit coupling, the result is to split some degenerate states as fig.1.4f shows. In weak octahedral fields, for example, $^4T_{1g}$, $^3T_{1g}$ and $^3T_{2g}$ have[92] three such components; $^2T_{2g}$ has 2 spin-orbit components; but $^1A_{1g}$, $^3A_{2g}$ and ^2Eg are unsplit.

Other effects of spin-orbit coupling are to allow an interaction between states differing in spin by $\Delta S=1$ and also to produce an orbital contribution to the magnetic moment. Such an interaction between

states, which may have different symmetry, can be important if ξ is large and if the levels are energetically close. These conditions are fulfilled by the Ni^{2+} ion at intermediate fields where the ^1E_g (D) state crosses $^3T_{1g}$ (F) and $^3T_{2g}$. This interaction can alter the observed ν_1 and ν_2 values,[121] and is discussed in Appendix A4. Whether these levels do approach closely is a matter of controversy. A diagram due to Liehr and Ballhausen[118] shows that they do not, but this depends on the values chosen for B, C and λ.

Vibronic Coupling[18]

The Born-Oppenheimer approximation allows the total wavefunction to be expressed: $\Phi = \varphi_e \psi_v \varphi_r$, where the subscripts e, v and r refer to the electronic, vibrational and rotational parts of the wavefunction; which are thus taken to be independent. A vibrational transition may occur simultaneously with an electronic absorption, and in this way vibrational structure is superposed on the electronic bands. Generally this results in a broad band at room temperature because many vibrational states may be populated, and because of the limitations of instrumental resolution. At low temperatures much of this structure is lost as only the vibrational ground state is appreciably occupied.

The Born-Oppenheimer approximation is not always obeyed. In

particular, a vibrational distortion of a complex may have a different electronic wavefunction to the undistorted complex. This 'vibronic' coupling means that it is more appropriate to treat a $\varphi_{e,v}$ wavefunction than to attempt its separation.

18,122-125

Intensity

The intensities of d-d electronic spectra are governed by two quantum-mechanical selection rules:

(i) The spin selection rule allows only transitions between states of the same spin multiplicity. Weak 'spin-forbidden' transitions are, however, often observed. This has been attributed to the action of spin-orbit coupling. Thus for d^7 ions, some quartet character can be mixed into the doublet excited states and transitions are therefore partially allowed from the quartet ground state.

(ii) The Laporte selection rule only allows a transition between an 'even' and an 'odd' state or vice versa. 'Even' and 'odd' parities refer to wavefunctions which are symmetric (g) or antisymmetric (u) with respect to the operation of a centre of inversion. Since all d-orbitals have even parity, all d-d transitions are 'Laporte-forbidden'. That d-d bands are

observed implies a break-down of the Laporte selection rule. The usual mechanism involves d-p mixing of wavefunctions, whereby the d-orbitals are able to gain some of the odd parity of the p-orbitals. However, such mixing is only possible in acentric complexes such as those of tetrahedral symmetry.

The much weaker bands observed in centrosymmetric complexes, such as octahedral species, are permitted by a further mechanism : vibronic coupling. A vibrational distortion of ungerade (u) symmetry will destroy the centre of symmetry when the nuclear displacements are non-zero. d-p mixing is then permitted, as for acentric complexes.

These mechanisms also account for optical dichroism[47]. Absorption only occurs if there is an electric dipole difference between the ground (φ_G) and excited (φ_E) states. Intensity is measured experimentally by the oscillator strength $f(\nu)$, which is related to the transition moment, $M=\int \varphi_G \mu \varphi_E d\tau$, where μ is the electric dipole moment operator. M is only non-zero if the product of the representations of the φ_G and φ_E contains one or more of the representations of μ. Since μ transforms as one of the cartesian vectors, the optical absorption will be anisotropic. A study of the polarisation properties of crystals allows, in favourable cases, the identification of the symmetry of φ_G and φ_E for each transition.

Similar studies have been made of the dichroism of vibrational spectra[126,127].

A further intensity-giving mechanism, sometimes available, is the mixing of the d-orbital excited states with charge-transfer excited states, through spin-orbit coupling. Charge-transfer bands are parity-allowed, and the mixing permits d-d bands to 'borrow' some of their intensity. Essentially this mechanism depends on the covalency which allows charge-transfer[128].

The occurrence of 'two-electron' transitions must also be considered. Such a simultaneous transition has a very low probability and will thus give rise to very weak bands. This might be expected for the $^4T_{1g}(F) \rightarrow {}^4A_{2g}(\nu_2)$ transition of octahedral d^7 ions, since the $^4T_{1g}(F)$ and $^4A_{2g}$ states are formally derived from the strong field $(t_{2g})^5(e_g)^2$ and $(t_{2g})^3(e_g)^4$ configurations.

Magnetic Properties[2,19,20,129-133]

The interaction of the unpaired electrons of suitable ions with an applied magnetic field is called paramagnetism. The diamagnetic[11a] interaction due to electron pairs is much smaller and of opposite sign. It is only important here in that a correction for diamagnetism must be made before the paramagnetism can be calculated.[133] Tables are available

for this purpose, though it is better to use experimentally determined values, where available.

The energy of the i'th paramagnetic ion of an array in a magnetic field H was expressed by Zeeman as a power series in H:

$$W_i = W_i^{(0)} + W_i^{(1)} H + W_i^{(2)} H^2 + \cdots\cdots\cdots$$

where $W_i^{(0)}$, $W_i^{(1)}$, $W_i^{(2)}$ ..... are coefficients of the zero'th, first, second ..... order Zeeman terms. The energy levels corresponding to this expression are generally closer together than the thermal energy, kT, and are populated according to a Boltzman distribution. The total energy (W) for all the N atoms can then be calculated, and hence also the paramagnetic susceptibility χ per unit mass:

$\chi = (-1/Hd)(\partial W/\partial H)$, where d is density.

χ may be measured conveniently on a Gouy balance by the vertical force exerted on a sample suspended partly in a horizontal magnetic field. Room temperature measurements are usually expressed in terms of the effective magnetic moment:

$$\mu_{eff} = (3kT\chi_M/N\beta^2)^{\frac{1}{2}}\beta,$$

where $\chi_M = \chi.M$, M is the molecular weight, and β is the Bohr Magneton

(B.M.). The magnetic moment is usually expressed in units of β, thus:

$$\mu_{eff} = 2.84\ (\chi_M T)^{\frac{1}{2}}\ \text{B.M.} \qquad \ldots\ 1.12$$

An application of quantum theory to the Zeeman energy levels predicts:

$\mu_{eff} = g(J(J+1))^{\frac{1}{2}}\beta$, if only the zero'th and first order terms are considered. Here g, the Landé splitting factor, characterises the energy intervals, $g\beta H$, caused by the magnetic field. Crystal field theory shows that:

$$g = 3/2 + (S(S+1)-L(L+1))/2J(J+1).$$

Experimentally, it is found that the orbital contribution to μ_{eff} is almost 'quenched' for 3d transition-metals. Ignoring the terms in L gives g=2 and:

$$\mu_{eff} = 2(S(S+1))^{\frac{1}{2}}\beta \qquad \ldots\ 1.13$$

which is the 'spin-only' moment (μ_{SO}).

That the orbital contribution is not always quenched completely is obvious from experimental μ_{eff} values. It is found that the extent of the orbital contribution depends on the degeneracy of the ground state of the complex.

An orbital contribution for a state φ only arises[20] if $\int \varphi \underline{L}^{*} \varphi \, d\tau$ is non-zero. The angular momentum operator ($\underline{L}$) has the symmetry properties of rotations about the x, y or z axes. Thus it transforms as T_{1g} in O_h or T_2 in T_d symmetry. The above integral is only non-zero if the direct product $\Gamma_\varphi \times \Gamma_{\underline{L}} \times \Gamma_\varphi$ contains the A_1 representation. Thus in the O_h group $A_{1g} \times T_{1g} \times A_{1g}$, $A_{2g} \times T_{1g} \times A_{2g}$ and $E_g \times T_{1g} \times E_g$ do not contain A_{1g} but $T_{1g} \times T_{1g} \times T_{1g}$ and $T_{2g} \times T_{1g} \times T_{2g}$ do. Similarly in T_d symmetry $A_1 \times T_2 \times A_1$, $A_2 \times T_2 \times A_2$ and $E \times T_2 \times E$ do not but $T_1 \times T_2 \times T_1$ and $T_2 \times T_2 \times T_2$ do contain A_1. In both groups T states give rise to an orbital contribution, but A and E states do not.

The triple orbital degeneracy of a T state can be lifted by spin-orbit coupling causing a splitting which is usually comparable to kT. A thermal population of levels results and μ becomes dependent on kT/λ. 'Kotani' plots of μ_{eff} against kT/λ have been given[19]. It is also possible for T state degeneracy to be raised by low symmetry crystal fields.

Though pure A and E states give rise to no orbital contribution, spin-orbit coupling can mix-in some excited T state wavefunctions leading to:[19]

$$\mu_{eff} = \mu_{SO}(1 - {}^{p}\lambda/10Dq)\beta \qquad \text{1.14}$$

where p is 4 for A_2 states and 2 for E states. E state degeneracy can

also be lifted by anisotropic crystal fields but the expression 1.14 is unaltered.

If the second order Zeeman term is included in the calculations a small extra contribution to the susceptibility arises. This 'temperature independent paramagnetic' (T.I.P.) term has been given[19] as $2pN\beta^2/10Dq$ for A and E states but is usually included in the T state Kotani diagrams.

Stability[20,28,134]

As figure 1.1c illustrates, the one-electron t_{2g} and e_g orbitals in an O_h field have energies (V_r-4Dq) and (V_r+6Dq) relative to the atomic parent term. The splitting caused by the V_o part of the potential results in an extra energy $(-4p+6q)Dq_o$ for a $(t_{2g})^p(e_g)^q$ configuration. This expression is a measure of the 'crystal field stabilisation energy' (C.F.S.E. = U_o) is an octahedral field. The analogous expression for an $(e_g)^q(t_{2g})^p$ configuration in a tetrahedral field is $U_t = (6q-4p)Dq_t$. Values for the C.F.S.E. of high-spin complexes are collected in table 1.3 along with the difference (U_o-U_t), after correcting for $|Dq_t| = |4/9Dq_o|$.

Table 1.3 shows that the octahedral stereochemistry is always at least as stable as the tetrahedral stereochemistry, for the same metal and ligands. The octahedral structure is especially stable for d^3 and

TABLE 1.3

High spin crystal field stabilisation energies (U) for d^n configurations in cubic fields.

n	U_o/Dq_o	U_t/Dq_t	U_t/Dq_o	$(U_o-U_t)/Dq_o$
0,5,10	0	0	0	0
1,6	-4	-6	-2.67	-1.33
2,7	-8	-12	-5.33	-2.67
3,8	-12	-8	-3.55	- 8.45
4,9	-6	-4	-1.78	-4.22

d^8 ions. If, perhaps because of steric hindrance, an octahedral structure is impossible, then the absolute U_t becomes more important than the relative $(U_o - U_t)$. Under these conditions, apart from the d^o, d^5 and d^{10} configurations, tetrahedral complexes are most likely to be formed with d^2 or d^7 ions.

Low-spin complexes involve an unfavourable spin-pairing contribution (Q) relative to the corresponding high-spin configuration. For square-planar d^8 ions, $U_p = (-12Dq_o - \Delta_2 + Q)$ giving $(U_o - U_p) = (\Delta_2 - Q)$ and $(U_t - U_p) = (8.45Dq_o + \Delta_2 - Q)$. Thus, a planar structure may be preferred to an octahedral one if Δ_2 is large, or preferred to a tetrahedral sterochemistry if Dq and Δ_2 are large.

Stability either in the solid state, or solution, is usually measured by the reciprocal (K) of the equilibrium constant for the dissociation reaction. Then: $-\Delta H_o + T\Delta S_o = -\Delta G_o = RT\log K$. Hence there is both an entropy and an enthalpy contribution to K. Entropy roughly correlates with disorder. Chelates are more stable than non-chelate complexes, since there is less disorder of the randomised ligands on dissociation.

Ligand Field Theory [18,20,31,135]

So far the theory has been presented on the assumption of a

purely electrostatic interaction between cation and ligands. Considerable evidence, however, exists [136-142] to indicate that covalency is often important. Thus hyperfine splitting due to ligand atoms has been detected in the paramagnetic resonance absorption of transition-metal ions [143]. The NMR spectra of metal ions and ligands also often show hyperfine structure due to the delocalisation of metal and ligand electrons [141]. Exchange interactions, via orbital-overlap, cause partially-paired spins on metal ions and thus reduce $\mathcal{N}_{eff}$ [19] and affect the ESR line width [144]. A study of nuclear quadrupole moments, or Mössbauer spectra [145], gives information on the S-electron density at the nucleus, which is related to the degree of covalency. The observation [69] of charge-transfer absorption spectra also confirms covalency. B and λ have also been predicted [146-148] to decrease in the presence of covalency; and this has been observed [149]. Certain aspects of the variation of Dq have also been attributed to covalency [137,138,150,151].

The molecular orbital theory of complexes is one way of dealing with covalency, [26,152,153] but it is simpler to treat B, C, λ and Dq as empirical parameters. This is the approach of 'ligand field' theory, and will be followed here as it preserves a physical picture.

The Spectrochemical Series[23,26]

Complexes placed in order of increasing Dq comprise a 'spectrochemical series'. For example:

$$CoI_4^{2-} < CoBr_4^{2-} < CoCl_4^{2-} < Co(NCS)_4^{2-}$$

or:

$$Mn(H_2O)_6^{2+} < Ni(H_2O)_6^{2+} \backsim Co(H_2O)_6^{2+}$$

By comparing complexes of different ligands, but with the same central ion and stereochemistry; or by comparing complexes of different metals with the same ligands, and stereochemistry; two series can be drawn up. The series for metal ions is commonly[26]:

$$M_n^{2+} < Ni^{2+} \backsim Co^{2+} < V^{2+} < Fe^{3+} < Cr^{3+} < Co^{3+} < Mn^{4+}$$

while for ligands[23]:

$$I^- < Br^- < Cl^- \backsim \underline{S}CN^- < F^- < OH^- \backsim \underline{N}O_2^- < H_2O < S\underline{C}N^-$$

$$< py \backsim NH_3 < en < phen < \underline{N}O_2^- \ll CN^-$$

(underlined atoms denote bonding sites in ambidentate ligands).

An expression: $10Dq = f(\text{ligands}).g(\text{central ion})$ has been given[23]

in an attempt to put these series on a more quantitative basis. Rough predictions of Dq for complexes of mixed ligands may be made using the rule of average environment[23]. Thus for a chromophore MA_xB_{n-x}:

$$Dq(MA_xB_{n-x}) = (x/n)Dq(MA_n) + ((n-x)/n)Dq(MB_n) \quad .. \quad .. \quad .. \quad .. \quad 1.15$$

The spectrochemical series for metal ions is seen to be one of increasing oxidation number, consistent with the larger electrostatic fields of the more highly charged central ions. For the same oxidation state Dq roughly follows an inverse relationship with ionic radius, consistent with an inverse relationship between the potential and the metal-ligand internuclear distance (equation 1.1). This is also consistent with the greater power of a small cation, to induce a dipole moment on (to 'polarise') a ligand, than a larger cation of the same charge.

An explanation of the spectrochemical series for ligands is more difficult since Dq does not depend simply on the electron charge density of the donor atom (ie. the basicity or the reducing power) or on ligand polarisability as might be expected if a purely electrostatic interaction were present. It was mentioned earlier that covalency could affect Dq, and in fact a molecular orbital formulation[92] shows

(Fig.1.6) this to be the case. The energy interval corresponding to 10Dq increases with σ-bond strength, and also with π-bond strength if the ligand originally has empty antibonding π-orbitals. Such 'backdonation' from the metal ion has been suggested[92] as the reason for the high position of CN^- in the spectrochemical series.

If backdonation is impossible, then Dq may be reduced by the reverse process, if the ligand only has filled π-orbitals[92] (eg: the halide ions). If neither type of π-bonding is possible (eg: NH_3, en), then Dq follows the order of ligand pKa quite closely.

Equation 1.1 shows Dq to depend on the internuclear distance, and accordingly it has been suggested[167,168] that it may be decreased if steric hindrance results in long M-L bonds.

The Nephelauxetic Series[23,149]

It was mentioned above that the Racah B parameters are usually reduced in complexes from the free ion values given in table 1.1. If complexes are placed in an order of decreasing observed Racah parameter ($B' = \beta B$), the 'nephelauxetic series' results. Such a series may be written in terms of metal ions or ligands:

$$V^{2+} \backsim Mn^{2+} > Ni^{2+} \backsim Co^{2+} > Cr^{3+} > Fe^{3+} > Co^{3+} > Mn^{4+}$$ and:

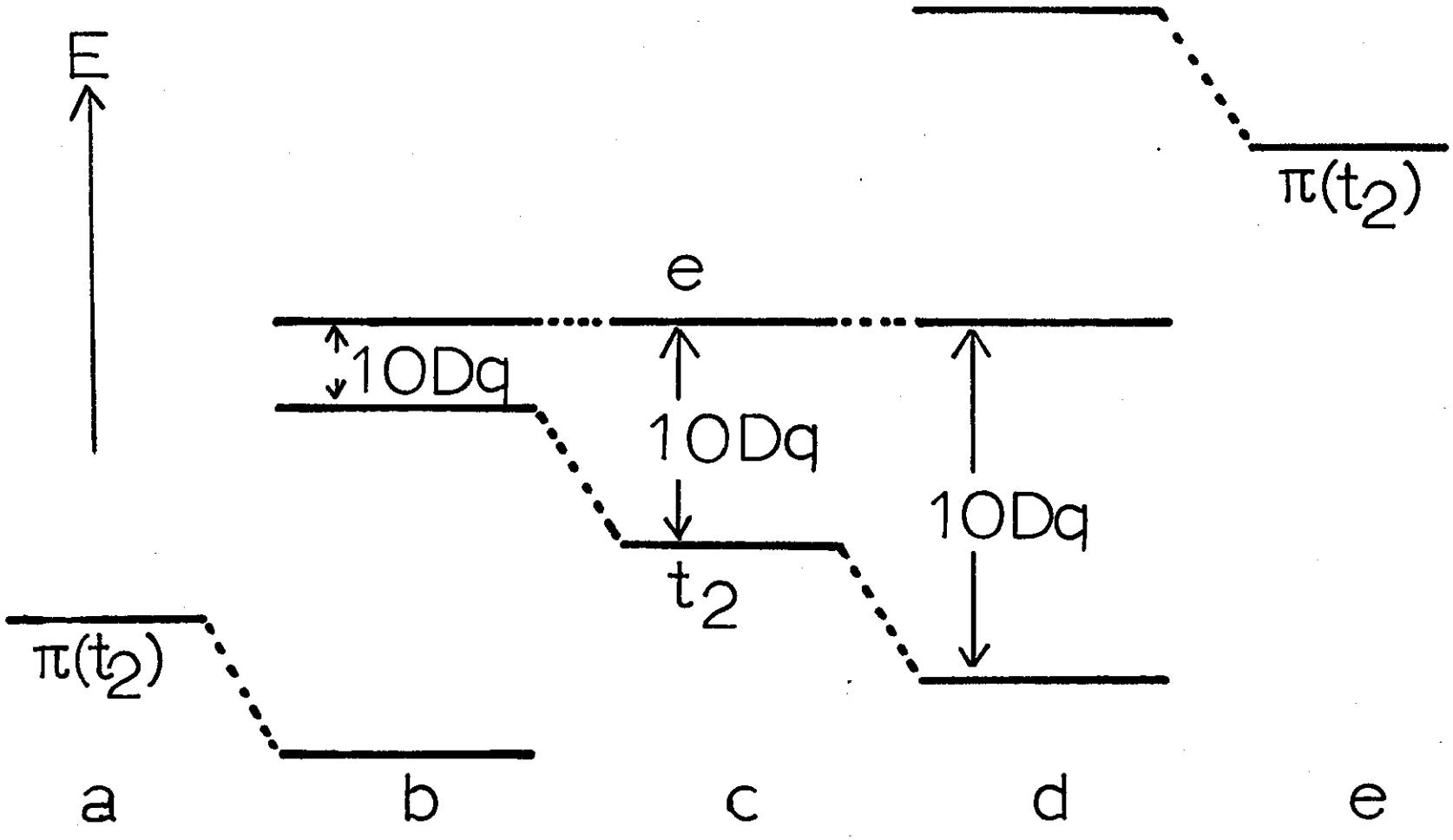

Figure 1.6

$$F^- > H_2O > NH_3 > en > \underline{N}CS^- > Cl^- > CN^- > Br^- > I^-$$

Expressions similar to those for the spectrochemical series may be used to separate ligand and metal contributions to the variation of B', or to deal with complexes of mixed ligands. The series in metal ions is seen to be one of increasing oxidation potential; while the ligand series correlates with reducing power, complexing power, polarisability, and other measures of electron availability on the donor atom (eg: pKa, heat of protonation, charge density). A steric effect has also been claimed [167] in that B' appears to be high when steric hindrance produces long bonds.

As mentioned above, the reduction of B has been ascribed [149] to covalency, and hence the correlation with redox potentials, polarisability, and electronegativity can be understood. The greater the affinity of the metal ion for electrons, and the greater the donor power (or induced dipole) of the ligands, so the greater will be the covalency accompanying charge-transfer.

The relationship of β to covalency has been discussed by Jørgensen [149], but the mechanism appears to be controversial. Some authors prefer to attribute the effect entirely to electron delocalisation but others relate it to a reduction in the size of the d-orbitals. Both effects may be important.

Covalency also provides an explanation of the reduction of the magnitude of the observed spin-orbit coupling constant ($\lambda' = \alpha\lambda$) from the free-ion value given in table 1.1.

Metal-Ligand π -Bonding

As explained above, the occurrence of metal-ligand π -bonding can be important [169] in determining the value of Dq and it will contribute to the reduction of B and λ. Molecular orbital treatments of metal-ligand bonding have successfully invoked π -bonding to explain physical properties [170,171] but there is little more direct evidence for backdonation.

A parameter $S_f = \log K_L' - \log K_L$, was devised by Irving and Da Silva [172] to measure the π -bonding in complexes of ligand L', relative to equivalent ones of L. Da Silva and Colado extended [173] this study and reported data on two series of complexes with substituted pyridines. S_f was found to correlate with the Hammett σ-value for the substituent, and also to have an inverse relationship with the ligand pKa. However, Yingst and McDaniel have shown [174] that S_f does not necessarily measure π -bonding. Thus, no clear evidence exists on the relative π-acceptor properties of these ligands. It has, for example, been argued that the smallness of the ligand infrared shifts due to co-ordination is both evidence for [89] and against [175] appreciable backdonation. Further, Bull

and Moore have suggested[176] that the positive resonance effect of halo-substituents on the pyridine nucleus will make halopyridines poorer π-acceptors than pyridine, while Nelson et al[153,177] have considered that the inductive effect is also important, and this being negative should make halopyridines better π-acceptors than pyridine, if the inductive effect is dominant.

Electroneutrality[178]

According to Pauling's principle of electroneutrality, a metal co-ordinates that number of ligands, which by charge transfer, will reduce its effective charge to zero. Thus fewer polarisable, or 'soft' ligands[179], (eg: I^-) can be co-ordinated to a given cation than hard ligands (eg: F^-), since more covalency is present in the former complexes. Polarisability (b) is defined[180] as the dipole moment induced by a unit field. It may be measured by means of refractivity (R) to which it is related: $b=3R_\infty/4N\pi$ (where R_∞ is the value obtained by extrapolating a graph of R against λ^{-2} to infinite wavelength.) R is additive in terms of atoms or of bonds and hence so is b.

If a chromophore, MX_4L_2, is considered and both X and L are soft, instability may result because the effective charge on the metal atom has been reduced below zero, thus violating the Pauling principle.

However, stability can be restored if L is a good π-acceptor so that the excess negative charge is reduced. The extent of M-L π-bonding will therefore depend on the charge accumulation which must be reduced, and thus on the anion polarisability. Nelson et al [181-183] found from studies of the solution equilibria of Co^{2+} and Ni^{2+} complexes of pyridine that their explanation of the entropy term as due to π-bonding deanded that the extent of M-L π-bonding should correlate with the order of anion polarisabilities ($I^- > Br^- > Cl^-$). Confirmation of this view has recently been reported [72] from proton NMR contact shifts of the Co^{2+} complexes with pyridine.

The basicity of L may also be expected to be important [153,177]. Thus a ligand of low pKa [184,185] will usually give rise to a weak σ-metal-ligand bond. Hence, only small charge-transfer from this ligand would contribute to the undesirable negative charge accumulation on the metal, and a stable complex could result.

If polarisable anions are present, along with other ligands of high basicity but low π-acceptor capacity, the only means to reduce the charge accumulation is a decrease of co-ordination -number. Thus with such ligands, the iodide complex may be four-co-ordinate while the chloride complex is six-co-ordinate. This is the case with the pyridine complexes. Thus α-$CoCl_2py_2$ [186] and $NiCl_2py_2$ [187, 188] are

both octahedral but CoI_2py_2[187] and NiI_2py_2[189,190] are tetrahedral. An alternative explanation of these facts is possible if more π-bonding is possible in a tetrahedral structure than in octahedral polymer.

Summary of Spectra & Magnetism[18,21,28]

All the complexes discussed in this work are of cobalt (II), nickel (II) or copper (I and II). Thus it is convenient to summarise the spectral and magnetic properties of the complexes with these metals.

(i) Cobalt (II): Three spin-allowed transitions are expected for both octahedral and tetrahedral complexes. Their assignment may be complicated by splitting, due to low symmetry fields or spin-orbit coupling; or by the presence of spin-forbidden transitions. Tetrahedral complexes will exhibit much stronger absorption bands than octahedral complexes because the former are acentric. Since Dq is smaller in tetrahedral complexes than analogous octahedral complexes, all frequencies will be lower in the former species. This results in ν_1 being obscured by ligand vibrational overtones in tetrahedral complexes.[47] Further ν_1 is electric-dipole-forbidden for tetrahedral symmetry, while ν_2 is a two-electron transition in octahedral complexes. Both bands may therefore be weak.

Transitions in the octahedral complex $(Co(H_2O)_6)^{2+}$ have been observed[28] at:

$\sim$ 8.5kK : ν_1, $^4T_{1g}(F) \rightarrow {}^4T_{2g}$

$\sim$ 17kK : ν_2, $^4T_{1g}(F) \rightarrow {}^4A_{2g}$

$\sim$ 20.5kK : ν_3, $^4T_{1g}(F) \rightarrow {}^4T_{1g}(P)$

With a molar extinction coefficient (ε) of about[17] 3.

On the other hand, the tetrahedral complex β-$CoCl_2py_2$ has $\varepsilon \sim 900$, for the most intense band, and frequencies[191] of:

$\sim$ 7kK : ν_2, $^4A_{2g} \rightarrow {}^4T_{1g}(F)$

$\sim$ 16kK : ν_3, $^4A_{2g} \rightarrow {}^4T_{1g}(P)$

Typical cobalt (II) spectra are illustrated in fig. 5.1 by α-$CoCl_2py_2$ (spectrum D) and $CoBr_2py_2$ (A).

Octahedral magnetic moments lie in a region[19] $\sim$ 5.2 B.M. somewhat higher than the range[19] ($\sim$ 4.4 B.M.) usually observed for tetrahedral complexes.

(ii) Nickel (II): The three spin-allowed bands have been observed in the octahedral $(Ni(H_2O)_6)^{2+}$ species at:[28]

8.6kK : ν_1, $^3A_{2g} \rightarrow {}^3T_{2g}$; ($\varepsilon \sim 2$)[55]

13.5kK : ν_2, $^3A_{2g} \rightarrow {}^3T_{1g}(F)$; ($\varepsilon \sim 2$)

25.3 kK : ν_3, $^3A_{2g} \rightarrow {}^3T_{1g}(P)$; ($\varepsilon \sim 5$)

The high values observed for ν_3 often cause this band to be obscured by charge-transfer absorption. The assignment may often be complicated due to the presence of shoulders caused by spin-forbidden transitions or by splitting in low symmetry crystal fields.

Tetrahedral complexes show stronger bands at lower frequencies than octahedral species[192,193]; for $NiBr_2Quin_2$ at:

$\sim$ 6.9kK : ν_1, $^3T_{1g}(F) \rightarrow {}^3T_{2g}$

9.9kK : ν_2, $^3T_{1g}(F) \rightarrow {}^3A_{2g}$; ($\varepsilon \sim 60$)

17.45kK: ν_3, $^3T_{1g}(F) \rightarrow {}^3T_{1g}(P)$; ($\varepsilon \sim 170$)

Square-planar complexes have strong singlet-singlet absorptions at high frequencies. It is thus difficult to differentiate between d-d and charge-transfer bands. [192] NiI_2Quin_2 has bands at:

11kK : $^1A_g \rightarrow {}^3B_{1g}, {}^3A_g$ ($\varepsilon \sim 5$)

15.43kK : $^1A_g \rightarrow {}^1B_{3g}$; ($\varepsilon \sim 200$)[190]

$\sim$ 21.7kK : $^1A_g \rightarrow {}^1B_{1g}$

25.0kK: $^1A_g \rightarrow {}^1A_g$

and its spectrum is shown in fig. 11.1 (B); while the octahedral spectrum of $NiCl_2py_2$ is illustrated in fig.6.1(A).

Square planar nickel complexes are diamagnetic[19] while tetrahedral meoments ($\backsim$3.4 B.M.)[19] may be slightly higher than octahedral values ($\backsim$3.2 B.M.)[19].

(iii) Copper (II): Weak bands are generally found for copper (II) complexes since these often have centrosymmetric, tetragonal structures. The number of peaks observed, and their frequencies, depend on the degree of tetragonality. Low frequencies are expected, unless the distortion is large, since all transitions occur between the components of a single atomic term. Up to three peaks may be produced but they may be poorly resolved, resulting in one broad band. A fourth component may appear, if a rhombic distortion is present.

In a $ZnSiF_6 \cdot 6H_2O$ lattice, copper takes up an octahedral stereochemistry[120]. Its spectrum shows only one band at 11.75kK ($\varepsilon \backsim 10$) with a low frequency shoulder due to spin-orbit splitting. The bands of the square planar $Cu(acac)_2$ complex may be assigned[55]:

13.5kK : $B_{2g} \rightarrow A_{1g}$

15.1kK : $B_{2g} \rightarrow B_{1g}$

17.5kK : $B_{2g} \rightarrow E_g$

$CuCl_2py_2$ has[186] a tetragonally distorted octahedral structure, but as fig.4.1(F) shows $(CuCl_2(3Brpy)_2$ has a practically identical spectrum and is in fact illustrated) only one broad band results; while the less distorted[194] complex $CuCl_2T$ gives rise (fig.4.1.B) to two bands.

The magnetic moment ($\sim$ 1.8 B.M.) of the Cu^{2+} ion is relatively insensitive[19] to stereochemistry, though a low value ($\sim$ 1.4 B.M.) may reflect exchange coupling.

(iv) Copper (I): The complete d-shell of the Cu^+ ion gives rise to no d-d spectrum and only a diamagnetic susceptibility. The visible spectrum may exhibit intense charge-transfer bands.

ARRANGEMENT OF THESIS

The work to be reported here will use the spectral and magnetic properties, listed above, to furnish stereochemical information on the complexes of cobalt, nickel and copper with two series of ligands : the halopyridines, and the quinoxalines. Though these studies are interlinked, it is convenient to divide this dissertation into two sections.

A brief survey in Chapter III of reported complexes of substituted pyridines will preceed the discussion in Chapters IV-VI of the work on halopyridines. Then will follow some introductory remarks on the quinoxaline ligands (Chapter VII) and an account in Chapters VIII-XI of their complexes.

It will be useful before this (Chapter II) to consider how the ligand-field parameters, Dq and B', may be calculated for cobalt (II) and nickel (II) complexes.

CHAPTER II

THE CALCULATION & USE OF LIGAND FIELD (Dq)

&

RACAH (B') PARAMETERS

Recently a number of papers have been published in which Dq and B' have been calculated from measurements of the electronic spectra of cobalt (II) [195,196] and nickel (II) complexes [152,197,198]. Useful information has been derived from discussions of these calculated parameters.

In those cases when all three spin-allowed bands were observed, the calculation was simple - involving only equations 1.4 or 1.6. However, as mentioned in Chapter I, it was frequently only possible to observe two of these bands, because:

(i) ν_1 was obscured by infrared overtones due to ligand vibrations. (e.g. in tetrahedral cobalt (II) and nickel (II) complexes [190,195,198-201]).

(ii) ν_2 was not observed (e.g. in octahedral Co(II) this band corresponds to a two-electron transition).

(iii) ν_3 was obscured by charge-transfer bands (e.g. in octahedral Ni(II) spectra [198]).

(iv) One of the bands was beyond the frequency range studied [183,202,203].

In these cases, the values of Dq and B' were often found by solving the secular equations (1.7-1.10) using trial and error methods [198].

While pursuing these calculations on the complexes described in this thesis it has been found possible to simplify considerably the solution of the secular equations. Calculations have been performed:

(i) To study the consistency of the values of Dq and B', calculated from the various pairs of observed absorption bands.

(ii) To investigate the reported spectral data on a large number of compounds.

The results of this work, and a discussion of the usefulness of the values obtained for Dq and B', are given in this chapter. It has been subsequently found[204] that Cotton and Goodgame have published equations for tetrahedral d^7 ions which lead to the equations derived here. In the following treatment the effect of spin-orbital coupling will be ignored.

Nomenclature

In this thesis the values of Dq and B', calculated from the ν_1 and ν_2 bands only, will be denoted by Dq_{12} and B'_{12}. The same convention will be used for values derived from other combinations of ν_1, ν_2 and ν_3.

(A) Calculation of Dq and B' for case (a) complexes (d^2 and d^7 ions in octahedral fields and d^3 and d^8 ions in tetrahedral fields).

To calculate Dq and B' from only two bands the interaction between the two T_1 states must be examined. This interaction is given[23] for case (a) complexes by the intermediate field secular equation 1.7. This quadratic equation may be solved to give two roots E_+ and E_- (whose subscripts refer to the sign of the square root term). These may be identified as the energies (E') of the $T_1(P)$ and $T_1(F)$ states after interaction, relative to an energy of $E(F)+V_r$. In the limits when $Dq \rightarrow 0$ or $Dq \gg B'$ there will be no interaction, but in these cases $E \rightarrow E'$ only if:

$$\left.\begin{aligned} E_+ &= E'(T_1P) \\ E_- &= E'(T_1F) \end{aligned}\right\} \quad .. \quad .. \quad .. \quad .. \quad .. \quad .. \quad .. \quad 2.1$$

Further, Figure 1.3 shows that:

$$\left.\begin{aligned} \nu_1 &= E(T_2)-E'(T_1F) = 2Dq - E'(T_1F) \\ \nu_2 &= E(A_2)-E'(T_1F) = 12\ Dq - E'(T_1F) \\ \nu_3 &= E'(T_1P) - E'(T_1F) \end{aligned}\right\} \quad .. \quad .. \quad .. \quad .. \quad 2.2$$

(i) Calculation from ν_2 and ν_3 only:

Equations 2.1 and 2.3 give:

$$\left.\begin{aligned} E_- &= E'(T_1F) = 12Dq - \nu_2 \\ E_+ &= E'(T_1P) = \nu_3 + E'(T_1F) = \nu_3 - \nu_2 + 12Dq \end{aligned}\right\} \quad .. \quad 2.3$$

Expansion of equation 1.7 gives:

$$E^2 - E(15B' - 6Dq) - 90B'Dq - 16Dq^2 = 0 \quad .. \quad .. \quad .. \quad 2.4$$

Thus, equation .2.3 and the sum rule for the roots E_+ and E_- of 2.4 lead, as before to:

$$\nu_3 - 2\nu_2 = 15B' - 30Dq \quad .. \quad .. \quad .. \quad .. \quad .. \quad .. \quad 1.3$$

While the product rule for E_+ and E_- yields, after substituting 15B' from 1.3:

$$340Dq^2 + 18Dq(\nu_3 - 2\nu_2) + \nu_2^2 - \nu_2\nu_3 = 0 \quad .. \quad .. \quad 2.5$$

and thus:

$$Dq_{(23\pm)} = (1/340)(9(2\nu_2 - \nu_3) \pm (81\nu_3^2 + 16\nu_2\nu_3 - 16\nu_2^2)^{\frac{1}{2}}) \quad 2.6$$

There are two solutions $Dq_{(23+)}$ and $Dq_{(23-)}$ (whose subscripted signs

refer to those of the square root term in 2.6) and two corresponding solutions $B'_{(23+)}$ and $B'_{(23-)}$ of equation 1.3.

In the weak field limit when Dq $\rightarrow$ 0, equation 2.5 becomes:

$$\nu_2(\nu_2 - \nu_3) = 0;$$

ie. $\nu_2 = 0$ or $\nu_2 = \nu_3$. $\nu_2 = 0$ is correct here, since figure 2.1 shows that the A_2 state crosses $T_1(P)$ (when $\nu_2 = \nu_3$) at finite Dq. Thus putting $\nu_2 = 0$ into equation 2.6 should give Dq = 0. This is only the case for $Dq_{(23+)}$ which must therefore be the meaningful solution.

The use of equations 1.3 and 2.6 allows the calculation of Dq and B' from ν_2 and ν_3 without recourse to the trial and error methods previously employed. Further, the position of the ν_1 band may be predicted from equation 1.4.

(ii) Calculation from ν_1 and ν_2 only:

Dq may be calculated directly from equation 1.4, and B' found in the following manner from the depression of the $T_1(F)$ state. The lower of the two solutions of equation 2.4 has already been identified

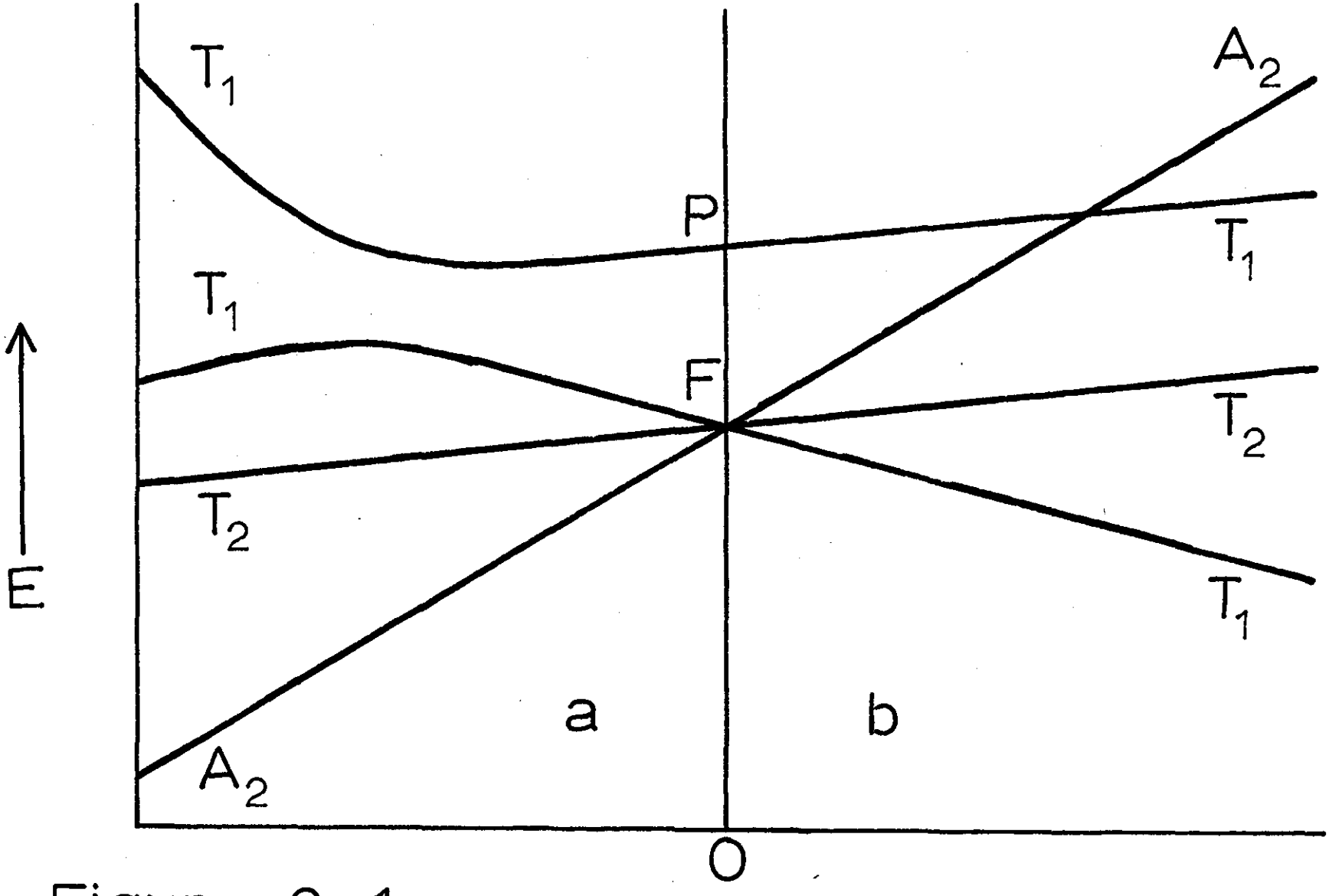

Figure 2.1

as $E'(T_1F)$, hence:

$$E'(T_1F) = E_- = (1/2)\left\{(15B'-6Dq)-(225(B')^2+180B'Dq+100Dq^2)^{\frac{1}{2}}\right\}$$

Substitution of this expression into equation 2.2 gives:

$$(225(B')^2 + 180B'Dq + 100Dq^2)^{\frac{1}{2}} = 15B'-10Dq + 2\,\nu_1$$

and on squaring both sides the terms in $(B')^2$ cancel leaving:

$$B'_{12} = \nu_1(10Dq- \nu_1)/15(\nu_1-8Dq) = \nu_1(\nu_2-2\nu_1)/3(9\nu_1-4\nu_2) \qquad 2.7$$

Equation 1.4 then allows ν_3 to be predicted.

(iii) Calculation from ν_1 and ν_3 only:

Dq may first be calculated after eliminating B' between equations 1.3 and 2.7:

$$80Dq^2 + 8Dq(\nu_3-2\nu_1)+\nu_1(\nu_1-\nu_3) = 0 \qquad .. \quad .. \quad .. \quad .. \qquad 2.8$$

giving:

$$Dq_{(13+)} = (1/20)\ ((2\nu_1-\nu_3)\pm(\nu_3^2 + \nu_1\nu_3-\nu_1^2)^{\frac{1}{2}}) \qquad .. \quad .. \qquad 2.9$$

The two solutions of 2.9 give two values of $B'_{(13)}$ from equation 1.3.

When Dq $\rightarrow$ 0, equation 2.8 becomes:

$\nu_1(\nu_1-\nu_3) = 0$; ie. $\nu_1 = 0$, or $\nu_1 = \nu_3$. However, figure 2.1 shows that the latter solution is impossible (except at infinite Dq) and that $\nu_1 = 0$ is correct. Putting this value into equation 2.9 only gives Dq = 0 for $Dq_{(13+)}$ which must, therefore, be the meaningful solution.

ν_2 can be predicted from equation 1.4.

(B) Calculations for case (b) complexes (d^3 and d^8 ions in octahedral fields and d^2 and d^7 ions in tetrahedral fields).

The interaction between T_1 states is given[23] for case (b) complexes by the intermediate field secular equation 1.8. This may be solved by methods (See Appendix A.1.) very similar to those given above. In addition to equation 1.6, the following are important:

$$Dq_{(23\pm)} = (1/340)(9(\nu_2+\nu_3) \pm (81\nu_2^2 - 178\nu_2\nu_3 + 81\nu_3^2)^{\frac{1}{2}}) \quad .. \quad .. \quad 2.10$$

where $Dq_{(23-)}$ is the meaningful solution.

$$B'_{12} = (2\nu_1-\nu_2)(\nu_1-\nu_2)/3(5\nu_2-9\nu_1) \quad .. \quad .. \quad .. \quad .. \quad .. \quad 2.11$$

$$B'_{13} = (2\nu_1-\nu_3)(\nu_1-\nu_3)/3(5\nu_3-9\nu_1) \quad .. \quad .. \quad .. \quad .. \quad .. \quad 2.12$$

(C) Verfication of Equations

A Ferranti Argus 100 Computer (See Appendix A2 for Programmes) was used throughout to calculate the parameters, except Dq_{13} and B'_{13} for which a desk calculator coped adequately with the small number of results. Many calculations were performed on data reported for complexes for which:

(i) Dq or B' were also reported (denoted Dq_r or B'_r), or:

(ii) All three spin-allowed bands were reported, allowing a comparison of Dq and B' values calculated using all methods.

Tables 2.1 and 2.2 give some results for case (a) complexes and Tables 2.3 and 2.4 for case (b) complexes. ν_{1p}, ν_{2p} and ν_{2p} denote values of ν_1, ν_2 and ν_3 predicted from each pair of measured frequencies.

A consideration of these tables lead to the following conclusions:

(i) The agreement between Dq and B' values calculated here and those previously reported, (or, in the absence of the latter, with Dq_{123} and B'_{123}) is a convincing verification of the equations developed above.

Table 2.1

Reported, and predicted, spin-allowed frequencies (kK) for some octahedral d^2 and d^7, and tetrahedral d^8 complexes.

Complex	Observed Bands			Predicted Bands			Reference
	ν_1	ν_2	ν_3	ν_{1p}	ν_{2p}	ν_{3p}	
V^3/Al_2O_3	17.4	-	25.2	-	36.08	-	21, 24
$V(H_2O)_6^{3+}$	17.1	-	25.2	-	35.51	-	23, 24
VOx_3^{3-}	16.45	-	23.2	-	34.04	-	23, 24
CoO	7.81	16.68	18.45	7.81	16.68	18.35	205
$Co(H_2O)_6^{2+}$	8.35	17.85	20.00	8.35	17.85	20.00	18, 23
$KCoF_3$	7.15	15.2	19.2	7.07	-	15.31	206
$NiCl_2Mp_5$	-	9.2	15.62	4.23	-	-	198
$NiBr_2Mp_5$	-	8.6	15.47	3.95	-	-	198
NiI_2Mp_5	-	8.1	15.40	3.71	-	-	198

Table 2.2

Ligand field and effective Racah parameters (kK) reported, and calculated for the complexes of Table 2.1.

Complex	Dq_{123}	Dq_{23+}	Dq_{23-}	Dq_{13+}	Dq_{13-}	Dq_r	B'_{123}	B'_{12}	B'_{23+}	B'_{23-}	B'_{13+}	B'_{13-}
V^{3+}/Al_2O_3	-	-	-	1.868	-.908	1.860	-	-	-	-	.605	-1.245
$V(H_2O)_6^{3+}$	-	-	-	1.841	-.941	1.840	-	-	-	-	.627	-1.227
VoX_3^{3-}	-	-	-	1.759	-.789	1.780	-	-	-	-	.526	-1.173
CoO	.887	.887	-.098	.887	-1.170	.888	.780	.773	.780	-1.190	.780	-.592
$Co(H_2O)_6^{2+}$	.950	.950	-.119	.950	-1.280	-	.853	.854	.853	-1.284	.853	-.633
$KCoF_3$	.805	.813	-.220	-	-	.770	.863	.604	.879	-1.187	-	-
$NiCl_2Mp_5$	-	.497	-.350	-	-	.500	-	-	.808	-.885	-	-
$NiBr_2Mp_5$	-	.465	-.374	-	-	.465	-	-	.815	-.862	-	-
NiI_2Mp_5	-	.439	-.396	-	-	.435	-	-	.824	-.846	-	-

Table 2.3

Reported and predicted spin-allowed frequencies (kK) for some octahedral d^3 and d^8, and tetrahedral d^7 complexes.

Complex	Observed bands			Predicted bands			Reference
	ν_1	ν_2	ν_3	ν_{1p}	ν_{2p}	ν_{3p}	
$VSO_4.7H_2O$	12.0	18.2	27.8	-	17.88	28.38	207
$Cr(H_2O)_6^{3+}$	17.4	24.6	37.8	-	-	38.53	23
$Cr(H_2O)_5F^{2+}$	16.8	24.0	37.6	16.99	24.1	37.48	23
Cr^{3+}/MgO	22.7	29.7	48.3	22.74	29.78	48.25	208
Cr^{3+}/Al_2O_3	18.1	24.4	39.1	18.2	-	38.99	23
Cr_2O_3	16.6	21.6	-	-	-	35.2	23
CrF_6^{3-}	14.9	22.7	34.4	-	-	35.44	23
$CrCl_3$	13.7	18.9	-	-	-	29.87	23
$Cr(NH_3)_6^{3+}$	21.55	28.5	-	-	-	46.01	23
$Cr(en)_3^{3+}$	21.85	28.5	-	-	-	46.38	23
MnF_6^{2-}	21.75	28.2	-	-	-	46.06	23
$CoCl_4^{2-}$	-	5.26	14.7	3.01	-	-	195
$CoBr_4^{2-}$	-	5.75	14.0	3.32	-	-	195
CoI_4^{2-}	-	4.93	13.2	2.83	-	-	195
$HgCo(NCS)_4$	-	8.3	16.7	4.88	-	-	209
$NiCl_3(Me_4N)$	6.60	11.20	21.20	6.65	11.13	22.13	197
$Ni(NH_3)_6^{2+}$	10.60	16.70	27.40	10.37	16.92	26.63	16, 150
$NiCl_2$	-	12.9	22.1	7.86	-	-	23
$KNiF_3$	-	12.5	23.7	7.42	-		23
$Nipy_6^{2+}$	9.479	15.57	26.15	9.56	-	26.70	210
$Ni(H_2O)_2py_4^{2+}$	10.15	16.50	27.00	10.27	16.38	27.58	23

Table 2.3 cont....

Complex	Observed bands			Predicted bands			Reference
	$\bar{\nu}_1$	$\bar{\nu}_2$	$\bar{\nu}_3$	$\bar{\nu}_{1p}$	$\bar{\nu}_{2p}$	$\bar{\nu}_{3p}$	
$NiCl_2py_2$	8.230	13.793	24.213	8.333	-	25.43	210
$NiCl_2(m\text{-}Tol)_2$	-	13.79	23.26	8.45	-	-	152
$NiBr_2(m\text{-}Tol)_2$	-	13.25	22.47	8.10	-	-	152
$NiBr_2(p\text{-}Tol)_2$	-	13.26	22.57	8.09	-	-	152
$NiCl_2Quin_2$	-	13.15	22.70	7.99	-	-	152
$NiCl_2Mp_5$	10.0	15.75	-	-	-	25.11	198
$NiBr_2Mp_5$	10.0	15.8	-	-	-	25.27	198
NiI_2Mp_5	11.4	15.8	-	-	-	24.92	198
$Ni(NCS)_2Mp_5$	10.5	16.65	-	-	-	26.74	198
$Ni(NCS)_2(2,6Dmp)_2$	10.4	16.15	-	-	-	25.45	198

Table 2.4

Ligand field and effective Racah parameters (kK) reported, and calculated, the complexes of table 2.3

Complex	Dq_{123}	Dq_{23+}	Dq_{23-}	Dq_r	B'_{123}	B'_{23+}	B'_{23-}	B'_{12}	B'_{13}	B'_r
$VSO_4.7H_2O$	1.200	-	-	1.200	.667	-	-	.705	.646	.6
$Cr(H_2O)_6^{3+}$	1.740	_	-	1.740	.680	-	-	.729	-	.7
$Cr(H_2O)_5F^{2+}$	1.680	1.699	1.562	1.680	.747	.708	.983	.738	.754	-
Cr^{3+}/MgO	2.270	2.274	1.855	2.270	.660	.652	1.489	.656	.665	.6
Cr^{3+}/Al_2O_3	1.810	1.820	1.542	1.810	.613	.593	1.150	.606	-	.6
Cr_2O_3	1.660	-	-	1.660	-	-	-	.467	-	.4
CrF_6^{3-}	1.490	-	-	1.490	.827	-	-	.896	-	.8
$CrCl_3$	1.370	-	-	1.370	-	-	-	.512	-	.5
$Cr(NH_3)_6^{3+}$	2.155	-	-	2.155	-	-	-	.657	-	.6
$Cren_3^{3+}$	2.185	-	-	2.185	-	-	-	.622	-	.6
MnF_6^{2-}	2.175	-	-	2.175	-	-	-	.601	-	.6
$CoCl_4^{2-}$	-	.756	.301	.301	-	-.181	.729	-	-	.7
$CoBr_4^{2-}$	-	.714	.332	.332	-	-.112	.653	-	-	.6
CoI_4^{2-}	-	.677	.283	.283	-	-.146	.643	-	-	.6
$HgCo(NCS)_4$	-	.833	.488	.488	-	-.005	.691	-	-	.6
$NiCl_3(Me_4N)$	.660	1.050	.665	.660	.840	.059	.830	.902	.835	.8
$Ni(NH_3)_6^{2+}$	1.060	1.297	1.037	1.060	.820	.345	.865	.769	.835	.8
$NiCl_2$	-	1.067	.786	.720	-	.199	.762	-	-	.7
$KNiF_3$	-	1.175	.742	.730	-	.064	.930	-	-	.9
$Nipy_6^{2+}$	.948	-	.956	-	.886	-	.870	.922	-	-
$Ni(H_2O)_2py_4^{2+}$	1.015	1.276	1.027	-	.870	.347	.847	.909	.862	-

Table 2.4 Cont....

Complex	Dq_{123}	Dq_{23+}	Dq_{23-}	Dq_r	B'_{123}	B'_{23+}	B'_{23-}	B'_{12}	B'_{13}	B'_r
$NiCl_2py_2$	.823	1.179	.833	-	.888	.176	.867	.969	-	-
$NiCl_2(m\text{-}Tol)_2$	-	1.116	.845	.845	-	.237	.780	-	-	.78
$NiBr_2(m\text{-}Tol)_2$	-	1.081	.810	.810	-	.219	.761	-	-	.76
$NiBr_2(p\text{-}Tol)_2$	-	1.087	.809	.810	-	.214	.770	-	-	.77
$NiCl_2Quin_2$	-	1.099	.799	.799	-	.191	.793	-	-	.79
$NiCl_2Mp_5$	1.000	-	-	1.000	-	-	-	.724	-	.72
$NiBr_2Mp_5$	1.000	-	-	1.000	-	-	-	.738	-	.73
NiI_2Mp_5	1.140	-	-	1.140	-	-	-	.435	-	.43
$Ni(NCS)_2Mp_5$	1.050	-	-	1.050	-	-	-	.793	-	.79
$Ni(NCS)_2(2,6Dmp)_2$	1.040	-	-	1.040	-	-	-	.694	-	.69

(ii) Except for the complexes of chromium (III), the results confirm the above selection of meaningful values of Dq. In the case of the octahedral complexes of Cr(III); $Dq_{(23+)}$ and $B'_{(23+)}$ were nearer to Dq_{123} and B'_{123} than were $Dq_{(23-)}$ and $B'_{(23-)}$. It has been pointed out[211] that the explanation for this effect lies in the comparatively large values of Dq commonly observed for Cr(III) complexes. In this case the strong field limit is more appropriate, as an aid to the selection of meaningful solutions, than the weak field limit so far considered. For octahedral d^3 ions, when $Dq \gg B'$ then ν_2 corresponds to the transition $t_{2g}^3 \rightarrow t_{2g}^2 eg^1$, while ν_3 corresponds to $t_{2g}^1 eg^2$ (Fig.2.1), and the energies given in Chapter I lead to: $\nu_2 = 10Dq$, and $\nu_3 = 20Dq$. Substitution of these values into equation 2.10 only yields a meaningful result for the $Dq_{(23+)}$ solution.

(D) Errors and Discrepancies in calculated parameters

The results in Tables 2.1-2.4 have usually been based upon reliable data from undistorted complexes. Many more results are given in Appendix A3, while Table 2.5 shows a selection of those which reveal

Table 2.5a

Data for some case a) complexes showing, to varying degrees, disagreement with theory. Units are kK, except those of P_2 (kK^2).

Complex	P_2	Dq_{123}	Dq_{23+}	Dq_{13+}	B'_{123}	B'_{23+}	B'_{13+}	B'_{12}	Reference
$V^{3+}/\alpha\text{-}Al_2O_3$	-165.59	1.710	1.792	1.868	.500	.655	.605	-.093	21
CoO	-0.38	.887	.887	.887	.780	.780	.780	.773	205
$Co(H_2O)_6^{2+}$	0.01	.950	.950	.950	.853	.853	.853	.854	18
$Co(NH_3)_6^{2+}$	-65.70	.950	.985	-	.840	.911	-	.214	23
$Coen_3^{2+}$	-124.26	.930	.997	-	.813	.947	-	-.032	23
$KCoF_3$	-13.80	.805	.813	-	.863	.879	-	.604	206
$CoCl_2$	-63.35	.670	.712	-	.717	.801	-	.035	206
$CoBr_2$	-88.84	.580	.644	-	.653	.781	-	-.106	206
$Co(2:6\text{-}DPNO)_2(NO_3)_2$	-472.71	.236	.654	-	.190	1.025	-	-.611	212
Ni^{2+}/CdS	-44.70	.400	.441	.486	.540	.623	.597	-.056	23
Co $enta^{2-}$	-235.08	.720	.871	-	.593	.894	-	-.345	23

Table 2.5b

Data for some case b) complexes showing, to varying degrees, disagreement with theory. Units are kK, except those of P_3 (kK^2).

Complex	P_3	Dq_{123}	Dq_{23} [a]	B'_{123}	B'_{23} [a]	B'_{13}	B'_{12}	Reference
$VSO_4.7H_2O$	9.80	1.200	b)	.667	b)	.646	.705	207
$Cr(H_2O)_6^{3+}$	24.48	1.740	b)	.680	b)	-	.729	23
$Cr(H_2O)_5F^{2+}$	-3.84	1.680	1.699	.747	.708	.754	.738	23
trans-$Cr(H_2O)_4F_2^+$	-41.76	1.630	1.745	.720	.491	-	.636	23
$Cr(H_2O)_4Cl_2^+$	-61.39	1.575	1.752	.783	.429	-	.650	23
Cr^{3+}/MgO	-2.92	2.270	2.274	.660	.652	.665	.656	208
Cr^{3+}/Al_2O_3	-4.58	1.810	1.820	.613	.593	-	.606	23
CoI_2dpa_2	23.47	.410 [c]	.448	.715	.639	.676	-.554	213
$NiCl_2Q_2$	15.78	.758	.781	.929	.883	-	1.278	152
$NiCl_3(Me_4N)$	3.16	.660	.665	.840	.830	.835	.902	197
$Ni(NCS)_2py_4$	54.99	1.045	b)	.517 [d]	b)	-	.900	153
$Ni(H_2O)_6^{2+}$	-11.75	.850	.834	.967	.998	-	.846	16
$Ni(NH_3)_6^{2+}$	-9.12	1.060	1.037	.820	.865	.835	.769	16
$Ni(NH_3)Enta^{2-}$	33.70	1.020	1.124	.900	.692	-	1.287	55
$Ni(NH_3)$Tetren	43.40	1.110	b)	.933	b)	-	1.385	55
$NiBdn^{2+}$	19.91	1.095	1.147	.917	.812	-	1.072	55
$Ni(H_2O)_2py_4^{2+}$	5.16	1.015	1.027	.870	.847	.862	.909	23
$Nipy_6^{2+}$	4.08	.948	.956	.886	.870	-	.922	210
Nitren SO_4	28.86	1.030	1.124	.880	.692	-	1.167	150

Notes: a) Values are of Dq_{23-} and B'_{23-}, except for Cr^{3+}, for which Dq_{23+} and B'_{23+} are given.

/cont.....

Table 2.5b Notes cont....

b) $(81\nu_2^2 - 178\nu_2\nu_3 + 81\nu_3^2) < 0$. Hence Dq_{23} and B'_{23} cannot be evaluated.

c) Accuracy of ν_1 doubtful.

d) Accuracy of ν_3 doubtful.

large disagreements between the calculated parameters. Before discussing the calculated parameters, some consideration must be given to the obviously spurious results which the large number of calculations revealed. Most of the discrepancies are of the following type:

(i) The values of Dq and B', derived from different combinations of the three bands for a complex, can differ by up to several hundred wavenumbers. Such disagreements are most marked for complexes containing mixed ligands and therefore not possessing strictly octahedral or tetrahedral symmetry.

(ii) Values of Dq and B' are very sensitive to changes in the position of band maxima. Values calculated from the ν_1 and ν_2 bands only are particularly sensitive. Thus B'_{12} may be either very small and even negative, or it may be very large and even greater than the free-ion value. Both such extremes are meaningless. It will be impossible to evaluate Dq_{23} ot Dq_{13} if the arguments of the square root terms are negative in equations 2.6, 2.9 or 2.10. This is sometimes observed for case (b) complexes.

Such discrepancies may be caused by two main types of error:

1. <u>Theoretical Inadequacy</u>:

(a) The theory of the T_1 state interaction only stricly applies to the few metal ions found in purely cubic fields.

(b) Some of the assumptions made in developing the theory may not be valid. These assumptions have been:

(i) That spin-orbit coupling may be safely ignored.

(ii) That the metal-ligand interaction is purely ionic.

(iii) That the interacting T_1 states mix equally.

2. Experimental Errors

Bands may be wrongly assigned or inaccurately measured if they are:

(i) Very broad

(ii) Split

(iii) Very weak

(iv) Obscured by infrared or charge-transfer bands

(v) Confused with unusally intense spin-forbidden peaks

Rather than discuss (for each complex) the variation of several values of Dq and B', it is convenient to develop a single parameter to express the deviation of the data from ideality. This may be done simply by equating any two expressionsfor Dq or B'; when for case (a) complexes:

$$17\,\nu_1^2 - 16\,\nu_1\nu_2 + 4\,\nu_2^2 - 9\,\nu_1\nu_3 + 4\,\nu_2\nu_3 \equiv P_2 = 0 \quad .. \quad .. \quad .. \quad 2.13$$

and for case (b) complexes:

$$17\nu_1^2 - 9\nu_1\nu_2 - 9\nu_1\nu_3 + 5\nu_2\nu_3 \equiv P_3 = 0 \quad .. \quad .. \quad .. \quad .. \quad 2.14$$

P_2 or P_3 will be zero in the absence of deviations, otherwise the magnitudes $|P_2|$ or $|P_3|$ will measure the error. The results in table 2.5 verify that agreement between the various Dq and B' values, for the same complex, is closest when $|P|$ is least. The parameter P may be of use in two ways:

(i) If 'theoretical' errors can be ignored, then a criterion of least $|P|$ may be used to select the best from several sets of data for the same complex.

(ii) If the experimental data is reliable then the magnitude of P may indicate the extent of distortion of the complex from cubic symmetry.

If P is to be of use it is important to have estimates of the sizes of various contributions.

(a) Wrong assignments may cause P to be very large, as table 2.6 shows. It is difficult to allow for this factor.

(b) Inaccuracies in actual band measurements are easier to anticipate as the following examples show:

Table 2.6

Disagreement amongst reported data.

Units are kK, except those of P (kK^2)

Complex	ν_1	ν_2	ν_3	P	Reference
$Co(H_2O)_6^{2+}$	8.35	17.85	20.00	0.01	18
$Co(H_2O)_6^{2+}$	8.20	16.00	19.40	-122.24	23
$Co(H_2O)_6^{2+}$	8.20	16.00	21.55	-143.31	23
Cr^{3+}/MgO	22.70	29.70	46.00	125.41	208
Cr^{3+}/MgO	22.70	29.70	48.30	- 2.92	208
Cr^{3+}/MgO	16.20	22.70	29.70	192.51	21
$Ni(H_2O)_6^{2+}$	8.50	14.00	26.00	-11.75	16
$Ni(H_2O)_6^{2+}$	8.50	13.50	25.30	-32.20	150
$Ni(H_2O)_6^{2+}$	8.50	13.80	18.40	34.55	24
$Ni(H_2O)_6^{2+}$	8.50	15.40	25.30	62.80	55
$Ni(H_2O)_6^{2+}$	8.50	14.30	25.30	7.80	150

(i) A typical octahedral Nickel (II) complex ($NiCl_3Me_4N$) has ν_2 = 11.2 kK and ν_3 = 21.2kK, from which ν_1 may be predicted at 6.648 kK. The fictitious Ni(II) complex which has these three spin-allowed frequencies should not be subject to error, and P_3 should be exactly zero. However, because the frequencies have not been given to more than four significant figures, P_3 is actually -0.0264 kK^2.

(ii) In practice, accuracy to four or more significant figures in all spin-allowed frequencies is far from the case. Even when the bands are narrow enough for accurate measurement, the frequencies may still be uncertain within $\sim\pm$ 0.025kK in ν_1; $\sim\pm$ 0.03 kK in ν_2 and $\sim\pm$ 0.05 in ν_3. These figures give the error in P_3 as $\sim\pm$ 9kK^2 for a typical octahedral Ni(II) complex ($NiCl_3Me_4N$).

(iii) Such narrow bands are unusual, and more typical limits of error might be ten times as great as above. The error in P_3 is then $\sim\pm$ 90kK^2.

If these values for experimental error in P seem large, it is because the dimensions of P (frequency^2) tend to emphasise errors.

(c) 'Theoretical' errors are difficult to assess. However, it is seen that a great number of complexes have values of P within the limits expected for purely experimental errors of type (b). This shows that in many cases 'theoretical' errors are not very important. P is thus often primarily a measure of experimental error.

The reason that distortions do not contribute much to P is unclear. Possibly the use of the baricentres of bands, broadened or partially split by low symmetry, eliminates the effects of distortion on the calculations.

(E) Intermediate Coupling

The interaction of ^3T and ^1E states of Ni(II), via spin-orbit coupling, has been mentioned in Chapter 1. Bostrop and Jørgensen have attempted[150] to correct ν_1 and ν_2 for the effect of this coupling but do not state their method. Table 2.7 gives their observed and corrected frequencies along with a parameter $\Delta X = X_{calc.} - X_{obs.}$. X is the energy interval between the $^3T_{1g}(F)$ and $^3T_{1g}(P)$ levels. Thus:

$$X_{obs.} = \sigma_3 - \sigma_2 \qquad)$$
$$)$$
$$X_{calc.} = (225(B')^2 - 180B'Dq + 100Dq^2)^{\frac{1}{2}} \qquad)$$

Table 2.7

Data (kK) reported, and corrected for the effects of intermediate coupling, by Bostrop and Jørgensen.[150]

	Observed bands				Corrected bands						
Complex	ν_1	ν_2	ν_3	ν_4 [a]	σ_1	σ_2	σ_3	σ_4 [a]	Dq_r	B'_r	Δ
$NiSO_4.7H_2O$	8.5	(14.1)[b]	25.7	(15.4)	8.5	14.7	25.7	14.8	.85	.993	.
$NiSO_4.6H_2O$	8.6	(15.4)	25.7	(14.2)	8.6	14.8	25.7	14.8	.86	.980	.
$(NH_4)_2Ni(SO_4)_2.6H_2O$	8.9	(15.5)	25.8	(14.4)	8.9	15.0	25.8	14.9	.89	.940	.
$Ni(H_2O)_6^{2+}$	8.5	(13.5)	25.3	(15.4)	8.5	14.3	25.3	14.7	.85	.940	.
$Nipy_4(SCN)_2$	10.1	16.7	26.7	(12.8)	10.2	16.7	26.7	12.8	1.02	.853	.
$Ni(NO_3)_2py_4$	10.15	16.5	27.0	13.5	10.2	16.5	27.0	13.5	1.02	.860	.
Ni tren SO_4	10.0	17.2	26.9	(12.9)	10.3	17.2	26.9	12.7	1.03	.880	1.
Ni tren $SO_4.7H_2O$	10.6	17.9	27.5	(12.9)	11.0	17.9	27.5	12.7	1.10	.827	.
Ni tren $(SCN)_2$	10.9	17.9	27.8	(12.8)	11.3	17.9	27.8	12.6	1.13	.787	.
Ni tren $(H_2O)_2^{2+}$	10.5	17.8	27.8	(12.8)	10.9	17.8	27.8	12.6	1.09	.860	.
$Ni(NH_3)_6Br_2$	10.8	17.7	28.2	-	10.8	17.7	28.2	-	1.08	.900	.
$Ni(NH_3)_6^{2+}$	10.75	17.5	28.2	13.15	10.8	17.5	28.2	13.1	1.08	.893	.
Ni en_3SO_4	11.3	18.5	29.0	(12.8)	11.7	18.5	29.0	12.6	1.17	.827	.

Notes:

a) ν_4 and σ_4 are the observed, and corrected, frequencies of the $^3A_{2g} \rightarrow {}^1E(D)$ transition.

b) Bracketed frequencies are uncertain.

σ_1, σ_2, and σ_3 are the frequencies ν_1, ν_2 and ν_3 after correction for intermediate coupling. These authors give values of σ_1 = 10Dq and of $\sigma_3 = \nu_3$ but not of σ_2, which has been inferred from $X_{obs.}$ and σ_3.

Table 2.8 gives Dq, B' and P_3 calculated from the observed and from corrected frequencies. From the P_3 values it is evident that the correction has usually improved agreement of the data with the theory for the T_1 state interaction.

Both $P_{3\sigma}$ (calculated from the corrected frequencies) and ΔX are measures of the departure from the theory for the T_1 state interaction. It is thus interesting to find a rough proportionality between $P_{3\sigma}$ and ΔX, and this is shown in Table 2.9. $(NH_4)_2NiSO_4.6H_2O$ does not fit this proportionality, but $P_{3\sigma}/\Delta X$ has a mean of 27.65kK (with standard deviation 1.49kK) for the rest of the complexes.

Bostrop and Jørgensen suggested that an experimental error of $\sim\pm$ 0.3kK was likely in $X_{calc.}$ and thus in ΔX. With the proportionality constant above, this figure corresponds to an experimental error of $\sim\pm$ 8.3kK in P_3. This is close to the error of $\sim\pm$ 9kK in P_3 noted earlier for narrow bands.

As the method used by Bostrop and Jørgensen for correcting frequencies was unclear, several attempts were made to carry out the

Table 2.8

Ligand field, effective Racah, and error parameters, calculated from the data of table 2.7. All units are kK except $P_3(kK^2)$.

Complex	Data calculated from ν_1, ν_2 and ν_3					Data calculated from σ_1, σ_2 and σ				
	P_3	Dq_{23-}	B'_{23-}	B'_{12}	B'_{123}	P_3	Dq_{23-}	B'_{23-}	B'_{12}	B'_{123}
$NiSO_4.7H_2O$	-4.60	.843	.966	.902	.953	26.60	.889	.915	1.584	.993
$NiSO_4.6H_2O$	55.08	.948	.844	10.200	1.020	24.42	.897	.906	1.459	.980
$(NH_4)_2Ni(SO_4)_2.6H_2O$	37.94	.955	.842	1.946	.973	13.49	.912	.896	1.116	.940
$Ni(H_2O)_6^{2+}$	-32.20	.803	.981	.648	.887	7.80	.862	.916	1.044	.940
$Nipy_4(SCN)_2$	18.56	1.057	.778	1.040	.873	14.01	1.057	.778	.966	.853
$Ni(NO_3)_2py_4$	5.16	1.027	.847	.909	.870	2.88	1.207	.847	.881	.860
Ni tren SO_4	44.40	1.124	.692	1.680	.940	28.86	1.124	.692	1.167	.880
Ni tren $SO_4.7H_2O$	40.21	a)	-	1.361	.907	23.65	a)	-	.993	.827
Ni tren $(SCN)_2$	24.70	a)	-	1.058	.867	11.14	a)	-	.847	.787
Ni tren $(H_2O)_2^{2+}$	39.25	1.167	.705	1.416	.940	20.61	1.167	.705	1.011	.860
$Ni(NH_3)_6Br_2$	17.10	1.125	.811	1.031	.900	17.10	1.125	.811	1.031	.900

/cont.....

Table 2.8 cont....

Complex	Data calculated from ν_1, ν_2 and ν_3					Data calculated from σ_1, σ_2 and σ_3				
	P_3	Dq_{23}	B'_{23}	B'_{12}	B'_{123}	P_3	Dq_{23}	B'_{23}	B'_{12}	B'_{123}
$Ni(NH_3)_6^{2+}$	10.59	1.100	.846	.973	.897	8.34	1.100	.846	.944	.887
$Ni\ en_3SO_4$	22.48	1.203	.761	1.070	.907	7.88	1.203	.761	.868	.827

Notes:

a) $(81\nu_2^2 - 178\nu_2\nu_3 + 81\nu_3^2) < 0$. Hence Dq_{23} and B'_{23} cannot be evaluated.

Table 2.9

Error parameters for the Ni(II) complexes of tables 2.7 and 2.8.

Complex	$P_{3\sigma}(kK^2)$	$\Delta X(kK)$	$P_{3\sigma}/\Delta X$ (kK)
$NiSO_4.7H_2O$	26.60	.9	29.6
$NiSO_4.6H_2O$	24.42	.8	30.6
$(NH_4)_2Ni(SO_4)_2.6H_2O$	13.49	.8	16.9
$Ni(H_2O)_6^{2+}$	7.80	.3	26.0
$Ni\ py_4(SCN)_2$	14.01	.5	28.0
$Ni(NO_3)_2py_4$	2.88	.1	28.8
Ni tren SO_4	28.86	1.1	26.2
Ni tren $SO_4.7H_2O$	23.65	.9	26.3
Ni tren $(SCN)_2$	11.14	.4	27.9
Ni tren $(H_2O)_2^{2+}$	20.61	.8	25.8
$Ni(NH_3)_6Br_2$	17.10	.6	28.5
$Ni(NH_3)_6^{2+}$	8.34	.3	27.8
$Ni\ en_3SO_4$	7.88	.3	26.3

correction. These are worked out in Appendix A4. It was found that the best expressions for minimising $|P_3|$ were often:

$$\left.\begin{aligned}\sigma_1 &= (1/2)\ \left\{(\nu_4+\nu_1)-((\nu_4-\nu_1)^2-3.81)^{\frac{1}{2}}\right\}\\ \sigma_2 &= (1/2)\ \left\{(\nu_4+\nu_2)-((\nu_2-\nu_4)^2-3.81)^{\frac{1}{2}}\right\}\end{aligned}\right\}\ \ldots\ \ldots \qquad 2.15$$

The correction can only be made on data which include the frequency (ν_4) of the spin-forbidden $^3A_{2g} \rightarrow {}^1E(D)$ transition.

(F) Survey of Results of Calculations with Reported Data

Appendix A3 contains all the Dq and B' values calculated in this work. A survey of these results was undertaken according to the following procedure:

(i) The criterion of least $|P|$ was used to select the best of the available data for each complex.

(ii) The calculated Dq and B' values, for complexes (MA_xB_{n-x}) with mixed ligands, were then used in the rules of average environment, to derive Dq and β for MA_n (n=4 or 6) species .

(iii) The spectrochemical and nephelauxetic series were then written for complexes of the same stereo-chemistry with:

(a) Different metal ions but the same ligands.

(b) Different ligands with the same metal ion.

(iv) The series for metal ions were examined for a correlation with oxidation potential, and the ligand series for a correlation with basicity.

(v) Attempts were then made to understand deviations from the ligand basicity series in terms of π-bonding, ligand polarisability, steric hindrance and bridging character.

The results of this survey broadly substantiate other reported spectrochemical [23,26] and nephelauxetic series [26,149]. Some original results have been obtained and those which appear to be the most reliable are collected in table 2.10.

The results for simple complexes of the type MA_n (n=4 or 6) are much easier to interpret than those for complexes with mixed ligands. This is expected, because with mixed ligands the following factors are introduced:

(i) Distortion due to low symmetry causes bands to split and thus inhibits accurate measurements. Two-electron transitions and spin-forbidden bands are often quite strong and can confuse the spectrum.

Table 2.10

Some new data for ligand field, and effective Racah parameters (kK).

Metal Ion	Environment	Reference	Dq	B'	β
V^{3+}	$4Cl^-$	214	.596	.434	.510
Co^{2+}	$6H_2O$	18	.950	.853	.879
Co^{2+}	$6NH_3$	23	.950	.840	.866
Co^{2+}	6py	210	.962	.831	.856
Co^{2+}	$6F^-$	206	.805	.863	.888
Co^{2+}	$6Cl^-$	206	.670	.717	.739
Co^{2+}	$6Br^-$	206	.580	.653	.672
Co^{2+}	4dpa a)	213	.314	.636	.655
Ni^{2+}	$6NCS^-$ a)	150	.973	.732	.703
Ni^{2+}	6 py a)	23	1.100	.801	.769
Ni^{2+}	Bdn	55	1.095	.917	.881
Ni^{2+}	3/2 tren a)	150	1.210	.807	.775
Ni^{2+}	6/5 tetren a)	55	1.120	.956	.919
Ni^{2+}	6 IQuin a)	153	1.053	.855	.821
Ni^{2+}	$4Cl^-$	199	.402	.789	.758
Ni^{2+}	$4Br^-$	23	.379	.712	.684
Ni^{2+}	$4I^-$ a)	199	.360	.656	.630
Ni^{2+}	$4O^{2-}$	24	.455	.870	.835
Ni^{2+}	$4S^{2-}$	23	.441	.623	.598
Ni^{2+}	$4\phi_3PO$ a)	199	.408	1.008	.966
Ni^{2+}	$4\phi_3ASO$ a)	199	.451	.942	.905

Notes:

a) Calculated using rules of average environment.

(ii) The calculations depend on the validity of the rules of average environment. The values obtained indicate good agreement with this rule for Dq, but only fair agreement for B'.

(iii) In order to use these rules, to derive parameters for unmixed species MB_n, from MA_xB_{n-x} results, it is necessary to know the values for MA_n. These may be unreliable. An example is the ion $NiCl_6^{4-}$, which is unknown except for the chromophore in $NiCl_2$, in which bridging chloride ions are involved.

(iv) Steric hindrance is often more acute in structures with bridging ligands. This can confuse the calculation of Dq and B', which requires using the rules of average environment. For example, data for the octahedral $CoI_2(pyz)_2$ polymer can be used in calculations for the $Co(pyz)_6^{2+}$ chromophore, only if values for CoI_6^{4-} are known. Since this CoI_6^{4-} is unknown, its parameters must first be calculated from other complexes containing Co-I bonds. These other complexes may not involve as much steric hindrance as in $CoI_2(pyz)_2$; thus the parameters used for CoI_4^{4-} may not be appropriate.

(a) Results for Simple MA_n Complexes

The most satisfactory results were obtained with the spectrochemical

and nephelauxetic series for metal ions. These were for Dq:

$$Co^{2+} \backsim Ni^{2+} < V^{2+} < Cr^{3+} < V^{3+} < Mn^{4+}$$

and for β :

$$V^{2+} \backsim Ni^{2+} \backsim Co^{2+} > Cr^{3+} > V^{3+} > Mn^{4+}$$

The positions of V^{3+} do not appear to have been reported before. As expected, the spectrochemical series is one of increasing oxidation-number and ionic radius; while the nephelauxetic series is one of increasing oxidation-number and oxidation-potential.

Three metal ions (V^{3+}, Co^{2+} and Ni^{2+}) have been studied in both tetrahedral and octahedral environments. The Dq and β series were found to be identical in the two stereochemistries. In these cases the ratio Dq_t/Dq_o was $\backsim$0.42-0.52, being quite near the expected ratio of 0.44. The B' values were more informative, in that for the same metal and ligand it was found that $B'_t \backsim B'_o$. This also does not appear to have been previously reported.

The spectrochemical and nephelauxetic series for the ligands generally agree with those previously reported. Thus for Dq:

$$I^- < Br^- < Cl^- < H_2O < S^{2-} < O^{2-} < \underline{N}CS^- < py$$

and for β :

$$H_2O > py > en > O^{2-} > Cl^- > \underline{N}CS^- \backsim Br^- > I^+ > S^{2-}.$$

The positions of O^{2-} and S^{2-} do not appear to have been reported before.

(b) Results for Complexes MA_xB_{n-x} with Mixed Ligands

Few reliable results were obtained from the survey of complexes with mixed ligands. The results, for octahedral complexes, calculated from Nelson and Shepherd's data[153] on the picoline complexes of Ni(II) were quite systematic:

$$Br^- < N_3^- < Cl^- < NCO^- < NCS^- < NCSe^- < 3Mepy < 4Mepy = py < IQuin$$

for Dq, while for β :

$$IQuin \backsim py \backsim 3Mepy \backsim 4Mepy > NSSe^- > NCS^- > NCO^- > N_3^- > Cl^- > Br^-$$

The positions of IQuin, 3Mepy, 4Mepy, $NCSe^-$, NCO^- and N_3^- are reported here for the first time.

In the tetrahedral complexes steric effects are often less important, and bridging ligands less common, than in octahedral species. In agreement with this, the results obtained were more consistent.

Thus the series:

$$Cl^- < \Phi_3PO < S^{2-} < \Phi_3AsO < O^{2-}$$

for Dq, and for β :

$$py > \Phi_3PO > \Phi_3AsO > O^{2-}$$

were deduced from the data reported [199] by Goodgame, Goodgame and Cotton for some tetrahedral Ni(II) complexes.

(G) Conclusions

In spite of these successful interpretations, the main conclusion, from the survey undertaken, must be that experimental error is usually to high for useful results to be obtained from comparisons of Dq or B', except for series involving similar ligands. Such errors are particularly large for octahedral complexes with mixed ligands. Experimental errors have obscured any evidence of π -bonding, steric hindrance and bridging ligands, in the values of Dq and B'. It was not generally possible to consider the relative effects of basicity, and ligand polarisability, on either the spectrochemical, or the nephelauxetic series.

CHAPTER III

A SURVEY OF THE COMPLEXES OF PYRIDINES

&

RELATED MOLECULES

In order to appreciate the relevance of the present work it is useful to have some knowledge of the properties of similar complexes, and also of the ligand molecules themselves.

(A) Properties of the Organic Ligands

Much has been written of the occurrence,[215-217] preparation[218-225] and properties[184, 185, 215, 216, 220, 226-233] of these heteroaromatic tertiary amines. Figure 3.0 gives the formulae of the molecules and the numbering system used for the ring positions. Attention will be confined here to the two most relevant properties of the compounds which appear to be their basicity and π-acceptor character.

(a) The Basicities of these amines, as measured by their pKa values,[185] are given in table 3.2. The alkyl-substituted pyridines are seen[184] to be stronger bases than the parent molecule, while the reverse is true of the halo and cyano- pyridines. It is generally assumed that the stability constants[234] for the formation of metal-ligand bonds will reflect, at least partially, the equilibrium constants (1/Ka) for protonation of the ligands. Therefore all these bases should form stronger σ- metal-ligand bonds than the anions (Cl^-, Br^- and I^- anions have pKa values [234] of -1.51, -4.65 and -9.5 respectively) present in most of their complexes.

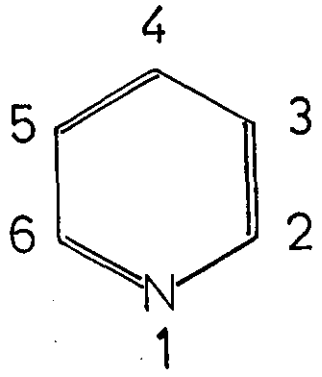

a

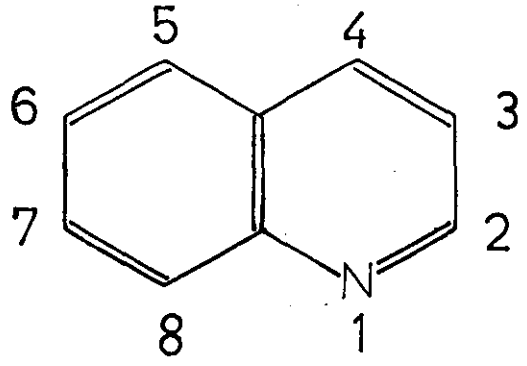

b

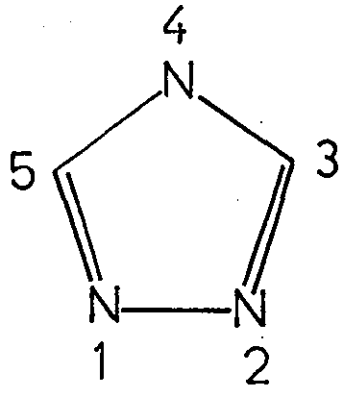

c

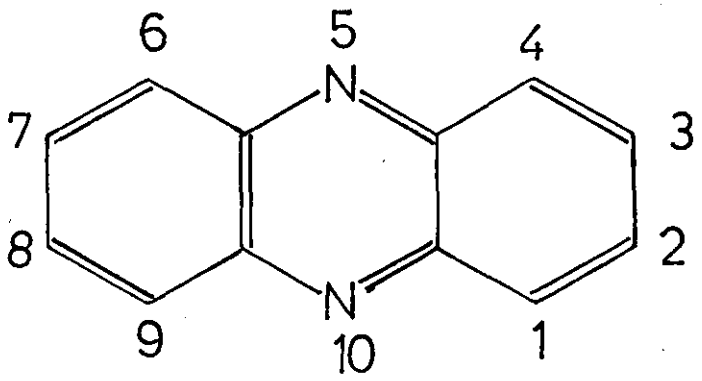

d

Figure 3.0

Table 3.2

Base strength (pKa) of the halopyridines, and related molecules, at room temperature.

Compound	pKa	Compound	pKa
2,4,6-TMepy	7.48	I Quin	5.42
2,6-DMepy	6.77	py	5.32
2,4-DMepy	6.72	2,3-DMeQuin	4.94
2,3-DMepy	6.60	Quin	4.89
3,4-DMepy	6.52	4-Clpy	3.84
2,5-DMepy	6.47	4-Brpy	3.78
4Me-py	6.19	3-Brpy	2.91
2Me-B	6.19	3-Clpy	2.84
3,5-DMepy	6.14	T	2.30
4-Etpy	6.02	4-CNpy	1.90
4-i-Prpy	6.02	3-CNpy	1.39
2-Etpy	5.99	P	1.19
2-Mepy	5.97	2-Brpy	0.71
2-MeQuin	5.83	2-Clpy	0.49
3-Etpy	5.70	2-CNpy	-0.26
3-Mepy	5.68		
3-MeIQuin	5.64		
A	5.58		
B	5.53		

(b) The π-acceptor capacity of the aromatic molecules will partly determine the strength of their π-bonds with metal ions. In principle, at least three methods of estimating π-acceptor character could be suggested:

(i) It might be correlated with stability of ligand π^* orbitals by measuring the $\pi \rightarrow \pi^*$ electronic band energies. These bands are at[220] lower frequency for pyridine that for benzene and this may indicate that pyridine is the better π-acceptor. However, the effect of substituents on the spectrum is more random, and this may be due to a dependence also on the π-orbital ground-state energies.

(ii) Resistance to electrophilic attack, and susceptibility to nucleophilic attack indicate[218, 231] that all these amines, with the exception of 1:2:4 -Triazole, are more π-electron-deficient that is benzene. Triazole is slightly more π-excessive than benzene, due to the presence of an acidic (-NH-) group. Generally it is difficult to measure π-acceptor capacity quantitatively on this basis.

(iii) The use of reduction potentials (E_o) or polarographic half-wave potentials of these molecules offers one method of measuring susceptibility to nucleophilic attack.

Unfortunately, little data of this kind has been tabulated. However, it is known that[215,230] the amines are more easily reduced than their parent arenes, and that additional aza-atoms enhance this effect. Further,[223] alkyl-substituents appear to lower E_o, thus decreasing the π-acceptor character. Halo- and cyano-substituents have the opposite effect.

(c) It is convenient to mention here a special property of 4- substituted halopyridines. These are unstable[220], giving (fig.3.8) N-(4'pyridyl)-4- -halopyridinium halides, which in the presence of moisture yield N-(4'-pyridyl)-4-pyridone. 4Cl-py was therefore prepared immediately before use, by shaking its hydrochloride with a 5N solution of sodium hydroxide. Portions of the lower layer were run off as required.

(B) Complexes with known crystal structures

(a) $CuCl_2py_2$ has been known since Lang, in 1888, reported[235] its precipitation on mixing pyridine and $CuCl_2.2H_2O$ in ethanol. An early crystal structure analysis indicated[236] that the compound was monomeric, with a square-coplanar stereochemistry around the copper atoms. However, in 1957, Dunitz redetermined[186] the

structure, finding the very tetragonally-distorted-pseudo-octahedral stereochemistry shown in Figure 3.1. The planar units are present, but catenated by very long (3.05Å) Cu-Cl bonds. This polymeric structure is perhaps best considered as based on a chain of Cu atoms bridged by pairs of Cl atoms. These pairs of chlorine bridges form rectangles containing both normal (2.28Å) and long Cu-Cl bonds. Pyridine molecules are co-ordinated (Cu-N = 2.02Å) above and below this chain, their ring-planes being stacked[103] almost perpendicularly to the chain axis. The bond angles about the Cu atoms vary little (88°-92°) from 90°.

(b) $CuBr_2py_2$ has a very similar structure[237], differing[238] only in that the Cu-Cu distance (4.04Å in the bromide; 3.87Å in the chloride) is determined by the Van der Waals radius of bromine, rather than the pyridine aromatic thickness.

The Bond lengths are given in Table 3.1.

(c) $Cu(NCS)_2py_2$ contains[239] bidentate thiocyanate groups acting as bridges and this places the Cu atoms further apart (5.65Å) than in the halide analogues. The only other differences from the halide structures are the packing of the chains (which are similarly orientated in the thiocyanate, but in two different orientations

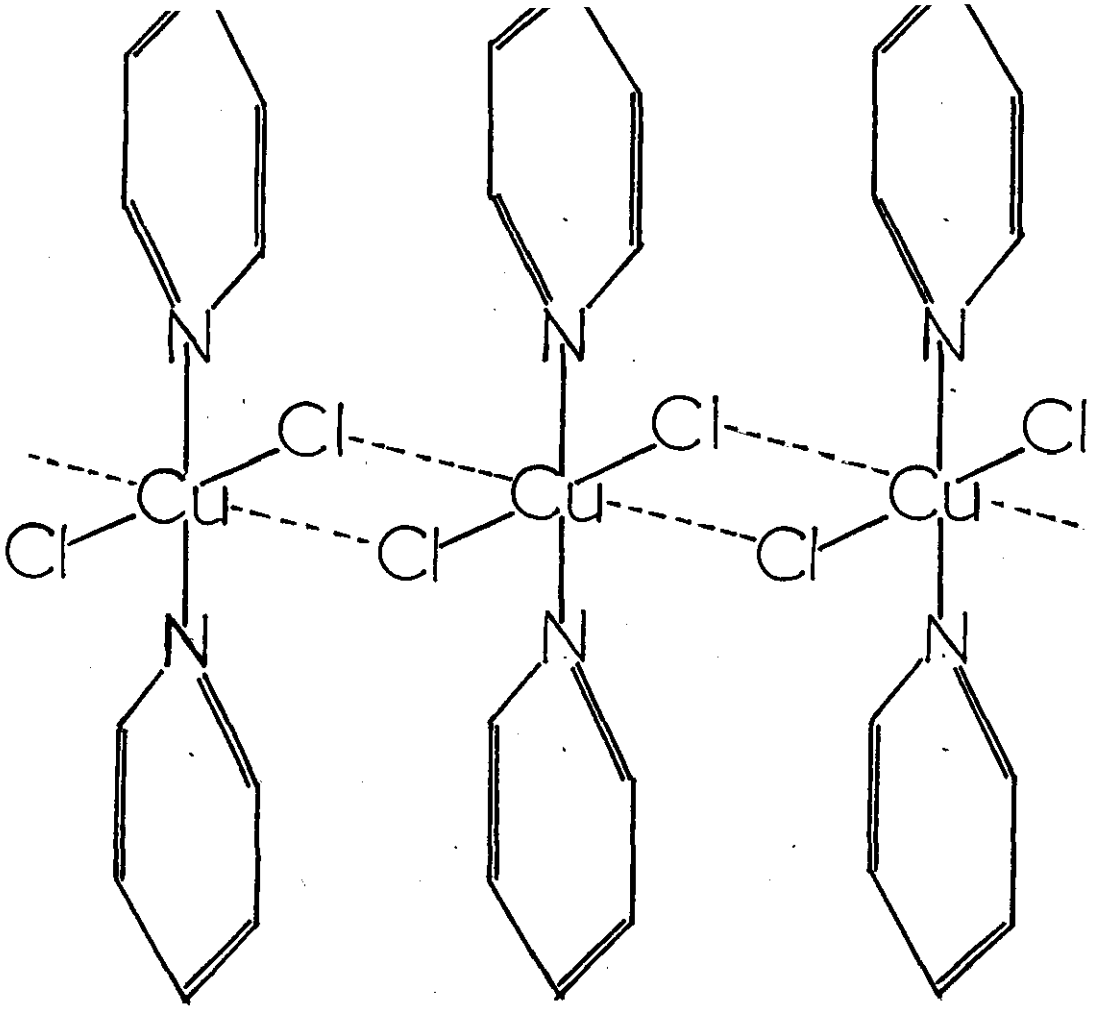

Figure 3.1

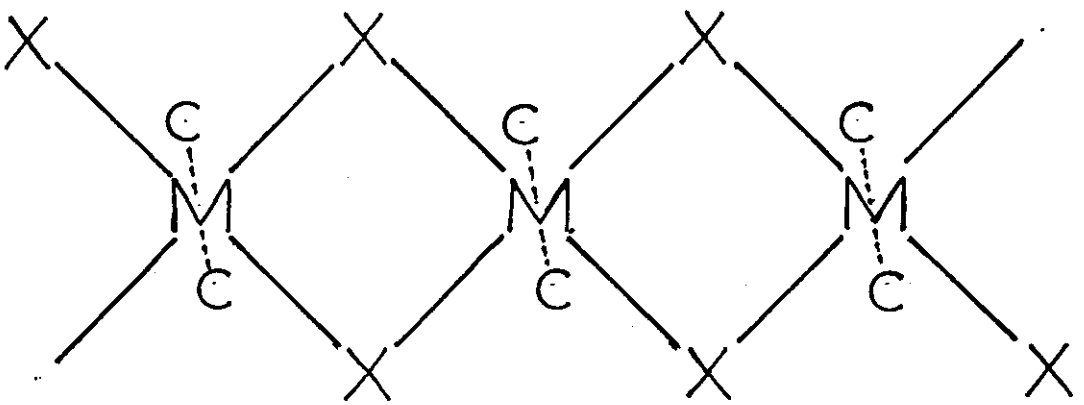

Figure 3.2

Table 3.1

Bond lengths in some pyridine complexes.

Complex	M-X(Å)	M-N(Å)
$NiCl_2py_4$	2.39	2.00
$NiBr_2py_4$	2.58	2.00
$CoCl_2py_4$	2.32	1.99
$CoCl_2py_2$	2.49	2.14
$CuCl_2py_2$	2.28, 3.05	2.02
$CuBr_2py_2$	2.46, 3.19	1.99

in the halides), and the greater twist of the pyridine rings in the thiocyanate.

(d) The violet α- isomer of $CoCl_2py_2$ was prepared[240] by Reitzenstein in 1894, and a partial crystal structure determination carried out[241] in 1937. Magnetic and other measurements have been given[242-244] but the full structure was not reported[185] until 1957. The polymeric chains are shown in plan-view in Figure 3.2. The equal Co-Cl bond lengths (2.49Å) cause a simplification of what is otherwise the same structure as $CuCl_2py_2$. The shorter M-M distance (3.66Å) than that of the copper complex, gives rise to a more efficient packing of the pyridine rings, which can twist only a little away from planes perpendicular to the chain axis. This is confirmed[185] by the smaller molecular volume of the cobalt complex, also by a calculation which reveals that the maximum twist in the cobalt complex is 10° but that the actual twist in the copper complex is about 17°.

Figure 3.7 shows how the steric requirements of these halide polymers limit the possible extent of M-N π-bonding. A p- orbital on the nitrogen atom does not have the correct symmetry to overlap with the d_{yz}, $d_{x^2-y^2}$ or d_{z^2} orbitals. Because the p orbital is directed nearly along the chain axis, it is misorientated relative

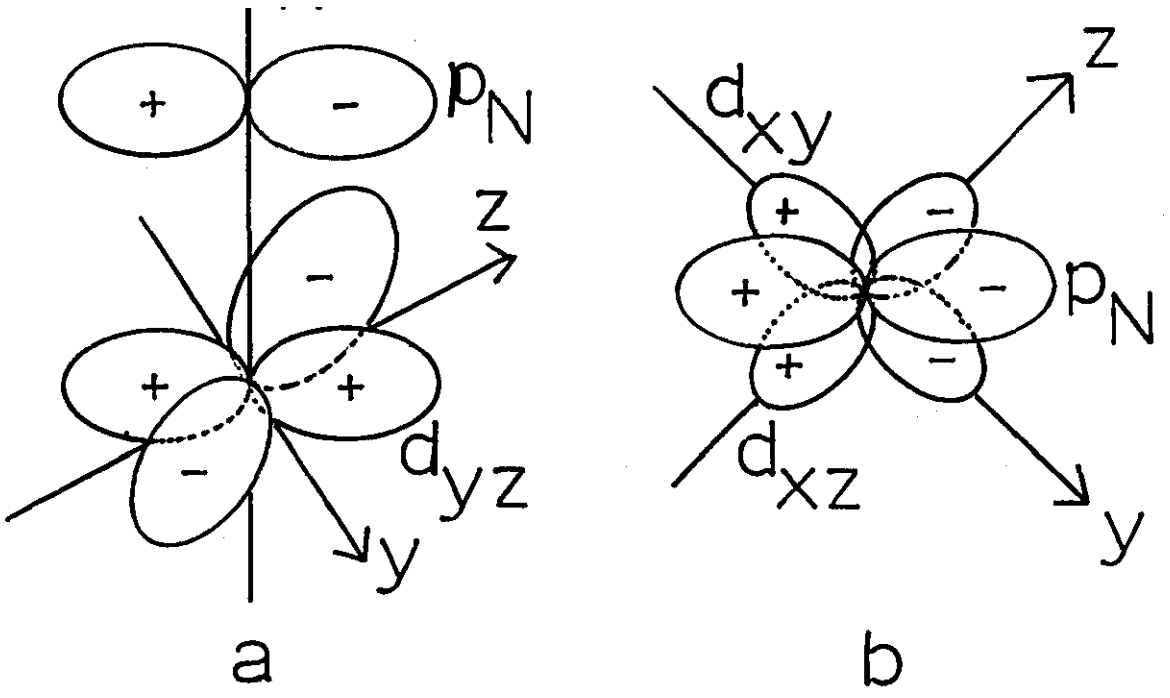

a b

Figure 3.7

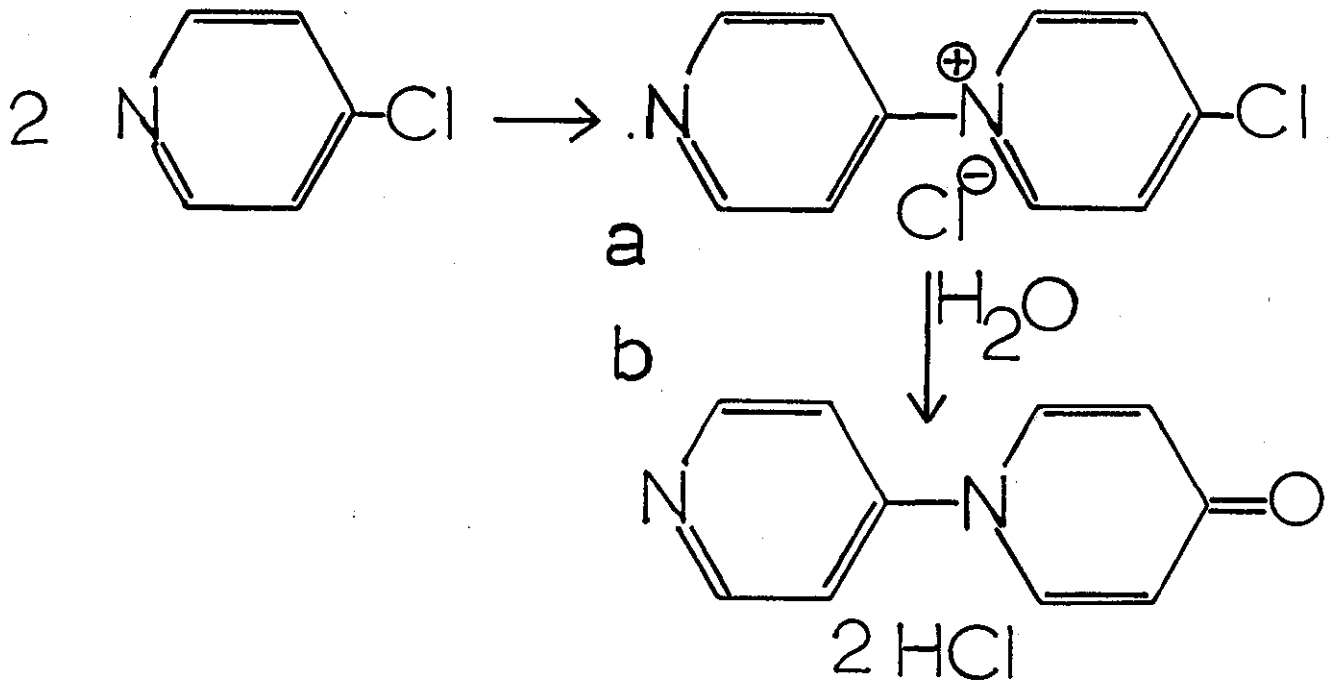

Figure 3.8

to the metal d_{xz} and $_{xy}$ orbitals (where the z axis is taken along the longer M-Cl bonds). This may explain why it is desirable for the pyridine rings to twist, if possible, to a more favourable orientation for π-bonding.

(e) $Co(NCS)_2py_2$ has [239] a polymeric structure like its copper analogue.

(f) $CuCl_2$ T was first described [245] by di Paolini and Goria, and its unit-cell dimensions were published [246] in 1936. The full structure[247,248] was not reported until 1960. This is a variant (fig.3.5) of the $CuCl_2py_2$ structure; the copper atoms being additionally bridged by bidentate triazole(Cu-N=1.98Å). The Cu-Cu distance is again quite small (3.46Å) and accommodating the stereochemistry of these organic ligand bridges, while maintaining near 90°(83.8°-89.6°) bond angles, necessitates the buckling of the $CuCl_2$ chains in a zig-zag manner. The tetragonal distortion, usual in copper (II) compounds, is evident, but is less marked (Cu-Cl=2.34Å, 2.78Å) than is $CuCl_2py_2$.

(g) The compounds of general formula MX_2py_4 (M=Co; x^-=Cl^-,NCS^-.M=Ni; x^-=Cl^-,Br^-, NCS^-) all have monomeric octahedral structures [249-252]. Bond lengths in some of these and other complexes are given in Table 3.1.

(h) $CuCl_2(2Mepy)_2$ has been shown [253] to contain dimeric units, in which each copper atom has a square-pyramidal stereochemistry.

(i) Several structure determinations have been reported on compounds containing these ligands, but these are not discussed here since they are not simply related to the complexes prepared in this work. Thus, for example, the square-pyramidal structures of $Cu(OAc)_2py$ and $Cu(acac)_2$ Quin have been determined.[254, 255]

(j) Gill, et al, have given [187] the conclusions of a study of the bis-pyridine complexes by X-ray powder-photography. $NiCl_2py_2$ gives a similar pattern to α-$CoCl_2py_2$ and it is proposed that they are isostructural. The blue β isomer of $CoCl_2py_2$ and also $CoBr_2py_2$ and CoI_2py_2 all have powder diffraction patterns similar to the known [256] tetrahedral monomer $ZnCl_2py_2$. It is proposed[187] that these complexes too are isostructural (Figure 3.4).

Finally, $CoBr_2py_4$ has been shown[250] to be isomorphous with $NiBr_2py_4$. A recent paper, however, illustrates[257] the danger of drawing firm conclusions from the observation of isomorphism.

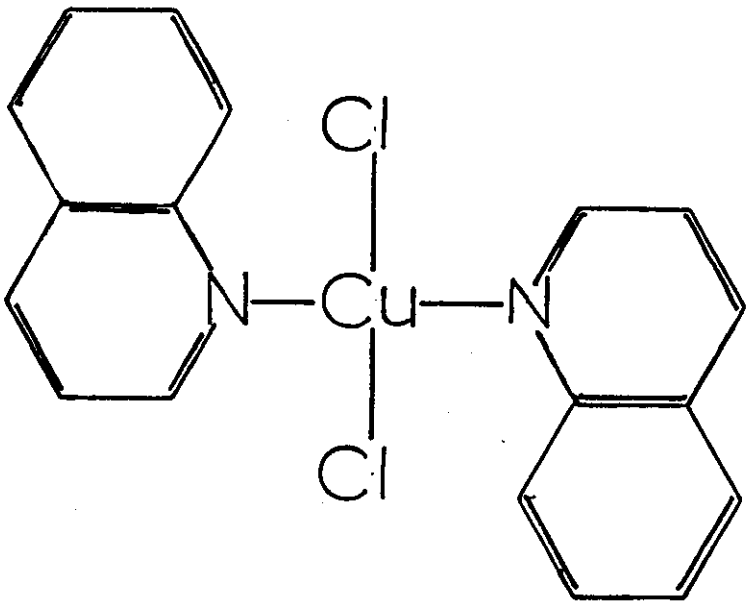

Figure 3.3

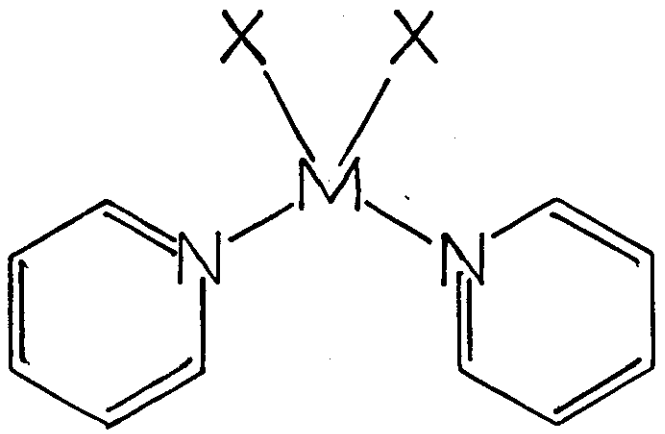

Figure 3.4

(C) Preliminary Work on Similar Systems

(a) Hexakis-amine complexes, such as $(Mpy_6)^{2+}$ species, have been reported in solution[23,258]. Their existence in the solid state is in greater doubt and, apart from reports of $CuBr_2py_6$[259-261] and $CoBr_2py_6$[262], appears to be confined to nitrato-complexes. Though several of these have been reported[261,263-266], evidence shows[266,267] that they must be formulated as $(Mpy_4(NO_3)_2).2py$ or $(Mpy_3(NO_3)_2).3py$. The existence of $(Mpy_6)^{2+}$ species in the solid MBr_2py_6 complexes therefore is placed in doubt.

(b) Heptakis- and Pentakis-Pyridine complexes were reported by Mitra and Sinha[263], on the basis of vapour pressure measurements, but could not be prepared by Biagetti et al.[267]

(c) Tetrakis-amine complexes are common for cobalt and nickel, but for copper appear to be confined to the solids of general formula CuX_2L_4 ($X^-=Cl^-$; L=2-NH_2py, 4Mepy. $X^-=Br^-$; L=4Mepy. $X^-=NO^-_3$; L=py. $X^-=ClO_4^-$, BF_4^-; L=py, 4Mepy)[90,260,261,267-272], and $CuCl_2py_4$[273] in solution.

(d) A small number of tris-amine complexes has been reported: MX_2L_3 ($X=NO_3^-$; L=py; M=Cu, Ni,Co)[258,266,270] and $Ni(SCN)_2L_3.\frac{1}{2}H_2O$ (L=2:3-DMepy, 2:5-DMepy)[200]; and a somewhat larger number of

mono-amine complexes: MX_2L(L=Quin; M=Ni, Co, Cu; X=Cl^-, Br^-. L=py, 4Mepy; M=Ni, Co, Cu; X=Cl^-. L=2Mepy, 3Mepy; M=Ni,Cu; X^-=Cl^-. L=py, 3Mepy, 4Mepy; M=Ni; X^-=Br^-. L=2:6-Mepy, 2:4:6-TMepy; M=Co; X^-=Cl^-. L=2:6-DMepy, 4Mepy, M=Co; X^-=Br^-. L=2Mepy; M=Cu; X^-=NO_3^-) 78,79,183,197,268,274-276,389.

(e) The bis-amine complexes, with which this thesis is mainly concerned, have more variety in their structures than those described above, which are all thought to involve pseudo-octahedral stereochemistries. The possible structures for the complexes of each metal are discussed below.

(i) Copper (II) complexes generally have tetragonally-distorted-octahedral, or square-coplanar structures; though many square-pyramidal[277-289], and some trigonal-bipyramidal[257,290-294] and tetrahedral[295-299] species have been reported. The octahedral complexes, which have already been discussed, show the usual elongated-tetragonal-distortion, but five examples of the compressed alternative are known[300-302], while other complexes have been found to exhibit rhombic distortions[303-304]. This does not exhaust the feasible pseudo-octahedral stereochemistries, and figure 3.6 shows a possible zig-zag polymer based on a cis-distortion. As yet there is no definite evidence for such a

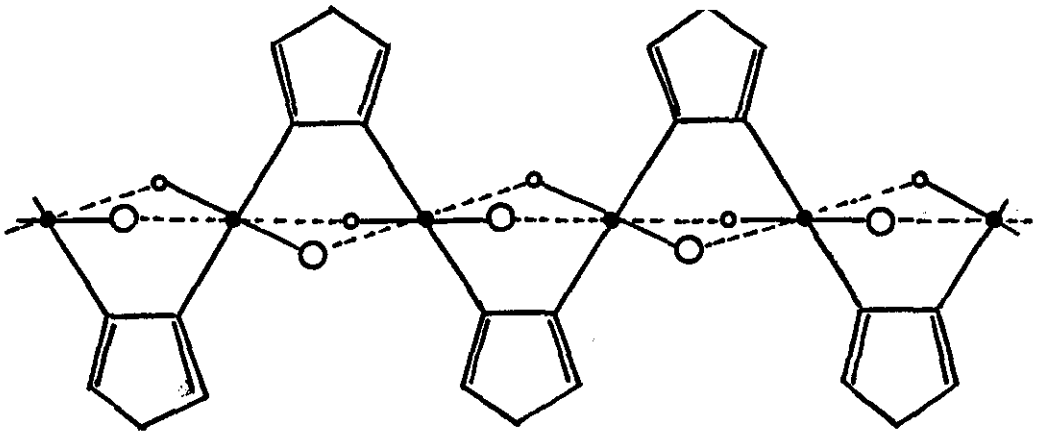

• = Cu ○ = Cl

Figure 3.5

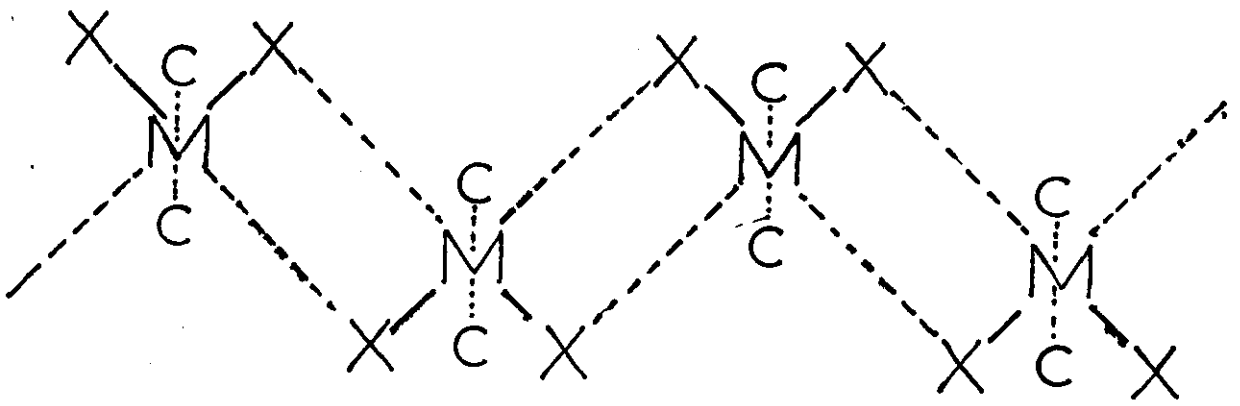

Figure 3.6

distortion[305], though the cations $Cu(en)_3^{2+}$, $Cu(bipy)_3^{2+}$ and $Cu(phenan)_3^{2+}$ may be executing a dynamic version of this deformation. A dynamic distortion[306,307] has been postulated[308] to account for the apparently regular octahedral structure[309] of $K_2PbCu(NO_2)_6$, and may similarly apply to the regular[310] $Cu(en)_3SO_4$ complex. Neither of these complexes is permitted to be regular, according to the Jahn-Teller theorem.

Besides the tetragonally-distorted-octahedral structure, its limiting case - the square-coplanar stereochemistry, is well established, some examples being: $Cu(acac)_2$[311], Cupc[312], $Cu(N\text{-}MeSalim)_2$[313], Cu Dithizonate[3] and $Cu(biuret)_2.2H_2O$[315]. No bis-amine copper (II) complexes with planar structures have been fully characterised by X-ray diffraction studies, but $CuCl_2Quin_2$ is thought[89] to have this structure, (figure 3.3) due to steric hindrance of co-ordination by the hydrogen atoms on the 8- carbon atoms.

(ii) Cobalt (II) is usually found in an octahedral or a tetrahedral stereochemistry. α-$CoCl_2py_2$[186] and $CoCl_2(p\text{-}tol)_2$[316] serve to illustrate these two structures. Some 5- co-ordinate complexes are known[317-322], and square-planar structures have been postulated[323].

The difference in structures, between the octahedral

α-$CoCl_2py_2$ complex and the tetrahedral $CoBr_2py_2$ and $CoCl_2(4Mepy)_2$[175] species, was explained in Chapter I in terms of the electroneutrality principle.

The above variations are due on the one hand to the greater polarisability of Br^- compared to Cl^-; and on the other hand to the greater bascicity of 4Mepy (See table 3.2) compared to pyridine.

(iii) The nickel (II) complexes $NiCl_2py_4$[249], $(\Phi_3MeAs)_2NiCl_4$[324] and Ni(salim)[3] illustrate the usual octahedral, tetrahedral and square-planar structures of this metal. Some five-co-ordinate structures are also known[317,318,319,320,326].

This difference, between the adoption of a tetrahedral structure by $CoBr_2py_2$ and an octahedral structure by $NiBr_2py_2$, can be explained as in Chapter 1, by the higher tetrahedral crystal-field-stabilisation energy of cobalt(II).

(D) Survey of Reported Work on Tetrakis- and bis- complexes

The discussion above, in section C, has dealt only with a number of representative complexes, in the bis- and tetrakis-cases. Most of the published work on these complexes will now be surveyed in tabular form. Tables 3.3, 3.4 and 3.5 describe the proposed stereochemistries respectively of copper (II), cobalt (II) and

Table 3.3

Stereochemistries proposed for some copper(II) complexes.

Complex	Reference
a) Octahedral species:	
CuX_2py_4 ($X^- = BF^-_4$, NO^-_3, NCS^-, $\frac{1}{2}(S_2O_8)^{2-}$, $\frac{1}{2}(SO_4)^{2-}$, ϕCOO^-)	90, 267, 271, 340-346
$CuCl_2L_4$ (L = 2Mepy, 3Mepy, 4Mepy, 2:6 DMepy, $2NH_2py$)	260, 268, 269, 347
$Cu(NO_3)_2py_4.2H_2O$	348
$CuBr_2(4Mepy)_4$	269
CuX_2I_4 ($X^- = Cl^-$, NO^-_3)	349, 350
CuX_2B_4 ($X^- = Cl^-$, Br^-, NCS^-, ClO^-_4, $\frac{1}{2}(SO_4)^{2-}$, NO^-_3)	351
$CuSO_4B_4 . 2\frac{1}{2} H_2O$	347
CuX_2py_2 ($X^- = Cl^-$, Br^-, NCS^-, NO^-_3, CN^-, NCO^-)	47, 59, 80, 188, 202, 267, 270, 340, 343, 352-357, 389
CuX_2L_2 ($X^- = Cl^-$, Br^-; L = 3Mepy, 4Mepy)	80, 213, 260, 269, 270, 358, 389
CuX_2Quin_2 ($X^- = NO^-_3$ NCS^-)	359, 360
$Cu(NO_3)_2L_2$ (L = 2Mepy, IQuin)	359
$CuCl_2L_2$ (L = 3:4 DMepy, 3:5 DMepy, $4NH_2py$, 4-i-Prpy, 4CNpy, $4NO_2py$, Th)	80, 270, 335, 350
$CuCl_2L_2.2H_2O$(L = py, 2Mepy, 3Mepy, 4Mepy, 2:3DMepy, 2:6DMepy, 2φpy, Quin, 2MeQuin, A)	347

Table 3.3 (a) cont.....

Complex	Reference
$Cu\ X_2py_2.2H_2O$ ($X^- = NO_3^-$, $\frac{1}{2}(SO_4)^{2-}$)	270, 361, 362

b) Square-Coplanar species:

$Cu\ X_2(2Mepy)_2$ ($X^- = Cl^-, Br^-, NO_3^-$)	80, 89, 268, 269, 270, 358, 359, 363, 389,
$Cu\ X_2\ L_2$ ($X^- = Cl^-, Br^-$; L = 2Etpy, 2:6DMepy,Quin)	80, 89, 202, 270, 360, 389

c) Complexes of unknown structure:

$Cu\ X_2\ L_2$ ($X^- = CN^-, NCO^-, NCS^-$; L= 2Mepy, 3Mepy, 4Mepy, 2:6DMepy)	356
$Cu\ Cl_2L_2$ (L= 2:3 DMepy, 2:4DMepy, 2:5DMepy)	80, 270
$Cu\ X_2$ (2:4:6-TMepy)$_2$ ($X^- = Cl^-, Br^-, CN^-$, NCO^-, NCS^-)	260, 356
$Cu\ X_2$ Quin$_2$ ($X^- = NO_3^-$ OAC^-)	360
$Cu\ X_2$ (PMH)$_2$ ($X^- = Cl^-, Br^-, NO_3^-$)	332

Table 3.4

Stereochemistries proposed for some cobalt(II) complexes.

Complex	Reference
a) Octahedral species:	
CoX_2py_4 (X^- = Cl^-, Br^-, I^-, NCS^-, $NCSe^-$, BF_4^-, ClO_4^-)	58,59,78,90,175,269, 270,272,340,364-370
$CoX_2(3Mepy)_4$	78,177
$CoX_2(4Mepy)_4$	78,175,177,213,269,272, 358
CoX_2L_4 (X^- = Cl^-, Br^-, I^-, NCS^-; L = 3Etpy,4Etpy)	177
CoX_2L_4 (X^- = Cl^-, NCS^-; L=4-Prpy,3:5DMepy,3:4DMepy)	177
$CoX_2(IQuin)_4$ (X^-= Cl^-, Br^-,I^-,NO_3^-,NCS^-,NCO^-,$NCSe^-$)	182, 359
$Co(NCO)_2(3Etpy)_4$	177
$CoCl_2(4Vpy)_4$	329
CoX_2py_2 (X^-=Cl^-,NO_3^-,NCS^-, $NCSe^-$)	59,78-80,181,188,270, 276,334,340,364,371-375.
$CoX_2(2Mepy)_2$ (X^-= $N(CN)_2^-$,$C(CN)_3^-$)	376
$Co(NO_3)_2L_2$ (L = 2Mepy, Quin, IQuin)	359
$Co(NCS)_2L_2$ (L=4Mepy,4Etpy,4Prpy,3:5DMepy)	175,177,269
$CoCl_2(Th)_2$	360
$CoX_2py_2.2H_2O$ (X^-=Br^-,NO_3^-)	187,270
b) Tetrahedral species:	
CoX_2py_2 (X^-=Cl^-,Br^-,I^-,NCO^-)	58,59,72,78,79,167,175, 181,188,191,276,334,352, 364,370,372-375
$CoX_2(2Mepy)_2$ (X^-=Cl^-,Br^-,I^-,NCS^-,NCO^-,$NCSe^-$)	78,167,175,196,276,334, 340,358
$CoX_2(3Mepy)_2$ (X^-=Cl^-,Br^-,I^-,NCS^-,NCO^-)	78,167,177,276,334,340,358

Table 3.4 cont....

$CoX_2(4Mepy)_2$ (X^-=Cl^-,Br^-,I^-,NCO^-)	78,167,175,177,213,269, 276,358
$CoX_2(2Etpy)_2$ (X^-=Br^-,I^-,NCS^-)	167
$CoX_2(3Etpy)_2$ (X^-=Cl^-,Br^-,I^-,NCS^-)	167,177
$CoX_2(4Etpy)_2$ (X^-=Cl^-,Br^-,I^-,NCO^-)	167,177,196
CoX_2(2:6 DMepy)$_2$ (X^-=Cl^-,Br^-,I^-)	78,276
CoX_2(2Pentyl py)$_2$ (X^-=Cl^-,Br^-,I^-,NCS^-)	167
CoX_2(3:4DMepy)$_2$ (X^-=Cl^-,NCS^-)	177
$CoCl_2L_2$ (L=4Prpy,2Vpy,4Vpy,3:5DMepy)	177,329
CoX_2L_2(X^-=Cl^-,Br^-,I^-; L= 2:4:6 TMepy,A)	78
CoX_2Quin_2 (X^-=Cl^-,Br^-,I^-,NCS^-,$NCSe^-$,NCO^-,ClO_4^-)	167,182,193,202,270,272, 276
CoX_2(IQuin)$_2$ (X^-= Br^-,I^-,NCS^-)	167,182,196
CoX_2(PMH)$_2$ (X^-=Cl^-,Br^-,I^-,NCS^-)	332
$CoCl_2I_2$	350
CoX_2B_2(X^-=Cl^-,Br^-,I^-,NO_3^-)	193,376
$Co(ClO_4)_2B_4$	376
(Et_4N) $[CoBr_3B]$	193,376
(ϕ_3MeAs) $[CoI_3B]$	193,376
c) Complexes of unknown structure:	
$Co(NO_2)_2py_2$	377
$Co(NO_2)_2py_2.H_2O$	377
CoI_2L_4(L = 2:6 DMepy, 2:4:6 TMepy,A)	78
$CoCl_2$(4CNpy)$_2$	335

Table 3.5

Sterochemistries proposed for some Nickel(II) complexes

Complex	Reference
a) Octahedral species:	
NiX_2py_4 (X^-=Cl^-,Br^-,I^-,NCS^-,$NCSe^-$,NCO^-,ClO_4^-,BF_4^-)	59,90,153,176,183, 190,258,270,272,275, 276,340,354,366,367, 370,378-380,387
$NiX_2(3Mepy)_4$ (X^-=Cl^-,Br^-,I^-,NCO^-,NCS^-,$NCSe^-$,ClO_4^-, BF_4^-)	59,153,176,183,190, 274,276,347,358,380
$NiX_2(4Mepy)_4$ (X^-=Cl^-,Br^-,I^-,NO_3^-,NCO^-,NCS^-,$NCSe^-$)	153,183,190,213,274, 276,347,358,380
NiX_2L_4 (X^-=Br^-,I^-,; L=3CNpy,4CNpy)	335
NiX_2L_4 (X^-=Cl^-,Br^-,NO_3^-; L=3:4DMepy, 3:5DMepy)	381
NiX_2L_4 (X^-=Cl^-,Br^-; L=4NH_2py, 2:4:6TMepy)	274,276
$NiCl_2L_4$ (L=2Mepy,2Φpy,2:3DMepy,2:5DMepy,A)	347
$NiClBrpy_4$	378
$Ni(ClO_4)_2L_4$ (L=4Etpy,3:5 DMepy, 4-i-Prpy)	176,382
$Ni\ I_2\ L_4$ (L=2:6DMepy, 3:4 DMepy,3:5DMepy)	190,276
NiX_2Quin_4 (X^-=Cl^-,$N(CN)_2^-$,$C(CN)_3^-$)	347,383
$NiX_2(IQuin)_4$ (X^-=Cl^-,Br^-,I^-,NO_3^-,NCO^-,NCS^-,$N(CN)_2^-$, $C(CN)_3^-$)	153,183,359,380,383,
$NiX_2(4Vpy)_4$ (X^-=Cl^-,NCS^-)	388
$NiCl_2(Th)_4$	350
$NiX_2L_4.2H_2O$ (X^-=Cl^-,BF_4^-; L=3Mepy,4Mepy)	274
$NiCl_2py_4.H_2O$	384
$Ni(ClO_4)_2py_4.2H_2O$	384

Table 3.5(a) cont.....

Complex	Reference
NiX_2py_2 (X^-=Cl^-,Br^-,NO_3^-,NCS^-,$NCSe^-$,N_3^-)	59,80,152,153,183,188,197,202, 275,276,334,340,370,380,385, 386,335,
$NiX_2(2Mepy)_2$ (X^-=NO_3^-,$N(CN)_2^-$,$C(CN)_3^-$)	274,359,376,383
$NiX_2(3Mepy)_2$ (X^-=Cl^-,Br^-,I^-,NCS^-,N_3^-)	152,153,183,274,276,340,358, 380,385
$NiX_2(4Mepy)_2$ (X^-=Cl^-,Br^-,NCS^-,N_3^-,$N(CN)_2^-$, $C(CN)_3^-$)	152,153,183,213,274,340,380,383, 385
NiX_2L_2 (X^-=Cl^-,Br^-;L=3Etpy,3CNpy,4CNpy)	152,335,385;
NiX_2L_2 (X^-=$N(CN)_2^-$,$C(CN)_3^-$;L=2:3DMepy,2:4DMepy)	383
$Ni(NO_3)_2L_2$ (L=2:3DMepy,2:4DMepy,2:5DMepy)	200
NiX_2Quin_2 (X^-=Cl^-,NO_3^-,NCS^-,$N(CN)_2^-$,$C(CN)_3^-$)	79,152,192,197,270,276,340,359, 383,385,
$NiX_2(IQuin)_2$ (X^-=Cl^-,Br^-,NO_3^-,NCS^-,N_3^-, $N(CN)_2^-$,$C(CN)_3^-$)	152,153,183,359,380,383
$Ni(NCS)_2(3MeIQuin)_2$	330
$NiX_2(4Vpy)_2$ (X^-=Cl^-,NCS^-)	388
$NiCl_2L_2.2H_2O$ (L=2Mepy,3Mepy,4Mepy,2Φpy, 2:3DMepy,3MeQuin,A)	347
$NiSO_4py_2.2H_2O$	378
$NiX(NO_2)py_2.2H_2O$ (X^-=Cl^-,Br^-,NO_2^-)	386
$Ni(NO_3)_2L_2.2H_2O$ (L=py,4CNpy)	270,335
$NiCl_2(2CNpy)_2.2H_2O$	335

Table 3.5 cont....

Complex	Reference
b) Tetrahedral species:	
NiI_2L_2 (L=py, 2Mepy, 3Mepy, 4Mepy, 2:6DMepy, 3:4DMepy, 2:4:6TMepy, 2MeB)	59,183,189,190,213,274, 276,330,334,370
NiX_2L_2 (X^-=Cl^-, Br^-; L=2Mepy, 2:3DMepy, 2:4DMepy, 2MeB, 3MeIQuin)	59,189,200,274,276,330
$NiCl_2(2:6DMepy)_2$	276
$NiBr_2(3:4DMepy)_2$	190,381
NiX_2Quin_2 (X^-=Cl^-, Br^-)	59,192,193,202,276
NiX_2B_2 (X^-=Br^-, I^-)	193
$(Et_4N)[Ni\ BBr_3]$	193
$Ni(ClO_4)_2(4Vpy)_4$	388
c) Square-coplanar species:	
NiX_2L_4 (X^-=ClO_4^-, BF_4^-; L=3Mepy, 4Mepy)	176,272,274,382
$NiX_2(4NH_2py)_4$ (X^-=Cl^-, Br^-, I^-, ClO_4^-)	176,272,274,382
NiI_2L_4 (L=2:4DMepy, 3:4DMepy)	190,381
$NiX_2(2Mepy)_2$ (X^-=I^-, NCS^-)	190,274,334
NiX_2L_2 (X^-=Br^-, I^-; L=2:3DMepy, 2:4DMepy, 2:5DMepy, 2:6DMepy, 2MeQuin, 2MeBT)	190,200,330
$NiCl_2(2:5\ DMepy)_2$	200
$Ni(SCN)_2(2:5\ DMepy)_2.\frac{1}{2}H_2O$	200
NiI_2L_2 (L=3MeIQuin, A)	190,330
$Ni(NCS)_2L_2$ (L=3MeIQuin, 2MeB, 2MeBT)	330
NiX_2Quin_2 (X^-=I^-, ClO_4^-)	59,190,192,272
d) Complexes of unknown structure:	
$Ni(C_2O_4)py_2$	378,386
$NiX_2(PMH)_2$ (X^-=Cl^-, Br^-, I^-)	332

nickel (II) complexes with monodentate-heteroaromatic-amines. These tables do not include the X-ray structural work previously discussed, nor has further work [73,327] on the triazole complexes been included. A restriction to the complexes of these three ions has been imposed here, because it was desired to develop comparisons with the complexes of quinoxalines, which are described later.

(E) Factors Affecting Structure and Properties

The effects most frequently suggested in order to account for the properties of these complexes appear to be steric hindrance (references: 58,78,80,89,152,167,175,196,200,268-270,274,328-332) and metal-ligand π-bonding (references: 72,89,90,152,153,161,169, 171-173,176,181,-183,192,200,328,333-338).

Steric hindrance has been shown to determine the preferred stereochemistry when a large 2-substituent is attached to the ligand molecules. A steric effect on Dq, and on the extent of electronic band splitting, has been claimed. The metal-ligand stretching frequencies have been found to be higher in unhindered complexes, because shorter M-L bonds are permitted.

π-bonding has been invoked to explain such diverse data as: NMR contact shifts, ESR parameters, infrared-frequency-shifts for

ligand molecules, the spectrochemical series, stabilities of complexes, and stereochemistry. For example, the preference of some Ni(II) complexes for a square-planar, rather than a tetrahedral structure, has been ascribed to better π-bonding in the former case.

The importance of π-bonding has not been universally accepted. Graddon, et al,[175,269] have interpreted the general smallness of the effect of co-ordination on ligand-infrared-frequencies as evidence against π-bonding.[175] They have sought to explain the spectrochemical series without recourse to π-bonding. The discrimination between the e_g and t_{2g} orbitals was said to be caused by coulombic repulsions between the ligand non-bonding electrons and the metal t_{2g} electrons. Nelson, et al, have objected[177,182] to this explanation on the grounds that the infrared evidence is ambiguous, and has also been interpreted[90] as evidence for π-bonding. In fact, all the effects explained by Graddon's steric model can be equally well treated in terms of π-bonding. This is not surprising since the two theories are practically equivalent, both depending on the effect of the non-bonding ligand orbitals on the metal t_{2g} orbitals. The difference is that Graddon's interaction is electrostatic, while the π- interaction is covalent (Figure 1.6) in nature. Since covalency has been established in metal-ligand bonding,[164] and since π-bonding arises quite naturally

in a molecular-orbital treatment of this system, it would seem unwise to reject π -bonding entirely. Further, NMR and ESR data are not readily explained without π -bonding.

Molecular-orbital theory tends to over-emphasize π -bonding contributions and it would seem wrong to attach a dominant importance to them. Such an unbalanced emphasis would denigrate the contributions of σ -bonding effects like ligand basicity and polarisability [200,270] [179,181,182,187,334,339].

These complexes are probably best approached in terms of steric hindrance, σ - and π -bonding. Further, the crystal-field-stabilisation energy, the chelate effect, and the various factors (bond energies, latent heats, solvation energies, etc.) which contribute to the lattice energy (and its dependence on molecular packing and hydrogen bonding), may be important.

CHAPTER IV

THE COMPLEXES OF COPPER (II) WITH HALOPYRIDINES

&

RELATED LIGANDS

In Chapter III the structural effect of various ligand properties was discussed. The conclusions about the effect of ligand basicity on the complexes of substituted pyridines had been based on studies of stronger bases than pyridine (see Table 3.3). It was therefore decided to extend this work to the weakly basic halopyridines. Table 3.2 lists the pKa values[185] of these, and related molecules. Further, the halo-substituents in these ligands have smaller Van der Waal's radii than the methyl group,[390-392] which had previously been used to study steric hindrance of co-ordination. The halopyridines therefore offered a method of extending the study of steric factors.

The investigation was begun by D.J.Walker, in this laboratory. He suggested[393], on the basis of the diffuse reflectance spectra, that the complexes $CuCl_2(2Clpy)_2$ and $CuBr_2(2Clpy)_2$ had a pseudo-octahedral structure with such a large tetragonal distortion as to be almost square-coplanar.

Table 4.1 shows the additional complexes which have now been prepared, with the ligands 2Brpy, 3Brpy, 4Clpy and also with 1:2:4: Triazole and Phenazine. The magnetic moments all lie in the range ($\backsim$1.7- $\backsim$2.0 B.M.) usually observed[131] for paramagnetic copper (II) compounds.

During this work, McWhinnie reported[394] the 2Clpy and 2Brpy complexes. From reflectance and far-infrared data he proposed that all

Table 4.1

Electronic spectral data (kK) and room temperature magnetic moments (B.M.) for the copper(II) complexes with halopyridines, and some related ligands.

Complex	μ_{eff}	Band maxima*	δ
$CuCl_2(2Clpy)_2$	1.79	14.9(0.8)	4.4
$CuBr_2(2Clpy)_2$	1.79	15.5(0.9)	7.1†
$CuCl_2(2Brpy)_2$		18.7(0.6), 15.3(0.6)	4.8
$CuBr_2(2BRpy)_2$		15.9(0.7)	4.1†
$CuCl_2(3Brpy)_2$	1.85	14.4(0.5)	3.5
$CuBr_2(3Brpy)_2$	1.79	14.2(0.6)	3.4†
$CuCl_2(4Clpy)_2$	1.83	14.3(0.6)	3.3
$CuBr_2(4Clpy)_2$	1.84	14.1(0.8)	3.3
$CuCl_2T$	1.81	13.9(0.8), 9.8(vb,sh)	4.7
$CuBr_2T$	1.84	13.8(0.8), 9.5(vb,sh)	5.3†
$CuCl_2P$**	1.68	20.8(1.0), 19.8(sh), 17.5(1.2), 14.3(1.0)	5.2
$CuCl_2py_2$		24.1(w), 14.5(0.5)	3.6
$CuBr_2py_2$		14.6(0.9)	3.4
$CuCl_2(2Mepy)_2$		17.1(0.6)	4.4
$CuCl_2Quin_2$		22.7(sh), 21.5(sh), 19.4(0.5), 15.9(0.5)	5.6†
$CuBr_2Quin_2$		16.7	

/cont....

Table 4.1 cont..

Complex	μ_{eff}	Band maxima	ε
$CuCl_2Quin$		12.5	
$CuBr_2Quin$		15.8(sh)	
$CuCl_2$		~11.5	
$CuBr_2$		~ 9.0	

Notes:

* Figures in brackets refer to absorption on the arbitrary Beckman scale. Abbreviations are listed at the beginning of this work.

† Estimated, since charge transfer bands overlap.

** Recorded with phenazine as reference.

four had square-coplanar structures. More recently Rogers, et al[80,270], have published studies of the far-infrared spectra and thermal stabilities of a series of related complexes which included $CuCl_2(4Clpy)_2$. They suggested that this compound might have an octahedral polymeric structure like that[186] of $CuCl_2py_2$. $CuCl_2(2Brpy)_2$ has also been reported[355], but without comment on its structure.

X-ray powder data

X-ray powder photographs were taken of the triazole complexes, in order to compare the structure of $CuBr_2T$ with that[194] of $CuCl_2T$. The results are given, as lattice d- spacings, in table 4.6. It is clear that the two complexes are isomorphous, with the bromide having the slightly larger unit cell.

Electronic Spectra

The reflectance spectra illustrated in figure 4.1, and detailed in table 4.1, may be divided into 3 main types.

(a) Complexes of py, 3Brpy and 4Clpy show a single, broad and moderately weak band near 14kK.

(b) The complexes of 2Clpy and 2Mepy exhibit an even broader band at slightly higher frequency, with some evidence of an unresolved shoulder.

(c) The complexes of 2Brpy, Quin, T and P show clearer evidence of

Table 4.6

d spacings (Å) measured from X-ray powder photographs on the copper(II) complexes with triazoles.

Complex	d*
$CuCl_2T$	6.2(b), 3.35, 3.2, (3.1), 2.9, (2.63), (2.38), 2.32, (2.20), 1.77
$CuBr_2T$	6.4(b), 3.4, (3.3), (3.2), (3.1), (2.70), (2.58), 2.45, (2.27), 1.87

* Results shown in brackets refer to weak lines.

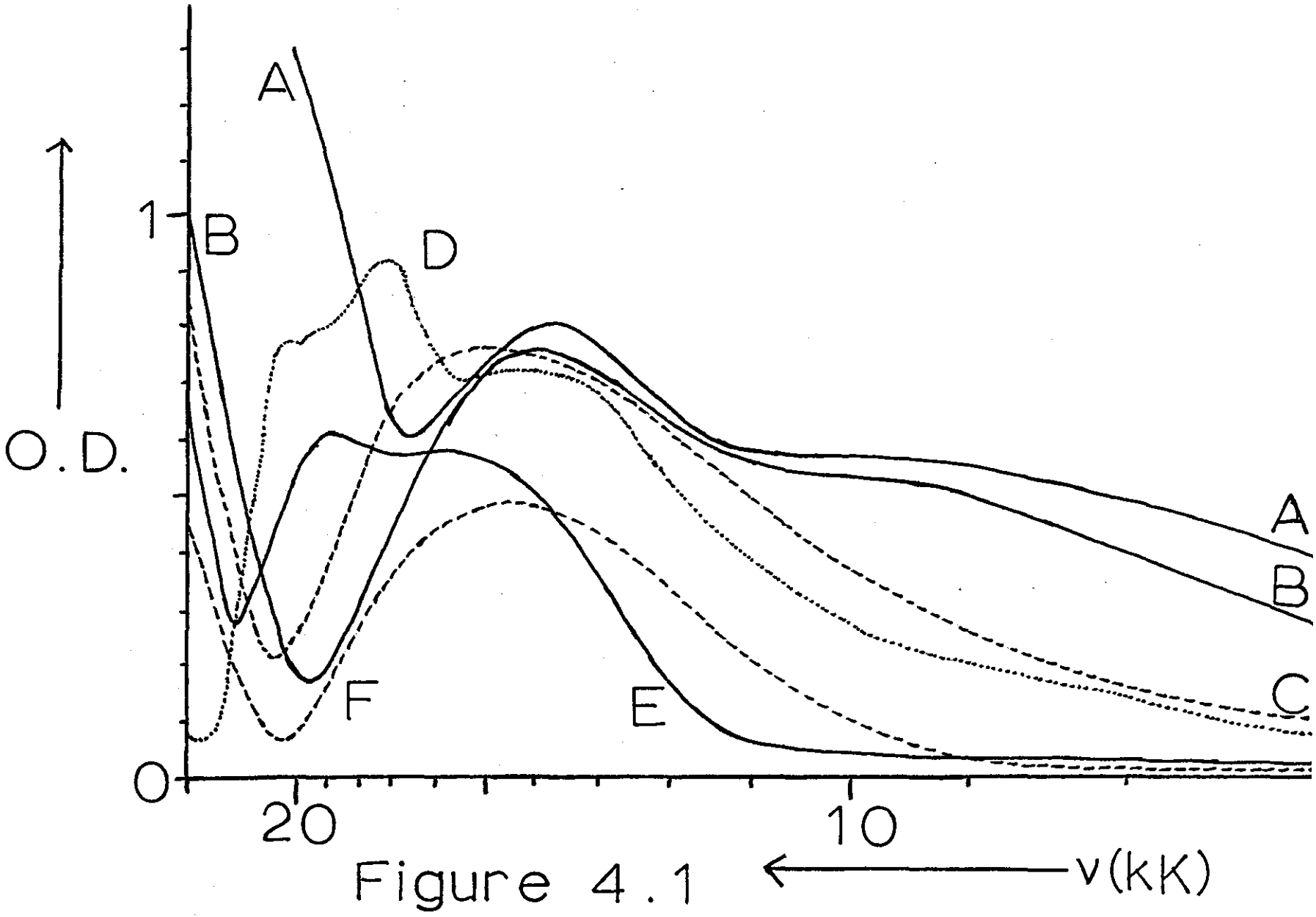

Figure 4.1

more than one component.

The bis-pyridine complexes

The single band at 14.5kK has been previously recorded by König and Schläfer[138] and by Ferguson[47], and assigned to the d-d transitions. No other band occurs between 4kK and 22kK. It is concluded that all the d-d transitions (see fig.1.2) lie unresolved within this broad envelope. This is in accord with general experience[17,120,395,397-412], which indicates that Copper (II) d-d transitions are normally close in energy; with ESR data[355] which indicates comparatively little splitting of the $^2T_{2g}$ state in $CuCl_2py_2$; and with the large value of the splitting Δ_2 (see fig.1.2) anticipated from the very tetragonally distorted structure[186] (see Table 3.1), and confirmed by the high value (1.76) of Jørgensen's[23,210] ratio ν_{Cu}/ν_{Ni}

A crude value of $10Dq \sim 7.7kK$ may be obtained for $CuCl_2py_2$ by using the baricentre rule[23], if all transitions are assigned an energy of 14.5kK. Allowing for the very approximate nature of this estimate, it is satisfactorily close to the value (8.3kK - see Chapter 6) for $NiCl_2py_2$. Jørgensen has suggested[23] that the positions of Ni(II) and Cu(II) should be close in the spectrochemical series.

The very similar spectrum of $CuBr_2py_2$ may be treated in the same way. The closeness of the d-d energies of these two complexes is

perhaps rather surprising in view of the difference between the positions of the two halides in the spectrochemical series. A comparison of the two crystal structures[186,237] shows that this may be due to the greater tetragonality, or to the slightly shorter Cu-N bonds in the bromide. A rough calculation based on the dependence of Dq on the sixth power of the internuclear distance (equation 1.1) shows that this latter factor could cause a shift of about 0.6kK in the band maximum.

The crystal structures reveal the further possibility that Dq may be raised in the bromide (see fig.1.6) by the easier π-bonding permitted (via ring twisting - see fig.3.) by the longer Cu-Cu distance. The higher polarisability of Br^- relative to Cl^- would contribute to this effect, as explained in Chapter I.

The d-d band of $CuBr_2py_2$ is also extremely similar in energy to that (14.8kK) recorded[413] for α-$CuBr_2(NH_3)_2$, which has the same structure[414]. Such a similarity, in spite of the lower basicity of pyridine (c.f. pKa of NH_3 is 9.48) and the shorter Cu-N bond (1.93Å) in the ammine, may be due to the smaller tetragonality (Cu-Br=3.08Å) and longer (2.54Å) equatorial Cu-Br band in α-$Cu(NH_3)_2Br_2$. However, it may also be connected with the impossibility of Cu-N π-bonding in the ammine.

All these bisamine complexes exhibit the tails of intense absorptions in the ultraviolet region. These bands are always lower in energy in the bromides, relative to the chlorides, and in the former cases often partially obscure the d-d bands. König and Schläfer[188] have assigned these bands to ligand and charge -transfer absorption. In common with general conclusions on the electronic spectra[415] of azines, co-ordination does not much affect the frequency of the ligand bands[416]. Jørgensen[417] has interpreted this as evidence of little metal-ligand π-bonding. However, this is uncertain since, as Perkins[416] has pointed out, the small effect is due to the N-atom's residing on the symmetry axis of the ligand.

The lowering of the halogen and pyridine charge-transfer bands in the bromide (27.4kK and 24.4kK respectively), relative to the chloride (34.0kK and 29.4kK), may be understood in terms of the greater reducing power and polarisability of Br^-, if the electron transfers are from halide to metal and from metal to pyridine. The higher frequency of the halogen charge-transfer band for the cobalt (II) and Nickel (II) complexes may similarly be attributed to the poorer oxidising power of Co^{2+} and Ni^{2+} relative to Cu^{2+}.

The complexes with 1:2:4 -Triazole

The spectra of both halides exhibit a main peak near 13.9kK and a pronounced shoulder near 9.8kK. It is apparent from the crystal structures that $CuCl_2T$ [194] is less tetragonally distorted than $CuCl_2py_2$ [186], and therfore figure 1.2 indicates that the ν_1 band may fall below the ν_2 and ν_3 transitions. It is then reasonable to assign the low energy shoulder to the $^2B_{1g} \rightarrow {}^2A_{1g}$ transition and the main band to the unresolved $^2B_{1g} \rightarrow {}^2B_{2g}$ and $^2B_{1g} \rightarrow {}^2E_g$ transitions. A similar assignment has been given [261], on the basis of polarised crystal spectra, for the complex $Cu\,en_2(NO_3)_2$, which [418] is also less distorted than $CuCl_2py_2$

With this assignment a crude value of 10Dq $\backsim$ 9.0kK is obtained for both halides. The value may be somewhat lower than this if the $^2B_{2g}$ state lies, unresolved, between the $^2E_{2g}$ and $^2A_{1g}$ levels. This high value of 10Dq indicates that triazole is acting as a more basic ligand than pyridine. This is not inconsistent with the low value [185] of pK_1(2.30) since this refers to the acidic hydrogen in the 4- position, and pK_2 should be more appropriate as a measure of complexing ability. The only data available is for 1:2:3 - Triazole [185] (pK_1=1.17, pK_2=9.51), but this may be taken as some support for a strong ligand field in CuX_2T.

$CuCl_2(2Mepy)_2$

The structure of this complex is said[253] to be a square-pyramidal dimer, but no details of the arrangement of ligands has yet been published. It is unlikely that the d-d energy would be comparable with that of $CuCl_2py_2$ unless both picoline molecules were co-ordinated equatorially. Thus the apical ligand is probably a chloride ion (see figure 4.2).

The higher frequency (17.1kK)of the main band, relative to that of the bis-pyridine complex, may be due to a combination of greater tetragonality and a more basic ligand. The unresolved shoulder near 14kK is therefore unlikely to be due to the ν_1 transition. If the shoulder is assigned to ν_2, with ν_1 and ν_3 contained within the main peak, 10Dq is calculated to be approximately 7.5kK, in satisfactory agreement with the value (7.2kK) estimated for $CuCl_2py_2$. This assignment also gives a ratio of $\nu_3/\nu_2 \sim 1.2$, which is identical to that obtained from the ESR data[355].

The Complexes of 3Brpy and 4Clpy:

The spectra of the complexes of known crystal structure have been discussed above, and the data obtained for the remaining complexes will be related to the assignments suggested there. It is not suggested

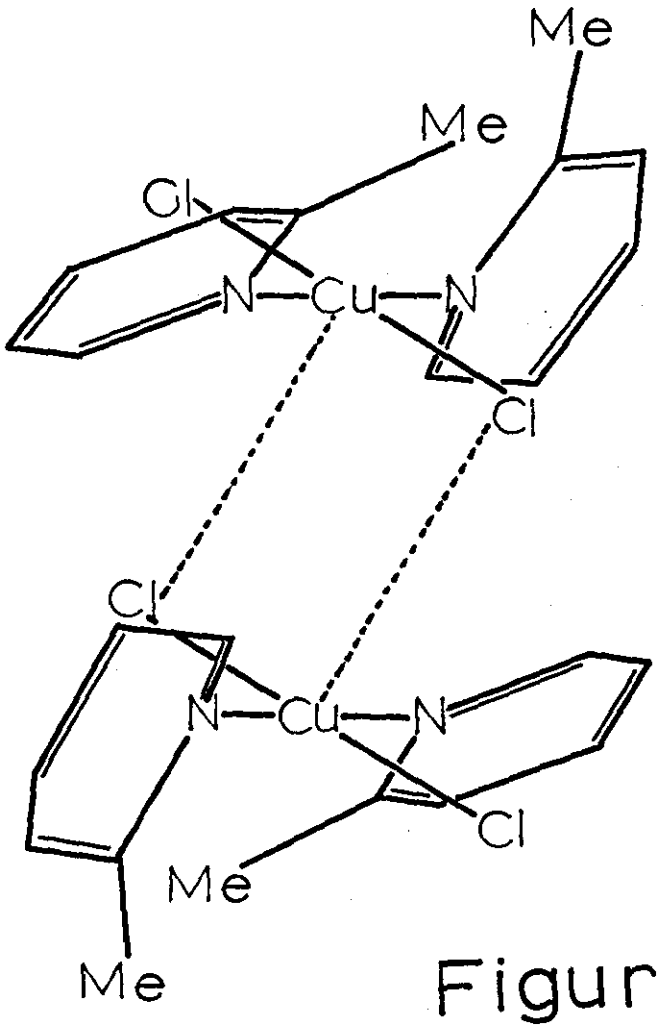

Figure 4.2

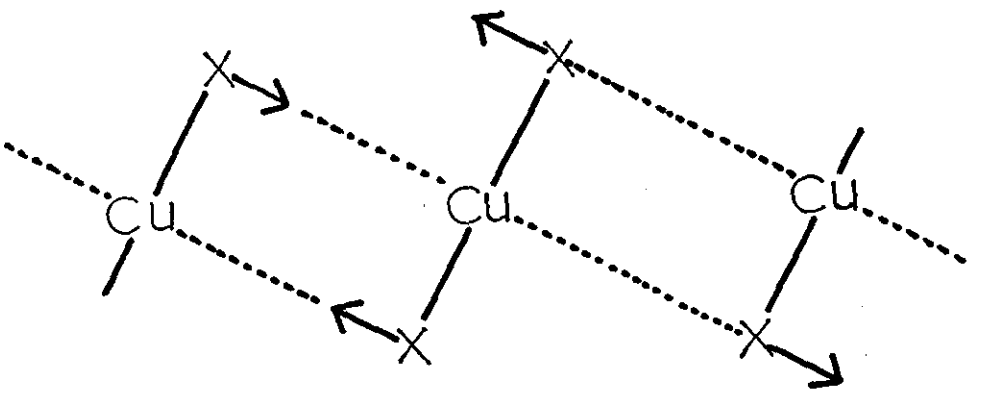

Figure 4.4

that these assignments are the only possible interpretations of the data, but that at least one consistent explanation is feasible.

The spectra of the 3Brpy and 4Clpy complexes are so similar to those of their pyridine analogues that there can be little doubt that they are all isostructural, as expected from the lack of steric hindrance. The closeness of the d-d bands of the three chlorides, in spite of differences of ligand basicity, may be due to some additional metal-ligand π-bonding in the halopyridine complexes. This is consistent with the higher π-acceptor character of the halopyridines, suggested in chapter 3.

The Complexes of 2Clpy

The d-d bands of both halide complexes of 2Clpy are at higher frequencies than for their pyridine analogues. This fact eliminates the possibility of tetrahedral or trigonal-bipyramidal species, which would absorb at lower energies.[120,166,351,398,406,412,419,420,445] Only a larger tetragonal distortion (and its limiting cases of square-pyramidal or planar species) or more extensive π-bonding can account for the position of the bands relative to those of the pyridine complexes. The observed bands are probably too weak for tetrahedral, trigonal-bipyramidal, or cis-octahedral species.[446-449]

The shape of the d-d band of $CuCl_2(2Clpy)_2$ is very similar to that

of $CuCl_2(2Mepy)_2$, being broad with an unresolved low-frequency (∽ 13kK) shoulder. A similar assignment is possible, yielding a rough value of 10Dq ∽ 6.8kK, and suggesting that the 2Clpy complex may also have a square- pyramidal structure.

The spectrum of the bromide is slightly different, having the unresolved shoulder at a higher frequency (∽17kK) than the main band. If this shoulder is assigned to the $^2B_{1g} \rightarrow {}^2A_{1g}$ transition then a value of 10Dq ∽7.0kK is obtained, which is in good agreement with the other values so far estimated.

$CuCl_2(2Brpy)_2$ and $CuBr_2(2Brpy)_2$

The chloride has a well-defined doublet peak in the visible region of the spectrum, being in this respect very similar to the square-planar species $Cu(acac)_2$ [395,400,336,421], $Cu(\varphi acac)_2$ [401] and Cu Ethylacetoacetate [4
A large tetragonality is expected, to account for the higher energy of the transitions compared with those of the pyridine complexes. This suggests that the ν_1 transition may be contained within the upper observed band.

The three g-factors [355] (2.05, 2.08 and 2.13) characterising the polycrystalline ESR absorption may be due to a crystal field of lower symmetry than axial [423]; or to exchange between several crystallographically

inequivalent sites, each having axial symmetry[144]. Whichever interpretation is correct, the data indicates that $\nu_3 < \nu_2$. This relative ordering of the ^2E and $^2B_2$ states is also indicated by the ESR data[355] for the bis-pyridine complex, and may be due to a large covalent contribution to the metal-ligand bonding.

The ESR data is consistent with an assignment of the lower electronic band to the ν_3 transition, while the upper band probably contains the ν_2 transition. If the exchange explanation is accepted[424] ν_3/ν_2 is estimated as $\sim$ 0.80 compared with a value of $\sim$ 0.82 given by the above optical assignment. The spin-orbit reduction factor may be calculated as $\alpha \sim$ 0.67, which low value reflects some covalency in the metal-ligand interactions[171].

The suggested assignment gives an approximate value of 10Dq $\sim$ 7.1kK, in good agreement with the value for $CuCl_2(2Clpy)_2$. This is expected from the closeness of the pKa values of the two halopyridines.

A similar assignment gives 10Dq $\sim$ 6.7kK for $CuBr_2(2Brpy)_2$, whose spectrum exhibits one main peak with an unresolved low frequency shoulder (14kK).

The Quinoline Complexes

The visible spectrum of $CuCl_2Quin_2$ consists of two peaks like that of its 2Brpy analogue, and a similar assignment may be made. The

crude value obtained, of 10Dq(~ 7.4kK), agrees well with those given above for $CuCl_2py_2$ and $CuCl_2(2Mepy)_2$, and also with that (8.0kK) of the octahedral complex $NiCl_2Quin_2$ (see Appendix A3).

The spectrum of the bromide complex is reported[79] to consist of one band, though further bands would be expected to be obscured by the charge-transfer absorption. The observed band is at higher frequency than that of the chloride complex, as noted earlier for the analogous complexes of 2Clpy and 2Brpy.

The spectrum of $CuCl_2Quin_2$ also exhibits two faint shoulders at 21.5kK and 22.7kK. It is not possible to say whether these are parts of the d-d system without polarisation data, a gaussian analysis,[17,422,425-428] or low-temperature spectra.[120,401,407,421] At lower temperatures it is often found that better resolution is obtained because the band width contributions from molecular vibrations are reduced.

$CuCl_2P$

The spectrum of this complex consists of three overlapping bands, but is quite similar to that of $CuCl_2Quin_2$, and a similar assignment can be given (ν_1=17.5kK, ν_2=20.8kK and ν_3=14.3kK). The rough value estimated for 10Dq(~7.7kK), is quite close to the value given above for $CuCl_2(2Brpy)_2$, as expected from the low basicity and good

π-acceptor character (see Chapter III) of each ligand.

Phenazine itself exhibits a strong electronic p-band at 27.4kK[429] which appears at 27.6kK in the complex and obscures the d-d system. The data given in table 4.1 were taken from a better resolved spectrum, recorded with phenazine as a reference instead of MgO. Probably because of the poor overall reflectance of the phenazine reference, the d-d band of the complex appears to gain intensity. The spectrum illustrated in figure 4.1 has been reduced to the original intensity to preserve uniformity.

The significance of a weak shoulder at 19.8kK is not clear at present, but may be due to a splitting of the upper ^2E state by a rhombic field. It was unnecessary to invoke rhombic fields to interpret the spectra of the other complexes, but this does not preclude a small and unresolved splitting of the upper ^2E state.

The assignment given above suggests that phenazine is bidentate and occupies equatorial positions in $CuCl_2P$. If this were not so the complex would absorb at lower energy (as does $CuCl_2Quin$ compared with $CuCl_2Quin_2$[79]) since the missing strong nitrogen donor would be replaced in the chromophore by the weaker chloride ligand.

Summary of assignments

Table 4.2 lists the very tentative assignments given above, and shows that at least one consistent interpretation of the spectra is possible. The complexes are shown in increasing order of ν_1, which (see fig.1.2) should correspond roughly with increasing tetragonality. If the assignments are accepted, this suggests (as expected) that the complexes of the more sterically hindered ligands are the more distorted.

Since more tetragonal structures, than those of the pyridine complexes, must involve practically no axial coulombic or covalent interaction it is probable that the complexes of2Clpy, 2Brpy, Quin and P involve square-pyra midal or square-planar structures. No sharp division is likely, and for this reason no conclusions can be reached on the structure of $CuCl_2(2Clpy)_2$.

The complexes may be divided on the basis of the relative orders of the ^2E and $^2B_2$ states, suggested above. No evidence is available for the complexes of T,3Brpy or 4Clpy, but those of py, P, 2Brpy and Quin appear to have $\nu_3 < \nu_2$, while those of 2Mepy and 2Clpy have $\nu_3 > \nu_2$. It has been suggested[19] that square-pyramidal complexes may have the reverse order of ^2E and $^2B_2$ states compared with octahedral or square-planar species. Covalency is probably responsible for the reversal of both these orders, compared with those given on the basis of crystal-field theory.

Table 4.2

A tentative assignment of the electronic spectra (kK) of the copper(II) complexes with substituted pyridines and related ligands.

Complex	ν_1 *	ν_2	ν_3	10Dq
$CuCl_2T$	9.8	13.9	13.9	9.0
$CuCl_2(4Clpy)_2$	14.3	14.3	14.3	7.1
$CuCl_2(3Brpy)_2$	14.4	14.4	14.4	7.2
$CuCl_2py_2$	14.5	14.5	14.5	7.2
$CuCl_2(2Clpy)_2$	14.9	13.0	14.9	6.8
$CuCl_2(2Mepy)_2$	17.1	14.0	17.1	7.5
$CuCl_2P$	17.5	20.8	14.3	7.7
$CuCl_2(2Brpy)_2$	18.7	18.7	15.3	7.1
$CuCl_2Quin_2$	19.4	19.4	15.9	7.4
$CuBr_2T$	9.5	13.8	13.8	9.0
$CuBr_2(4Clpy)_2$	14.1	14.1	14.1	7.0
$CuBr_2(3Brpy)_2$	14.2	14.2	14.2	7.1
$CuBr_2py_2$	14.6	14.6	14.6	7.3
$CuBr_2(2Brpy)_2$	15.9	15.9	14.0	6.7
$CuBr_2(2Clpy)_2$	17.0	15.5	15.5	7.0

* See Figure 1.2

Far-Infrared Spectra

Further support for the above order of tetragonality is supplied by the far-infrared data, previously reported and listed in table 4.3 in decreasing order of copper-halogen stretching frequencies. Adams and Lock[353] have concluded that, although terminal and bridging copper-halogen frequencies cannot be confidently distinguished, a correlation exists between ν_{Cu-X} and the length of the long Cu-X bonds. In agreement with this, table 4.3 shows that the complexes of the sterically hindered ligands are mostly grouped at higher Cu-X frequencies than those of the less hindered ligands.

Since both ν_{Cu-X} and the frequency of the ν_1 electronic band are related to the tetragonality of a complex, a correspondence may be expected between the two parameters. A rough correlation of this kind is apparent and is shown by figure 4.3 . Considerable scatter is evident, as would be expected from the approximate nature of the ν_1 values. Further, for the unhindered ligands, ν_{Cu-Cl} shows an inverse correlation with basicity. This effect accounts for the high Cu-Cl frequencies of the complexes of the weak bases $4NO_2$py and 4CNpy. Strongly basic ligands are generally poor π-acceptors (see Chapter III) and either this factor, or their high polarisability (via the electroneutrality principle - see chapter I), may account for some low values of ν_{Cu-Cl}.

Table 4.3

Metal-ligand vibrational frequencies (cm^{-1}) for some Copper(II) complexes of substituted pyridines and related molecules.

Complex	ν_{Cu-x}	δ_{Cu-x}	ν_{Cu-N}	δ_{Cu-N}	Reference
$CuCl_2P$	362s		<200		210
$CuCl_2(2Brpy)_2$	333		236		394
$CuCl_2Quin_2$	330	151	257	151	89
$CuCl_2(2Etpy)_2$	320	147	246	183	89
$CuCl_2(2:6DMepy)_2$	314	154	246	154	89
$CuCl_2(4NO_2\text{-}py)_2$	313		235		270
$CuCl_2(2Mepy)_2$	308,300sh	160	260,257 253	191	89,363
$CuCl_2(2Clpy)_2$	308s,vb		234s		210
$CuCl_2(4CNpy)_2$	307		242		270
$CuCl_2(4Mepy)_2$	299		266		270
$CuCl_2(3Mepy)_2$	294		267		270
$CuCl_2(4Clpy)_2$	294s,b		243s		210
$CuCl_2(4\text{-}iPrpy)_2$	287		275		270
$CuCl_2py_2$	287,229(?)	177	266	200	89
$CuCl_2(3Brpy)_2$	305s* (?), 281s		261s		210
$CuCl_2T$	273vb		252s,244		210
($CuCl_2$	329,277	189)			89,430
$CuBr_2Quin_2$	266		256		89
$CuBr_2(2Clpy)_2$	256s,249		234s		210
$CuBr_2py_2$	256,204(?)		268		89
$CuBr_2(Etpy)_2$	251		251		89

Table 4.3 cont....

Complex	ν_{Cu-x}	δ_{Cu-x}	ν_{Cu-N}	δ_{Cu-N}	Reference
$CuBr_2(2Brpy)_2$	244		239		394
$CuBr_2(3Mepy)_2$	238		269		356
$CuBr_2(4Mepy)_2$	234		256		356,260
$CuBr_2(4Clpy)_2$	234		240sh		210
$CuBr_2(2Mepy)_2$	231		268,259		89
$CuBr_2(2:6DMepy)_2$	230		244		89
$CuBr_2(3Brpy)_2$	230s		259s		210
α-$CuBr_2(NH_3)_2$	216s		510m	318m	353
$CuBr_2T$	225w,206s		251s, 244		210
($CuBr_2$	254,223)				430

* Ligand band enhanced in $CuCl_2(3Brpy)_2$

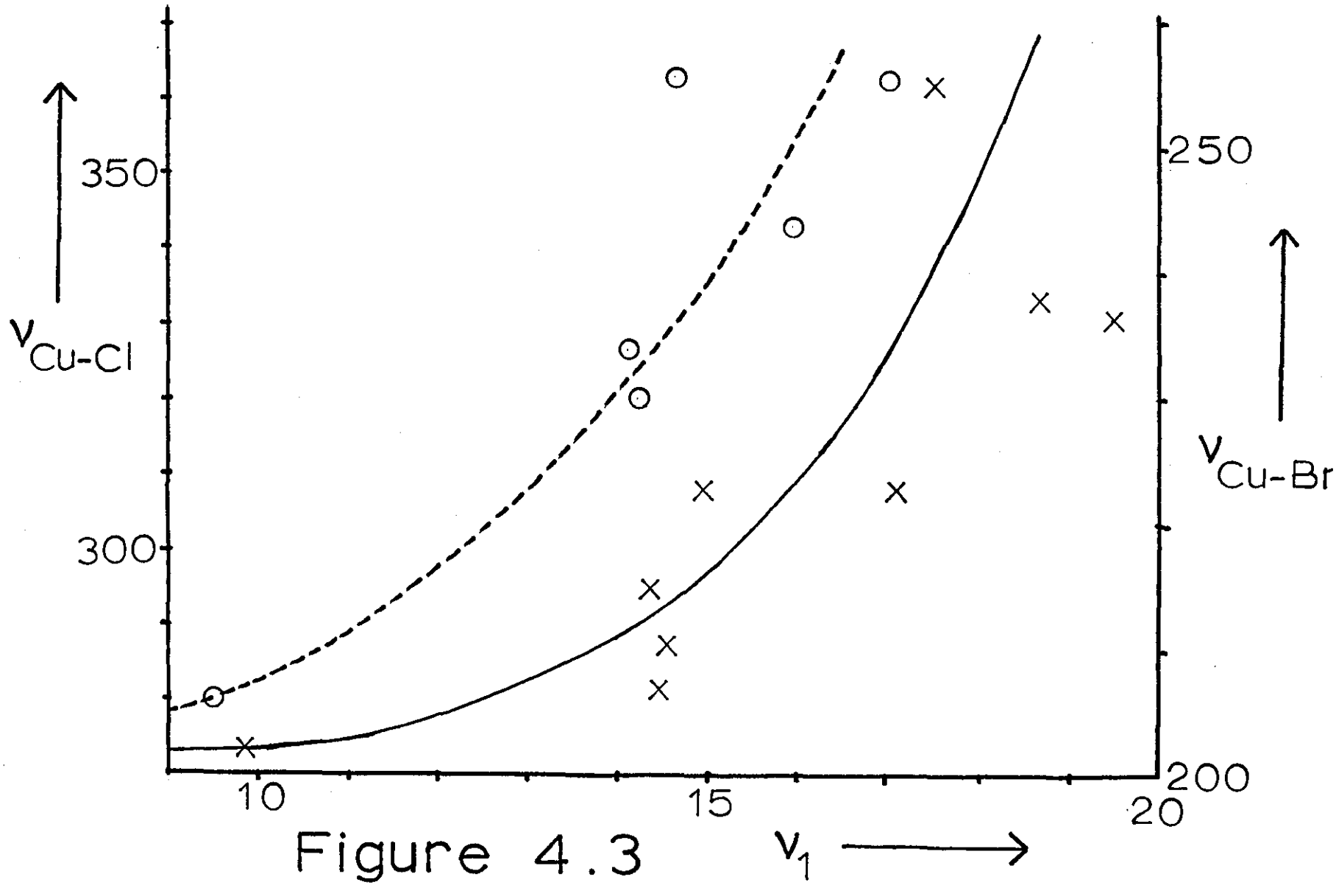

Figure 4.3

Another correlation exists, as demonstrated[270] by Frank and Rogers, between the ligand basicity and the Cu-N frequency. This relationship has not been plotted since it is perturbed by the presence of longer Cu-N bonds in the complexes with sterically hindered ligands. The absence of a strong dependence of frequency on ligand mass may suggest that the vibration does not involve displacement of the whole ligand, and that the Cu-N modes couple with those of the heteroaromatic rings.

Table 4.3 also shows that the Cu-N bending mode roughly follows ν_{Cu-N}, while the Cu-Cl deformation mode has an inverse correlation with the length of the long Cu-Cl bonds ($CuCl_2$ is taken to be the limiting case when two sets of Cu-Cl bonds are equivalent.) Figure 4.4 shows that this is expected, since the vibration in question may be described, either as a short Cu-Cl bending mode, or as a long Cu-Cl stretching mode. (See Appendix A.5.) In the case of the $CuCl_2py_2$ complex this interpretation is in accord with the conclusions[353] of Adams and Lock, who demonstrated that the 229cm^{-1} band was not due to long-bond stretching. The origin of this band is unclear.

The occurrence of multiple bands for $CuCl_2(2Mepy)_2$ is explicable, since the dimeric structure suggested has C_{2h} symmetry (if each monomer has a trans-configuration and these are joined by long Cu-Cl bonds) in which two stretching modes for the short Cu-Cl bonds ($2B_u$) and two Cu-N

stretching modes ($A_u + B_u$) are expected to be infrared active. The appearance of three ν_{Cu-N} components cannot be explained by any configuration and is probably due to site symmetry.. None of the other complexes exhibit both multiple Cu-X and multiple Cu-N bands, apart from those of triazole (which only have C_2 symmetry). There is, therefore, no evidence from the far infrared spectra in support of square-pyramidal structures for any of these complexes.

Other features of table 4.3 call for comment. The relative orders of the ligands differ occasionally in the chloride and bromide series. $CuCl_2(2Brpy)_2$, for example, appears (on the basis both of ν_1, and ν_{Cu-X}) to be more tetragonal than $CuCl_2(2Clpy)_2$, while the reverse obtains for the bromide analogues. The very different Cu-N frequencies of the 4Clpy and 3Brpy complexes are difficult to interpret. The high Cu-Cl stretching frequency recorded for the phenazine complex can probably be attributed to the absence of any halide bridging, and also to the low basicity and high π-acceptor capacity (see Chapter III) of the organic ligand. It is possible that any conclusions drawn from the table are invalidated because the modes compared do not all have the same form.

Near-Infrared Spectra

The Halopyridines

Table 4.4 records the infrared maxima of the halopyridines and their metal complexes in the region 375-1700cm^{-1}. The assignments given

Table 4.4 Section A Infrared spectra (375-1700cm^{-1}) of the halopyridine complexes of copper(II)

2Clpy	$CuCl_2(2Clpy)_2$	$CuBr_2(2Clpy)_2$	Vib^n No.	2Brpy	$CuCl_2(2Brpy)_2$	$CuBr_2(2Brpy)_2$
407ms	441sh	443w	16a	405ms	431m	428m
425ms	437m	436m	6a			
478m	487mw	482mw	11	466ms		471m
615m	640mw		6b	611ms	641mw	647w
720vs	728m	732m	4,12	695vs	703m	698m
762vs	761ms	768m	10b	756vs	760ms	759s
787sh,w	774sh	783mw				
823	801vw	804w	16a+16b			
880mw	878w	893w	10a	883mw,b	887vw	
920w,b		936w	5	930mw		
960m	972w	970m,b	17a	958w	962w	961w
988s	1019m	1025mw	1	984s	1023m	1020mw
1042s	1049m	1050mw	18a	1040s	1047m	1046mw,b
1082s	1093mw	1093mw	18b	1076vs	1082m	1078m
1119vs	1129m	1137sh	13	1106vs	1117m	1116m
1150s	1157m	1153mw	9a	1146ms	1148m	1151m

Table 4.4 Section A cont....

2Clpy	$CuCl_2(2Clpy)_2$	$CuBr_2(2Clpy)_2$	Vib^n No.	2Brpy	$CuCl_2(2Brpy)_2$	$CuBr_2(2Brpy)_2$
1240mw	1236w		2x6b	1238mw		
1286ms	1290m	1294w	3	1282m	1282mw	1279mw
1363m 1370sh	1392ms	1381w	14	1351mw		
1421vs	1430m	1420m	19b	1417vs	1416ms	1414m
1455vs		1460m,b	19a	1450vs	1473ms,b	
1550sh,w	1520m	1522w	2x10b			
1571 1582 vs	1560m	1560mw	8b	1564 1574 vs	1557m	1556m
	1591mw	1587w	8a		1588m	1585m
1611m	1596m	1600mw	10a+4			

Table 4.4 Section B

Infrared spectra (375-1700cm^{-1}) of the halopyridine complexes of copper(II)

3Brpy	Vib^{n} No.	$CuCl_2(3Brpy)_2$	$CuBr_2(3Brpy)_2$
410ms	16a	407ws(?)	408m(?)
430ms	11		
499s	2 x 15	473w	474w
591ms	6b	644s	644ms
690s	4	679s	678vs
	12	721m	717, 728 m,b
787ms	10b	798s	795vs
820mw		841w,b	842w,b
	10a	914m	912m
946mw	5	938mw	937mw
	17a	969mw,b	965mw,b
1005s	1	986w	984w
		1027sh	1027
		1029m	1029
			1036
1022m	18a	1050mw	1049

Table 4.4 Section B cont....

3Brpy	Vib^n No.	$CuCl_2(3Brpy)_2$	$CuBr_2(3Brpy)_2$
1083 } ms	13	1059 } ms	1087ms
1093 }	18b	1099 }	1100s
1117m	6a + 10b	1116m	1114m
		1167mw,b	1167mw,b
1189mw	9a	1191m	1193m
	3	1232mw	1230mw
		1304sh	1310sh
1320m	14	1318m	1318ms
1388mw		1370w,b	1370w,b
		1419sh	1416sh
1411s	19b	1427s,b	1422s,b
		1460sh	1460ms,b
1452s	19a	1475ms	1475mw
1558m	8b	1558ms	1557ms
1564ms	8a	1592ms	1592ms

Table 4.4 Section C

4Clpy	Vib^{n} No.	$CuCl_2(4Clpy)_2$	$CuBr_2(4Clpy)_2$
492m	11	497vs(?)	500m(?)
	6b	658mw	653mw
	15 + 16a	708mw	711sh
708ms	12	718w	721sh
	4	728ms	729s
807ms	10b	806s	807vs
	5	835m	832ms
	10a	915w	919sh
	17a	947w	949sh,b
984w	2 x 11	968mw,b	970m,b
999w	1	1000mw,b	1000w
		1027m	1026m
1060mw	18a	1056ws	1056ms
	18b	1092mw	1093mw
1102m	13	1110ms	1111ms
1130w	12 + 6a	1170mw,b	1169mw,b
1213mw	4 +11	1210m	1213m

Table 4.4 Section C cont....

4Clpy	Vib^{n} No.	$CuCl_2(4Clpy)_2$	$CuBr_2(4Clpy)_2$
1220 mw	9a	1230mw	1227mw
1318w	3	1315m	1315m
	14	1350w,b	1341w,b
	12+6b	1377w,b	1372w,b
1407ms	19b	1417s	1416s
1452w	2 x 4	1473s,b	1473s,b
1482ms	19a	1487s	1486ms
	8b	1521w	1520w
		1560ms	1559ms
1573ms,b	8a	1595s	1596s
1642m,vb	2 x 10b	1618w	1618w
	5 + 10b	1654mw	1654m

follow from the work of Green et al,[431] since the spectra are little changed by co-ordination[89,90]. The data for the 2-halopyridine complexes agree well with those of McWhinnie[394], while the spectra of the other complexes have not previously been reported.

The ligand vibrations generally increase in frequency on co-ordination[89], in agreement with the conclusions of extensive work[432] on the simpler cyanide ligand. The smallness of the shifts due to co-ordination has been attributed[90] to backdonation which weakens bonds by partially occupying the ligand π^* orbitals. This is also consistent with the work on cyanides[432], which indicates that the frequencies of the metal-ligand bands increase and those of the ligand bands decrease, as the negative charge accumulated on the metal increases or as metal-ligand π-bonding increases. If partial π-bonding is assumed the higher polarisability of Br^-, relative to Cl^-, explains why the ligand frequencies are generally slightly lower in the bromide complexes.

Table 4.5 details a study made of those ligand modes which have been reported[59,213] to be sensitive to the stereochemistry of the metal ion. It was found that the shift on ν_{6a} (a substituent-sensitive band), due to co-ordination, showed a rough inverse correlation with steric hindrance (measured by ν_1); while that of ν_{10b} (a γ_{CH} band) roughly correlated with ligand basicity.

Table 4.5

Selected ligand vibration frequencies (cm^{-1}) for copper(II) complexes of substituted pyridines.

	Vibration Number							
Compound	16b	6a	12	10b	1	9a	8a	Reference
2Etpy	152	497	796	749	995	1147	1595	433
$CuCl_2(2Etpy)_2$	147	473	809	773	1014	1166	1612	89
$CuBr_2(2Etpy)_2$	154	472	807	769	1011	1166	1611	89
2:6DMepy	216	541		778	995	1155	1592	89
$CuCl_2(2:6DMepy)_2$	285	543		805	1029	1167	1615, 1605	89
$CuBr_2(2:6DMepy)_2$	286	543		805	1030	1166	1616, 1607	89
3Mepy	217	538	800	788	1025	1190	1594	431
$CuCl_2(3Mepy)_2$	212*	542	824	799	1036	1196	1608	356
$CuBr_2(3Mepy)_2$		540	822	799	1035	1198	1608	356
2Brpy	178	315	701	761	991	1146	1573	431
$CuCl_2(2Brpy)_2$		321†	703	760	1023	1148	1588	This work
$CuBr_2(2Brpy)_2$		323†	698	759	1020	1151	1585	This work
2Mepy	207	548	800	751	994	1143	1590	431
$CuCl_2(2Mepy)_2$	204	559	809,816	783,768	1033	1155	1612	89
$CuBr_2(2Mepy)_2$	207	559	808,805	785,770	1034	1155	1612	89
2Clpy	190	428	727	763	994	1150	1577	431
$CuCl_2(2Clpy)_2$		437	728	761	1019	1157	1596	This work
$CuBr_2(2Clpy)_2$		436	735	768	1025	1153	1600	This work
4Mepy	211	515	800	800	997	1224	1608	431
$CuCl_2(4Mepy)_2$	209‡	549	809	815	1034	1230, 1241	1618	356

Table 4.5 cont....

	Vibration Number							
Compound	16b	6a	12	10b	1	9a	8a	Reference
$CuBr_2(4Mepy)_2$		550	809	816	1033	1232, 1238	1618	356
py	403	601	1031	749	991	1217	1578	59
$CuCl_2py_2$	440	641	1041		1015	1219	1600	59
$CuBr_2py_2$	439	640	1038		1015	1223	1600	59
4Clpy	182	414	712	811	996	1219	1575	431
$CuCl_2(4Clpy)_2$	195**	497(?)728		806	1000, 1027	1230	1595	This work
$CuBr_2(4Clpy)_2$		500(?)729		807	1000, 1026	1227	1595	This work
3Brpy	182	319	705	792	1008	1189	1573	431
$CuCl_2(3Brpy)_2$	208†**	410**(?)721		798	1027, 1029	1191	1592	This work
$CuBr_2(3Brpy)_2$		410**(?)717, 728		795	1027, 1029	1193	1592	This work

Notes:

* From reference 270

** From reference 210

† From reference 394

‡ From reference 213

Gill and Kingdon found[356] that stereochemistry affected the relative intensity of the ν_1 (ν_{cc}) and ν_{18a} (β_{CH}) bands. In agreement with this, it is seen that the ν_1 peak is the stronger for the complexes of sterically hindered ligands, and vice versa for those of the unhindered ligands. Further, none of the bands generally split in the complexes of the hindered ligands, but splitting is often seen in the bands of the unhindered ligands. Since the most likely cause of this splitting is coupling of the vibrations of the two organic ligands co-ordinated to the same metal ion, the observed trend is in agreement with the higher symmetry of the planar species expected for hindered ligands. (less bands are infrared-allowed in the higher symmetries).

Phenazine

The spectrum recorded for phenazine agrees well with previous reports,[429,434-436] and is given in table 4.7 with that of $CuCl_2P$ and the assignment of Neto, et al[436]. Since this assignment is incomplete for the A_u and B_{1u} modes, the table also gives the assignment for anthracene[437-441], which is formally analogous. The data offers tenuous evidence for bidentate co-ordination of phenazine in $CuCl_2P$, since the intensities of the bands in the complex are nearly always closer to those of phenazine (which, like bidentate phenazine, has D_{2h} symmetry)[435] than to those of its mono-hydrochloride (which has the lower C_{2v} symmetry.)

Table 4.7

Infrared spectra (cm^{-1}) and assignment for $CuCl_2P$

$CuCl_2P$	Phenazine	PHCl[a]	Anthracene[b]	Assignment: Phenazine[c]	Assignment: Anthracene[d]
422m	393s				$B_{3U}(\beta_{CC})$
452m,b			465s		$B_{IU}(\gamma_{CC})$
472, 480 m,b	477w		473s 492w	$A_u(\gamma_{CC})$	$B_{1U}(\gamma_{CC})\nu_{42}$
578m	594vs		601m	$B_{3u}(\beta_{CC})$	$B_{1u}(\gamma_{CC})\nu_{42}$
633m			620sh		$B_{3u}(\beta_{CC})\nu_{66}$
650, 658 m	655w		656w	$B_{2u}(\beta_{CC})$	$B_{2u}(\beta_{CC})\nu_{55}$
708m	743 s	740vs	726s	$B_{1u}(\gamma_{CH})$	$B_{1u}(\gamma_{CH})\nu_{41}$
735ms	751 s	760vs	743s		$B_{2u}(\beta_{CC})\nu_{54}$
774mw,b		775ms	775w		A_u
834m,b	821ss	825ms	809w	$B_{3u}(\beta_{CC})$	A_u
	856m	880w	886s	$A_u(\gamma_{CH})$	$B_{1u}(\gamma_{CH})\nu_{40}$
897mw	902m	900ms	907m	$B_{2u}(\nu_{CC})$	$B_{2u}(\beta_{CC})\nu_{53}$
934, 945 mw	939sh 944m	920ms 955vw		B_{2u}	
970ms,b	956m	975vw	957s	$A_u(\gamma_{CH})$	$B_{1u}(\gamma_{CH})\nu_{39}$
1000mw	991m	1030s	980mw		$A_u(\gamma_{CH})$
	996m			$B_{3u}(\beta_{CH})$	
1030mw	1004mw		999mw		$B_{3u}(\beta_{CH})\nu_{64}$
1080mw	1068 w		1065w		$B_{3u}(\beta_{CH})$
1100mw	1074 w				
1122m	1108m	1130vs	1125w	$B_{1u}(\gamma_{CH})$	$B_{3u}(\beta_{CH})\nu_{65}$

Table 4.7 cont....

				Assignment	
$CuCl_2P$	Phenazine	PHCl[a]	Anthracene	Phenazine[c]	Anthracene[d]
1149 m,b	1139sh		1150m	$B_{2u}(\beta_{CH})$	$B_{2u}(\beta_{CH})\nu_{52}$
1169 m,b	1146m	1175w	1169w		$B_{3u}(\beta_{CH})\nu_{63}$
1210m	1205sh	1210	1216w		B_{2u}
1215m	1209mw	1225w	1347w	$B_{3u}(\nu_{CC})$	
1306 w	1307w		1298w	$B_{2u}(\nu_{CC})$	$B_{2u}(\beta_{CH})\nu_{51}$
1318 w	1323w	1320w	1316s		$B_{2u}(\nu_{CC})\nu_{50}$
1342mw,b	1357m	1355ms		$B_{2u}(\nu_{CC})$	$B_{3u}(\nu_{CC})\nu_{61}$
		1380ms	1398w		$B_{3u}(\beta_{CC})\nu_{60}$
1433m	1429m	1425m	1448m	$B_{3u}(\nu_{CC})$	$B_{2u}(\beta_{CC})\nu_{49}$
1455sh	1457w	1465vs	1462		$B_{3u}(\nu_{CC})\nu_{59}$
	1476mw			B_{2u}	
1475m,b	1507s				$B_{3u}(\nu_{CC})\nu_{62}$
1519m	1512vs	1520ms	1533w	$B_{3u}(\nu_{CC})$	$B_{3u}(\nu_{CC})\nu_{58}$
1577mw	1576w	1570m	1620m		$B_{2u}(\nu_{CC})\nu_{48}$

Notes:

xy is the ring plane. The x axis bisects all three rings.

a) From reference 435

b) From references 437-441

c) From reference 436

d) From references 437, 439, 440

Triazole

In the absence of an infrared assignment for 1:2:4-Triazole, table 4.8 shows that a good correlation was obtained with the treatment given [442,443] for pyrrole, which has the same symmetry (C_{2v}).

Discussion

The reflectance and far-infrared data concur in suggesting that the complexes, with the exception of $CuCl_2(2Clpy)_2$, may be divided into two groups:

(a) Those of 3Brpy and 4Clpy which probably have polymeric, tetragonally, distorted, octahedral structures similar to those (fig.3.1) of the bis-pyridine complexes [186,237].

(b) $CuBr_2(2Clpy)_2$ and those of 2Brpy, Quin and P which may have even more distorted structures. The far-infrared spectra suggest that all these complexes are square-planar (fig. 3.3; or, in the case of phenazine- fig.7.3) rather than square-pyramidal.

The data on $CuCl_2(2Clpy)_2$ is inconclusive.

While these effects would appear to be connected with the steric hindrance caused by 2-substituents, models show that the matter is finely balanced and depends on the value [390-393] taken for the Van der Waals radius of chlorine. If the value for a covalently bound chlorine atom is used then all these ligands can co-ordinate,

Table 4.8

Infrared spectra (cm^{-1}) and tentative assignments for the copper(II) complexes of 1:2:4-Triazole.

$CuCl_2T$	$CuBr_2T$	Triazole	Pyrrole[442]	Vibration Number[442]	Symmetry*	Form
	414mw	415mw				
480mw	477mw					
514m	499mw	502mw	510w	18	A_2	γ_{CC}
552mw	551mw		565w,b	21	B_2	γ_{NH}
619, 622 ms	618ms		618	5-22		
659mw	662mw	645m	647w	10	B_1	β_{CC}
716w	707 ms,b	717w	711w	1	A_1	β_{CC}
730ms,b	726 ms,b	673vs	768s	22	B_2	γ_{CH}
871m	868ms	882vs	868m	20	A_2	γ_{CH}
942 m,b	946m	927s	1015vs	11	B_1	β_{CH}
		952s	1046vs	12 or 24	B_1 or B_2	β_{CH} OR γ
968	972m	975s	1076vs	2	A_1	β_{CH}
1076ms	1070ms	1050s	1046vs	12 or 24	B_1 or B_2	β_{CH} or γ C
1135m	1130m	1139vs	1146vs	3 or 13	A_1 or B_1	ν_{CC} or β_N
1165m,b	1168m,b	1170s	1146vs	3 or 13	A_1 or B_1	ν_{CC} or β_N
1210mw	1208mw	1247vs	1202w	†		
1236mw		1263vs	1237ω	4	A_1	β_{CH}
1312ms	1307ms	1293ms	1289m	2 x 10		
		1325mw	1313	†		

Table 4.8 cont....

$CuCl_2T$	$CuBr_2T$	Triazole	Pyrrole[442]	Vibration Number[442]	Symmetry*	Form
		1376mw	1384m	5	A_1	ν_{CC}
1415, 1423 ms	1423ms	1415w,b	1418s	14	B_1	ν_{CC}
1481, 1500 mw,b	1466, 1479 mw	1480ms	1467s	6	A_1	ν_{CC}
1515m	1513m	1525, 1538 m,b	1530s	15	B_1	ν_{CC}
1547m	1541m					

*The molecular plane is taken as xz; z is the diad axis

†Not given by Lord and Miller [442]

at normal bond lengths, to a $CuCl_2$ chain like that present in $CuCl_2py_2$. If the value for an ionic chloride ion is used then none of the ligands can co-ordinate in this way. The observation of steric hindrance may, therefore, be attributed to the presence of some ionic copper-halogen bonding, consistent with the co-ordination of strongly basic organic ligands like Quin and 3Mepy. The influence of ligand basicity would stem from the electroneutrality principle. The planar structures of the complexes of the weaker bases may be necessitated in order to obtain maximum metal-ligand π-bonding.

Experimental

The reflectance spectra were determined at room temperature on a Beckman DK2A spectrophotometer fitted with a standard reflectance attachment. Infrared spectra were recorded on a Unicam SP100 spectrophotometer as mulls in Nujol or Halocarbon oil, thin sheets of polythene being used to protect the windows. The Gouy method was used for room-temperature, magnetic measurements, and the tube calibrated[132] with $HgCo(NCS)_4$. X-ray powder photographs were taken using a 9cm. diameter Unicam camera and CuK_α radiation, measurements being made with a Solus-Schall ruler. Copper and ionisable halide (denoted X') were determined gravimetrically[444] as $Cuen_2HgI_4$ and AgX. Analytical grade copper salts were used,

and ligands obtained from Messrs. Koch-Light Ltd. All products were dried at 20°C/25mm.

Dichlorobis (2-chloropyridine) Copper (II)[393]

Copper (II) chloride dihydrate (1.5g, 1 mol.) was dissolved in hot ethanol (30ml) and 2-chloropyridine (2.8g. 3 mol) added. After 1 hour the blue-green crystals of product (1.6g,54%) were filtered off and washed with ethanol. (Found:Cl'19.9; Cu, 17.6. $C_{10}H_8Cl_2Cl'_2CuN_2$ requires Cl',19.6; Cu,17.6%).

Dibromobis (2-chloropyridine) Copper (II)[393] (Found: Br,35.6; Cu14.1.$C_{10}H_8Cl_2Br_2CuN_2$ requires Br, 35.5; Cu,14.1%) was similarly prepared as dark green crystals (89%).

Dichlorobis (2-bromopyridine) Copper (II) Copper (II) chloride dihydrate (1g.1mol) was dissolved in ethanol (10 ml) and 2-Bromopyridine (2.2g; excess) added. After 3 mins. the violet crystals of product (1.8g.68%) were filtered off and washed with ethanol. (Found: Cl.15.7, Cu 14.2. $C_{10}H_8Br_2Cl_2CuN_2$ requires Cl, 15.7; Cu,14.1%).

Dibromobis (2-bromopyridine) Copper (II) 2-bromopyridine (1.4g.2 mol) was added, with stirring, to a solution of copper (II) bromide (1g. 1 mol) in ethanol (20 ml). The dark green crystals of product (1.5g.62%) were

filtered off and washed with ethanol and ether. (Found: Br',30.0; Cu,11.6. $C_{10}H_8Br_2Br'_2CuN_2$ requires Br',29.6; Cu,11.8%).

Dichlorobis (3-bromopyridine) Copper (II) Copper (II) chloride dihydrate (0.85g. 1mol) was dissolved in water (30 ml) and 3-bromopyridine (1.6g 2 mol.) added, with stirring. After 4 hours the product (2 g.89%) was filtered off and washed with water. (Found: Cl,15.8; Cu.14.1. $C_{10}H_8Br_2Cl_2CuN_2$ requires Cl, 15.7; Cu, 14.1%).

Dibromobis (3-bromo pyridine) Copper (II) was prepared in a similar manner. (Found: Br', 29.6; Cu, 11.4. $C_{10}H_8Br_{2/2}^{Br}CuN_2$ requires Br'.29.6; Cu,11.8%).

Dichlorobis (4-chloropyridine) Copper (II) 4-chloropyridine (1.33g. 2 mol) was run into a stirred solution of Copper (II) chloride dihydrate (1g. 1 mol.) in water (50 ml). After standing overnight the pale blue-green product (1.2g. 56%) was filtered off and washed with a little water. (Found: C,33.6; H,2.5; Cl',19.6; Cu, 17.8. $C_{10}H_8Cl_2Cl'_2CuN_2$ requires C,33.2; H,2.2; Cl',19.6; Cu,17.6%).

Dibromobis (4-chloropyridine) Copper (II) was likewise prepared. (Found: Br, 35.6; Cu, 14.1. $C_{10}H_8Cl_2Br_2CuN_2$ requires Br, 35.5; Cu,14.1%).

Dibromo (4-H, 1,2,4-triazole) Copper (II) Sufficient aqueous ammonia solution (6M) was added to a solution of copper sulphate pertahydrate (3.5g. 1 mol), in water (30 ml.) to redissolve the initial precipitate.

To this solution was added 1:2:4;triazole (1.95g. 2 mol) dissolved in water (10 ml). After standing for 2 hours the violet precipitate was filtered off, washed with water and dissolved in cold aqueous ammonia solution (900 ml; 6M). The solution was allowed to lose ammonia, when violet crystals formed. These were filtered off, washed with water, dissolved in warm aqueous hydrobromic acid (600 ml; 4M) and the solution filtered. On standing for 2 months, dark brown crystals precipitated from the filtrate. This product (1.5 g. 37%) was filtered off and washed with water. (Found: C, 8.1; H, 1.2; Br, 54.6; Cu, 21.7. $C_2H_3Br_2CuN_3$ requires C, 8.2; H, 1.0; Br, 54.7; Cu, 21.7%)

Dichloro (phenazine) Copper (II) A solution of copper (II) chloride dihydrate (0.5g. 1 mol) in cold acetone (40 ml) was added, with stirring, to a solution of phenazine (0.53g. 1 mol) in cold acetone (50 ml). The fine brown crystals of crude product (0.7g. 76%) were filtered off and washed with acetone and ether. Purification was achieved by heating these crystals for 3 hours at 85°C in an oven. (Found: Cl, 22.5; Cu, 20.9. $C_{12}H_8Cl_2CuN_2$ requires Cl, 22.5; Cu, 20.2%)

CHAPTER V

COMPLEXES OF THE HALOPYRIDINES WITH COBALT (II) HALIDES

The effect of steric hindrance of amine co-ordination on the structures of the copper (II) complexes of substituted pyridines has been discussed in Chapter IV. The smaller molecular volume of α-$CoCl_2py_2$ compared[186] with that of $CuCl_2py_2$ suggested that these effects might be even more pronounced in the complexes of Cobalt (II). The work was therefore extended to these complexes. The halopyridine ligands were employed in order to study the effects of their low basicity.

After D.J. Walker had prepared[393] and characterised the tetrahedral complexes $CoX_2(2Clpy)_2$ (where $X^-=Cl^-, Br^-, I^-$), the complexes listed in Table 5.1 were obtained. Subsequently McWhinnie reported[394] some of these complexes of the 2-halopyrdines, and suggested, on the evidence of electronic and far-infrared spectra, that they had tetrahedral structures. Very recently Gill and Kingdon have described[358] the infrared and far-infrared spectra of most of these compounds. On the basis of the colour of the complexes they proposed that all those containing 2-halopyridines were tetrahedral, while those of the 3- and 4- halopyridines were octahedral; with the exception of the tetrahedral $CoI_2(3Brpy)_2$, $CoBr_2(4Brpy)_2$ and $CoI_2(4Brpy)_2$ species. In all cases the present work confirms these conclusions.

Results

In addition to the complexes listed in table 5.1, impure

Table 5.1

Reflectance spectra (kK) and room temperature magnetic moments (B.M.) of the cobalt(II) halopyridine complexes.

Complex	μ_{eff}	Band Maxima
$CoBr_2py_2$	4.50	16.5(vs,sh),15.9(1.19),15.3(1.22),9.1(.73),6.8(.85), 6.0(.83)
$CoCl_2(2Clpy)_2$	4.53	17.2(1.02),15.9(1.12),8.7(.65),7.2(.85),6.1(.87)
$CoBr_2(2Clpy)_2$	4.45	15.7(1.65),7.8(.80),7.0(.95),6.0(.85)
$CoI_2(2Clpy)_2$	4.63	15.8(vs,sh),15.0(1.22),7.8(.74),6.7(.82),5.7(s,sh)
$CoCl_2(2Brpy)_2$	4.52	17.1(1.11),15.7(1.28),8.6(.63),7.3(.80),6.1(.76)
$CoBr_2(2Brpy)_2$	4.61	15.5(1.41),8.2(.73),7.0(.88),6.1(.79)
$CoCl_2(3Brpy)_2$	5.25	18.9(.27),18.0,16.4(.21),14.7,8.9(.05,b),6.5(.08,b)
$CoBr_2(3Brpy)_2$	5.19	18.3(.53),17.4,15.2(.38),12.6,8.2(.15,b),5.6(.26)
$CoI_2(3Brpy)_2$	4.77	16.0(vs,sh),15.3(.99),14.6(.99),9.0(.54),7.0(.62),6.1(.
$CoCl_2(4Clpy)_2$	5.12	18.9(.31),17.9,16.1(.31),14.7,8.7(.05),6.2(.11)
$CoBr_2(4Clpy)_2$	5.16	15.1(sh,vs),14.5(.87),7.6(sh),5.2(.60,b)
$\alpha CoCl_2py_2$	5.15	18.8(.42),18.0,15.9(.32),8.6(.10,b),5.9(.17,b)

specimens of $CoI_2(2Brpy)_2$, $CoBr_2(4Clpy)_4$ and $CoI_2(4Clpy)_2$ were obtained. Gill and Kingdon have isolated the 2Brpy complex [358]. No other tetrakis-complexes could be prepared, and the nature of $CoBr_2(4Clpy)_4$ is not clear at the present.

Diffuse Reflectance Spectra;

The data of table 5.1 and the considerations of Chapter I indicate that the complexes contain tetrahedral or octahedral high-spin Cobalt (II) species. Figure 5.1 illustrates some of the spectra obtained.

Tetrahedral Complexes

All the complexes of the 2-halopyridines, together with $CoI_2(3Brpy)_2$ show two intense bands near 7kK and 16kK. The spectra are very similar to those [191] of the tetrahedral complexes $CoBr_2py_2$ [451,187] and $CoCl_2(p\text{-}tol)_2$, suggesting that the two bands are due to the ν_2 and ν_3 spin-allowed transitions. The data agree well with those of McWhinnie, [394] though he reported weak bands near 4kK, where ν_1 is expected. Such bands have been found, [210] using a Unicam SP200G spectrophotometer, but were extremely weak. Since these bands are also exhibited by the pure ligands, it is considered that they are due to infrared overtones, and that the electronic ν_1 band is weak (as it is forbidden in pure T_d symmetry [452]).

Both ν_2 and ν_3 show splitting which confuses the measurement of

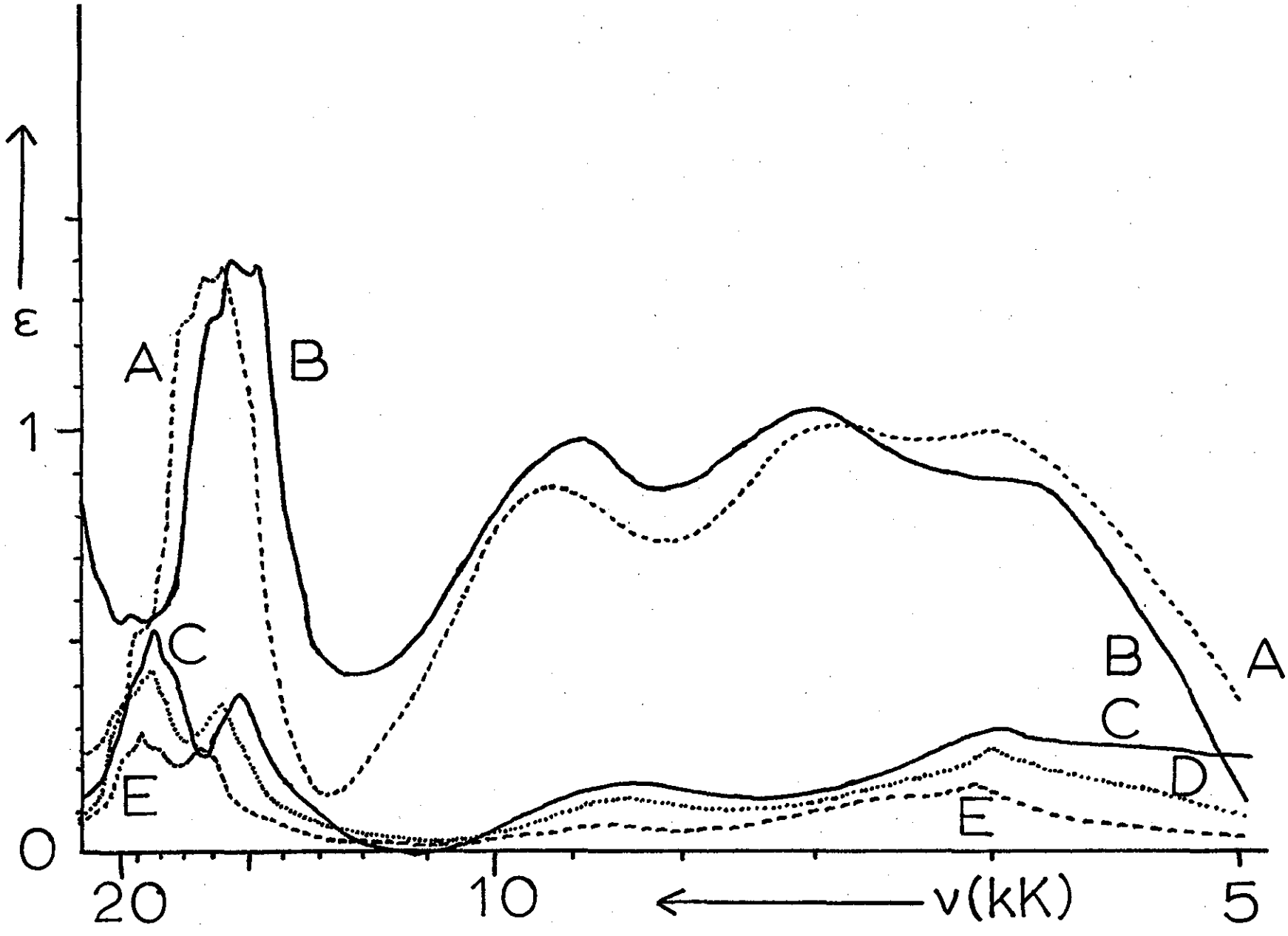

Figure 5.1

the precise band centres. In the case of the ν_2 band this has been[191,452] attributed to the $^4A_2$, $^4B_1$ and $^4B_2$ components in C_{2v} symmetry, of the $^4T_{1g}(F)$ state. The splitting of the ν_3 band is further complicated by spin-orbit coupling[452] of the $^4T_{1g}(P)$ state with the components of a close-lying ^2G term, or by intercomplex interaction[191].

Following Cotton, et al,[195] the centres of gravity of each of the ν_2 and ν_3 systems were estimated visually. The parameters, given in table 5.2, were calculated using the methods of Chapter II. These values are approximate, but do conform to the usual spectrochemical and nephelauxetic series for the halide ligands (See Chapter I).

The highest component of ν_2 appears at 9.1 kK for $CoBr_2py_2$, but at 7.8kK for $CoBr_2(2Clpy)_2$; and at 9.0kK for $CoI_2(3Brpy)_2$, but at 7,8kK for $CoI_2(2Clpy)_2$[167,196]. This data therefore supports the suggestion that the frequency of this component is influenced by steric hindrance.

Octahedral Complexes

The spectra of $CoCl_2(4Clpy)_2$ and the remaining complexes of 3Brpy are extremely similar to that of the octahedral complex.[186] α-$CoCl_2py_2$; consisting of two weak peaks near 17kK and two broad, weak peaks near 8.5kK and 6.0kK. After Ferguson[371], the peak at 16kK is assigned to the ν_2 transition, and the components near 18.5kK to ν_3. The ground-state may be $^4B_{3g}(F)$, and the components of ν_3 are

Table 5.2

Calculated ligand field parameters (kK) for the cobalt(II) complexes with halopyridines.

Complex	Stereochem.	Observed Frequencies			Calculated parameters			
		ν_1	ν_2	ν_3	Dq	B'	λ '	ν_1
$CoBr_2py_2$	T_d		6.8	15.9	.39	.72	-.12	3.9
$CoCl_2(2Clpy)_2$	T_d		7.2	16.4	.41	.74	-.13	4.1
$CoBr_2(2Clpy)_2$	T_d		7.0	15.7	.41	.70	-.11	4.1
$CoI_2(2Clpy)_2$	T_d		6.7	15.0	.39	.67	-.15	3.9
$CoCl_2(2Brpy)_2$	T_d		7.3	15.7	.42	.69	-.13	4.2
$CoBr_2(2Brpy)_2$	T_d		7.0	15.5	.41	.68	-.15	4.1
$CoCl_2(3Brpy)_2$	O_h	7.7	16.4	18.9	.87	.82		7.7
$CoBr_2(3Brpy)_2$	O_h	6.9	15.2	18.3	.81	.82		7.1
$CoI_2(3Brpy)_2$	T_d		7.0	15.3	.41	.67	-.20	4.1
$CoCl_2(4Clpy)_2$	O_h	7.5	16.1	18.9	.86	.83		7.5
$\alpha CoCl_2py_2$	O_h	7.3	15.9	18.8	.85	.83		7.4

probably due to transitions in D_{2h} symmetry, to the $^4B_{1g}$(P), $^4B_{2g}$(P) and $^4B_{3g}$(P) levels. ν_3 was estimated as the centre of gravity of the $^4T_{1g}$(P) system, and the parameters of table 5.2 were obtained from this value and that of ν_2. The value predicted for ν_1 is seen to be close to the mean of the two low frequency bands (this mean is given in table 5.2 as the observed frequency ν_1), which are therefore probably components of the ν_1 transition. It is not clear why two, rather than three, components of this band are observed. The calculations above are tentative, since the extent of the ground-state splitting is unknown.

These estimated values of Dq and B' do conform to the spectrochemical series for the halide ligands, but no significant trend in B' is apparent. The order of Dq for the amine ligands is py < 4Clpy < 3Brpy, which is the reverse of that for basicity but identical to that (See Chapters 1 and 3) expected if Co-N π-bonding is present. Since the differences in Dq values are so small they offer extremely unreliable evidence for π-bonding.

A comparison of the ligand-field parameters (using the rules of average environment: $Dq_t \backsim 4Dq_o/9$, and $B'_t \backsim B'_o$) reveals that B' values are slightly lower, but Dq values are similar in the tetrahedral complexes relative to the octahedral species.

The spectrum of $CoBr_2(4Clpy)_2$ has an intensity intermediate

between those of typical [56] octahedral and tetrahedral chromophores. This complex may be a mixture of tetrahedral and octahedral isomers. Apart from a shoulder at 7.6kK (which may be the octahedral ν_1, band), the spectrum is similar to (but weaker than) that of the tetrahedral $CoBr_2(4Clpy)_4$ complex. $CoBr_2(4Clpy)_2$ may, therefore, be octahedral, but mixed with sufficient of the tetrakis-complex to dominate the spectrum without affecting the magnetic moment (see later) or analysis results. None of these spectra bear any resemblance to those of square-planar [323] or five-co-ordinate [318,322,453-460] Co(II) complexes.

Magnetic Susceptibilities

The room-temperature magnetic moments of the complexes are given in table 5.1 . They are typical [19] of high-spin Cobalt (II) complexes and fall cleanly into two ranges: 4.45-4.77B.M. and 5.12-5.25B.M.

The former range is generally characteristic [19] of tetrahedral species, according to equation 1.14 for a $^4A_2$ ground-state, and includes $CoI_2(3Brpy)_2$ and all the complexes of the 2-halopyridines. Table 5.2 lists the values of the effective spin-orbit coupling constant (λ'), calculated using equation 1.14. These are generally higher than the free-ion value (-0.172kK), as usual [149] in the presence of covalent bonding. Differences in the values of λ' are probably not significant since the estimation of Dq is subject to error.

The remaining complexes of 3Brpy and those of 4Clpy have moments in the higher range, which is generally observed[19] for octahedral structures.

Other stereochemistries are not excluded by the magnetic data. Square planar $Co(Sal)_2.2H_2O$[323] and square-pyramidal $CoCl_2(paphy)$[322] have moments of 4.74B.M. and 4.84B.M. at room-temperature. Further, the octahedral complexes CoF_2[19] and $Co(PAH)_3I_2$[461] have moments as low as 4.73B.M. and 4.71.BM.

Magnetic data over a temperature range would resolve these ambiguities, but was not available. The observed moments are not conclusive evidence for octahedral or tetrahedral structures, but support the other results which indicate these sterochemistries.

Electronic Spectra in Solution

Polymeric octahedral structures have been indicated above for the complexes $CoCl_2(3Brpy)_2$ and $CoBr_2(3Brpy)_2$. These complexes were insoluble in acetone or benzene, but the bromide was slightly soluble in dichloromethane and the chloride in nitromethane. In these solvents, the complexes (in the presence of excess ligand to prevent dissociation) gave spectra consistent with tetrahedral configurations, have strong ν_3 bands at 16.6kK (ε=800) for the chloride and at 15.7 kK (ε=1,000) and 16.85(sh) for the bromide.

Similar changes from solid-state, octahedral, polymers to tetrahedral monomers in solution have been previously observed for $CoCl_2py_2$,[187,191] $Co(NCS)_2py_2$ and $Co(NCS)_2(4Mepy)_2$[175]. The spectrum of $CoI_2(3Brpy)_2$ in chloroform solution was similar to that in the solid state, having an intense ($\epsilon \sim 900$) ν_3 band consisting of three components (14.6vs, 15.5sh, 15.9 sh) with a centre of gravity at 15.2kK. The values of ν_3 for the three complexes of 3Brpy, in solution, reflect the expected variations in Dq and B' according to the spectrochemical and nephelauxetic series for the halide ligands.

Ligand Infrared Spectra

The observed frequencies of the complexes in the region 375-1700 cm^{-1} are collected in table 5.3 and have been assigned in the same way as those of the copper (II) complexes. The data agree well with those of McWhinnie[394] and of Gill and Kingdon[358].

It has been suggested[90,175,394] that the splitting of infrared bands may be expected in tetrahedral sterochemistries. The ν_1, ν_4, ν_{10a}, ν_{10b}, ν_{11}, ν_{16a}, ν_{18a} and ν_{19b} bands often split in the complexes of 2Clpy and 2Brpy and also in $CoI_2(3Brpy)_2$. These splittings are in agreement with the tetrahedral structures.suggested above for these complexes, while the infrequency of splitting for the other complexes is consistent with octahedral structures. Caution has been suggested[90,394] in the use of such an observation as a stereochemical

Table 5.3

Infrared spectra (375-1700cm^{-1}) of Co (II) complexes with substituted pyridines.

2Clpy	$CoCl_2(2Clpy)_2$	$CoBr_2(2Clpy)_2$	$CoI_2(2Clpy)_2$	Vib. No.	2Brpy	$CoCl_2(2Brpy)_2$	$CoBr_2(2Brpy)_2$
407ms	419m	418m		16a	405s	417s	432m
425ms	443mw	442w		6a			
478m	478m	477m		11	466s	463ms	467mw
615m	641mw	641mw	640sh	6b	611ms	639m	640mw
655w,b			651m				
720vs	727mw	726m	728m	12 4	695vs	699vs 723mw,b	694m
762vs	752 760 ms	755ms	757m 763sh	10b	756vs	751 760 vs	749s 757ms
823mw		837w	839w	16a + 6a			
880mw		878 884 mw	895ms	10a	883mw	881m	882mw
920w,b		928w		5	930mw	931w	
960m	966mw,b	969mw,b	965ms	17a	958w	960w	
988s	1018 1021 m	1018m	1018m	1	984s	1018 1021 ms	1013 1018 m
1042s	1053 1057 m	1052 1056 mw	1052mw	18a	1040s	1058ms	1052m

Table 5.3 cont....

2Clpy	$CoCl_2(2Clpy)_2$	$CoBr_2(2Clpy)_2$	$CoI_2(2Clpy)_2$	Vib. No.	2Brpy	$CoCl_2(2Brpy)_2$	$CoBr_2(2Brpy)_2$
1082s	1087mw	1085mw	1075w	18b	1076vs	1081ms	1079m
1119vs	1130m	1128m	1120ms	13	1106vs	1116s	1111ms
1150s	1152m	1152m	1152m	9a	1146ws	1151s	
	1170mw,sh,b	1177w	1167sh	6a + 12			
1240mw		1250w	1249w	2 x 6b	1238mw	1240w,b	1267w
1286ms	1292, 1297 mw	1289, 1294 mw	1291mw	3	1282m	1289, 1296 m	1286, 1292 m
1363sh, 1370m	1377m	1377mw	1370w	14	1351mw		
1421vs	1424mw	1423m	1420m,b	19b	1417vs	1410, 1421 vs	1409, 1418 s
1455vs	1474vs	1475m,b	1487sh	19a	1450vs	1457s,b	1459m,b
1550sh,w	1559mw	1557mw	1557mw	2 x 10b		1555s	1552m
1571, 1582 vs	1596m	1581w,sh 1595m,b	1580, 1594 m	8b 8a	1564, 1574 vs	1561sh 1591vs	1558sh 1589s
				6 b + 1	1603mw	1638w	1636w
1611m		1658w		10a + 10b	1642, 1659 w,b	1653w	1653mw

Table 5.3 cont....

Vib. No.	3Brpy	$CoCl_2(3Brpy)_2$	$CoBr_2(3Brpy)_2$	$CoI_2(3Brpy)_2$
16a	410ms	409m	402m	404ms
11	430ms	433sh		444sh
2 x 15	499ms			493mw 553mw
6b	591ms	635ms	636m	646m
12, 4	690s	676s 705mw	679ms 713w	678ms 719sh
			723mw	731m
10b	787ms	781s	786ms	765mw, 790ms
	820mw			838mw,b
10a		900mw	909mw	888, 899 mw
5	946mw	934w	938w	939mw
17a		976w	979w	970m,b
1	1005s	1022s	1027m	1036, 1050 m
18a	1022m	1041m	1041mw	
13	1086, 1093 ms	1083mw	1084mw	1082mw
18b		1094ms	1098m	1100mw
10b+ 6a	1117m	1119m	1113mw	1112mw
		1167w	1168w	1167mw,b
9a	1189mw	1190m	1189m	1192mw
3		1230w	1230w	1238mw
		1262w	1263w	
14	1320m	1320m	1316mw	1305m
				1386ms

Table 5.3 cont....

Vib. No.	3Brpy	$CoCl_2(3Brpy)_2$	$CoBr_2(3Brpy)_2$	$CoI_2(3Brpy)_2$
19b	1411s	1422s	1419m,b	1420m
19a	1452s	1454w	1453b,mw	1460sh
				1475ms
8b	1558m	1557m	1558m	1552m
8a	1564ms	1589ms	1588m	1591m

Vib. No.	4Clpy	$CoCl_2(4Clpy)_2$	$CoBr_2(4Clpy)_2$
6a		437w,b	
11	492m	492s	493ms
6b		658mw	
12, 4	708ms	710sh 722s,b	726m
10b	807ms	805vs	801m
		803m	
5		887w	893w
17a		967w	972mw,b
2 x 11	984w	994w	
1	999w	1017ms	1018mw
18a	1060mw	1055ms	1057mw
18b		1089m	
13	1102m	1109ms	1110mw
12 + 6a	1130w	1155mw,b	1159, 1168 mw

Table 5.3 cont....

Vib. No.	4Clpy	$CoCl_2(4Clpy)_2$	$CoBr_2(4Clpy)_2$
4 + 11 9a	1213 mw 1220	1208m,b 1224sh	1212mw
3	1318w	1313m	1314w,b
19b	1407ms	1412ms	1412mw
19a	1482ms	1486ms	1485w
8b		1562m	1562w
8a	1573ms,b	1592s	1593m
2 x 10b 5 + 10b	1642m,vb	1650w,b	1619w

criterion.

As in the previous chapter, the bands were examined for structural information. In agreement with Gill and Kingdon[358] the ν_{16a} band shows a larger shift due to co-ordination in the tetrahedral complexes than in the octahedral species. The opposite trend was apparent for the ν_{10b} and ν_{12} bands. However, generally the band shifts due to co-ordination are larger in the tetrahedral complexes. This is probably caused by the stronger σ-bonding permitted by the shorter bands in this stereochemistry[58,175].

Other frequency shifts were found when the complexes of the same amine, with different anions, were examined. For the tetrahedral complexes, the chlorides generally had higher ligand frequencies than the bromides. This may be explained by the higher polarisability of Br^- which, as discussed in Chapter I, can cause more transfer of metal electrons into the ligand π^* orbitals. Such π-bonding cannot be so extensive in the polymeric octahedral complexes, because of the unfavourable orientation of the heteroaromatic rings, and it is not surprising that the opposite direction of shifts prevails. This latter effect is consistent with the shorter Co-N bands, expected in the bromides by comparison[186] with the structureal studies on the Copper(II) complexes. The ligand frequencies were even lower (as expected from the argument above) in the iodide complexes than in the bromides,

when both were tetrahedral. However, a larger, opposite effect was apparent for the complexes of 3Brpy, due to the change in stereochemistry.

Far-Infrared data

McWhinnie[394] and Gill and Kingdon[358] have recorded the Co-N and Co-X stretching frequencies for the tetrahedral complexes, and these are listed in table 5.4. The metal-ligand bands of the octahedral complexes were generally too low for the instruments available to measure because of the weaker bonding mentioned above.

In T_d or C_{2v} symmetry, two ν_{Co-X} and two ν_{Co-N} bands should be infrared active. The two observed ν_{Co-X} frequencies confirm the tetrahedral nature of the complexes of the 2-halopyridines. A second ν_{Co-N} band would probably fall below the range studied.

The lower basicities of the 2-halopyridines compared with that of pyridine lead, as discussed in Chapter IV, to lower Co-N stretching frequencies. However, the slightly higher values of ν_{Co-N} and ν_{Co-X} for the 2Clpy complexes, relative to those of 2Brpy, do not follow pK_a and may be connected with the mass-effect and π-acceptor character.

As noted by Clark and Williams[59,352], the ν_{Co-X} bands in these complexes occur at somewhat higher frequencies than are found[462] in the tetrahalocobalt(II) anions. This is presumably due to the back-donation possible when heteroaromatic molecules are co-ordinated.

Table 5.4

Reported far infrared data (cm^{-1}) for cobalt(II) complexes with substituted pyridines.

Complex	ν_{Co-X}	ν_{Co-N}	Reference
$CoCl_2(2Clpy)_2$	332,312	227	358
$CoBr_2(2Clpy)_2$	260,242	224	358
$CoI_2(2Clpy)_2$	239,211	226	358
$CoCl_2(2Brpy)_2$	328,317	216	358
$CoBr_2(2Brpy)_2$	251,236	215	358
$CoI_2(2Brpy)_2$	228,203	218	358
$CoI_2(3Brpy)_2$	235(?)	226(?)	358
$CoCl_2py_4$	230	217	59
$CoBr_2py_4$	<200	214	59
α-$CoCl_2py_2$	234	227	270
β-$CoCl_2py_2$	344,304	252	59
$CoBr_2py_2$	274,242	250	59
CoI_2py_2	237	246	59
$CoCl_4^{2-}$	300		60
$CoBr_4^{2-}$	227		60

Discussion

The electronic spectra and magnetic moments strongly support the assignment of tetrahedral structures to $CoI_2(3Brpy)_2$ and the complexes of 2Clpy and 2Brpy; also octahedral structures to the remaining complexes of 3Brpy and 4Clpy. The data on the ligand and metal-ligand infrared frequencies are consistent with these proposed structures. The stoicheiometry of the complexes indicates that the tetrahedral species are monomeric (figure 3.4) while the others have polymeric octahedral structures, probably like that of α-$CoCl_2py_2$[186] (figure 3.2). The trans- rather than cis- configuration is preferred for the polymers, because of the relatively low intensity and large splitting[18] of the electronic bands, and the general absence of ligand infrared band splittings.

The following comments may be made on these structures:

1. The complexes of $CoCl_2$ and $CoBr_2$ with 3Brpy and 4Clpy have octahedral structures, in contrast to the tetrahedral complexes with the 3- and 4-alkylpyridines[167,177]. This can be explained, as in Chapter I, via the electroneutrality principle and the small negative charge transferred to the metal ion by the weaker bases.

2. The tetrahedral natures of the complexes of cobalt(II) iodide with 3Brpy and 4Brpy (and also the impure $CoI_2(4Clpy)_2$ complex)

may be compared with all the tetrahedral iodo-complexes in table 3.4. This preferred stereochemistry has earlier (see Chapter I) been attributed to the high polarisability of the iodide ion, aided by the high C.F.S.E. for tetrahedral cobalt (II).

3. As anticipated earlier, the influence of steric hindrance appears to be greater in the cobalt (II) complexes than in those of copper (II). The CoX_2L_2(L=2Clpy,2Mepy)[175,269] complexes are definitely four-co-ordinate whereas $CuCl_2(2Clpy)_2$ may have a structure intermediate between four- and six-co-ordination, and $CuCl_2(3Mepy)_2$ is five co-ordinate[253].

4. The absence of tetrakis-complexes of the 2-halopyridines may be attributed to steric hindrance. The virtual absence of tetrakis-complexes of 3Brpy and 4Clpy (the nature of $CoBr_2(4Clpy)_4$ is uncertain) cannot be explained in this way, and by comparison py[78,59] and the 3- and 4- alkylpyridines[175,269,177] do form such species (see table 3.4). The complexes CoX_2py_4 are also known[273,334] in solution, whereas even in the presence of excess ligand, $CoX_2(3Brpy)_4$ did not form.

Thermochemical cycles,[370] constructed for these systems, show that many factors may be involved. The ligand latent heat of vaporisation is involved as well as subtleties of crystal packing such as hydrogen bond formation. In solution, heats of solvation enter the cycle.

However, it appears that if the main effect is due to the relative energies of bond formation in the various species, then the ligand basicity may be important. Thermal[78], far-infrared[59,270] and stability-constant data all[273,370,334] indicate that CoX_2L_4 complexes are less stable than either octahedral or tetrahedral CoX_2L_2 complexes of the same ligands.[270] Far-infrared spectra show, further, that the M-N bond strengths decrease with the ligand basicity. Hence, weakly basic amines will yield even less stable CoX_2L_4 species because these contain four Co-N bonds, whereas CoX_2L_2 complexes only contain two (per cobalt ion.)

Experimental

Solution spectra were recorded using 1 cm. silica cells and a Beckman Dk2A or a Unicam SP700 spectrophotometer. A saturated solution ($\sim 2.10^{-4}$M) of $CoCl_2(3Brpy)_2$ in $MeNO_2$ was used. The spectra of $CoBr_2(3Brpy)_2$ and $CoI_2(3Brpy)_2$ were recorded in CH_2Cl_2 ($\sim 1.10^{-3}$M). Large concentrations ($\sim 7.10^{-2}$M) of 3Brpy were added to these solutions to prevent dissociation. Further additions of 3Brpy were observed to have no effect on the position of ν_3 (but slightly altered the band shape). In each case a solution ($\sim 7.10^{-2}$M) of 3Brpy, in the appropriate solvent, was placed in the reference beam.

Cobalt was determined gravimetrically as the anthranilate[444]. Other details have been given in the previous chapter.

Dichloro bis (2-chloropyridine) cobalt (II)[393]

2 chloropyridine (2.9g.3 mol) was added to a hot solution of cobalt (II) chloride hexahydrate (2 g. 1 mol) in ethanol (25 ml). The solvent was evaporated to leave dark blue crystals of the product (1.8g, 60%). (Found: Cl', 20.0; Co, 16.7. $C_{10}H_8Cl_2Cl_2'N_2Co$ requires Cl', 19.9- Co, 16.5%). Blue crystals of Dibromobis (2-chloropyridine) Cobalt (II)[393]. (Found: Br, 35.8; Co, 13.1.$C_{10}H_8Cl_2Br_2CoN_2$ requires Br,35.8; Co,13.2%) and green-black crystals of Di iodobis (2-chloropyridine) cobalt (II)[393]. (Found: I,47.7; Co,11.2.$C_{10}H_8Cl_2I_2CoN_2$ requires I,47.0;Co,10.9%) were similarly prepared.

Cobalt(II) chloride dihydrate Powdered Cobalt (II) chloride hexahydrate was heated at 80-100°C in a vacuum oven for 2 days.

Cobalt (II) bromide Cobalt (II) bromide hexahydrate was dried in a vacuum desiccator at room temperature for some hours. The sample was then placed in a vacuum oven and the temperature gradually raised to 80°C and maintained at this level for 24 hours.

Dichlorobis (2-bromopyridine) cobalt (II). Cobalt (II) chloride dihydrate (.9g. 1 mol) and 2-bromopyridine (1.9g; excess) were stirred together at 110°C for 15 minutes. Benzene (20 mol) was added, with stirring, and the mixture filtered after cooling. The bright blue product (2.2g. 91%) was washed with benzene and acetone. (Found: Cl, 16.2; Co,13.5. $C_{10}H_8Br_2Cl_2CoN_2$ requires Cl,15.9; Co,13.2%).

Dibromobis (2-bromopyridine)cobalt (II) (Found: Co, 10.9. $C_{10}H_8Br_2Br'_2CoN_2$ requires Co, 10.6%) was similarly prepared from cobalt (II) bromide.

Dichlorobis (3-bromopyridine)cobalt (II)

3-bromopyridine (1.3g, 2 mol) was added to a solution of cobalt (II) chloride hexahydrate (1 g. 1 mol) in water (10 ml). After allowing to stand over-night the pale violet product (0.4g. 21%) was filtered off and washed with water (Found: Cl, 16.1; Co, 13.4. $C_{10}H_8Br_2Cl_2CoN_2$ requires Cl, 15.9; Co, 13.2%).

Dibromobis (3-bromopyridine) cobalt (II)

3-bromopyridine (1.3g, 2 mol) was added to a solution of cobalt (II) bromide hexahydrate (1.3 g. 1 mol) in ethanol (5 ml). On scratching the walls of the vessel, the pale violet product (1.3g, 59%) was precipitated. This was filtered off and washed with ethanol and ether. (Found: Br', 29.6; Co, 10.7. $C_{10}H_8Br_2Br_2'CoN_2$ requires Br', 28.8; Co, 10.6%).

Di iodobis (3-bromopyridine) cobalt (II)

3-bromopyridine (1.1g, 2 mol) and cobalt (II) iodide dihydrate (1.2g, 1 mol) were stirred together at 110°C for 15 mins. Ether (20ml) was added, and after cooling the green product (1.8g, 83%) filtered off and washed with ether. (Found: C,18.4; H,1.3; Co,9.9; N,4.3. $C_{10}H_8Br_2I_2CoN_2$ requires C, 19.1; H,1.3; Co,9.4; N,4.5%).

Dichlorobis (4-chloropyridine) cobalt (II)

4-chloropyridine (1.5g. 2 mol) was added to a stirred solution of cobalt (II) chloride hexahydrate (1.2g. 1 mol) in ethanol (8 ml). The pale violet product (1.7g. 94%) was filtered off and washed with ether. (Found: Cl', 19.9; Co,16.3. $C_{10}H_8Cl_2Cl_2'CoN_2$ requires Cl', 19.9; Co,16.5%)

Dibromobis (4-chloropyridine) cobalt (II)

A pink compound (Co=12.2%) was obtained by a method similar to that employed for the chlorocomplex. When heated at 70°C, overnight, this gave the green product. (Found: Co,13.2. $C_{10}H_8Cl_2Br_2CoN_2$ requires Co,13.2%).

CHAPTER VI

THE COMPLEXES OF NICKEL (II) WITH HALOPYRIDINES

The structures listed in table 3.5 show the influences of both steric and basicity factors. A similar conclusion was reached in the previous chapter concerning the complexes of cobalt (II) with the halopyridines. The complexes listed in table 6.1 were prepared in order to study these effects in the halopyridine complexes of nickel (II) halides. None of these complexes, nor any nickel (II) halide complexes with weak bases, had been previously reported.

No evidence was found for the existence of complexes of the 2-halopyridines with $NiCl_2$ or $NiBr_2$, and only impure $NiI_2(2Clpy)$ and $NiI_2(2Brpy)$ species of uncertain structure, could be prepared. Likewise, it was not possible to prepare the pure $NiI_2(3Brpy)_2$ or $NiI_2(4Clpy)_2$ complexes. Attempts to prepare a tetrakis complex of 3Brpy with $NiCl_2$ also failed.

Diffuse Reflectance Spectra

The electronic band maxima for these complexes are detailed in Table 6.1. Figure 6.1 compares the reflectance spectra of the 3Brpy complexes with that of the octahedral[187] $NiCl_2py_2$ polymer. The spectra are very similar to those[197] of $NiCl_2py_2$ and $NiBr_2py_2$, exhibiting weak peaks near 24kK, 14kK and 8kK. In addition, all show a shoulder near 12kK and a broad, very weak peak close to 6kK.[250] The octahedral monomer $NiBr_2py_4$ has a similar spectrum (see table 6.1), differing only in the addition of a broad 10.7kK band and the absence of the 6kK peak.

Table 6.1

Diffuse reflectance maxima (kK) and room temperature magnetic moments (B.M.) of the nickel(II) complexes with halopyridines.

Complex	μ_{eff}	Band Maxima
$NiCl_2(3Brpy)_2$	3.24	24.1(.27), 14.1(.15), 12.3(sh), 8.5(.13b), 6.2(.06,vb)
$NiBr_2(3Brpy)_2$	3.20	23.0(.44), 19.4(sh), 13.3(.21), 11.4(sh), 8.0(.15,b) 6.0(
$NiCl_2(4Clpy)_2$	3.35	24.1(.47), 14.1(.24),12.3(sh),8.5(.20,b), 6.2(.09,vb)
$NiBr_2(4Clpy)_2$	3.21	23.8(.58), 20.0(sh), 13.7(.27), 11.4(sh), 8.2(.28,b) 6.0(.18,vb)
$NiCl_2py_2$	3.37	24.2(.26), 22.7(sh), 13.8(.18), 11.9(sh), 8.2(.18,b) 6.0(.13,vb)
$NiBr_2py_2$	3.35	23.4, 21.4(sh), 19.8(sh), 13.7, 11.6(sh), 8.0, 5.8(sh)
$NiBr_2Py_4$	3.22	25.2(.26), 20.4(sh,w), 15.5(.16), 13.3(sh), 10.7(.10,b) 8.0(.17,vb)

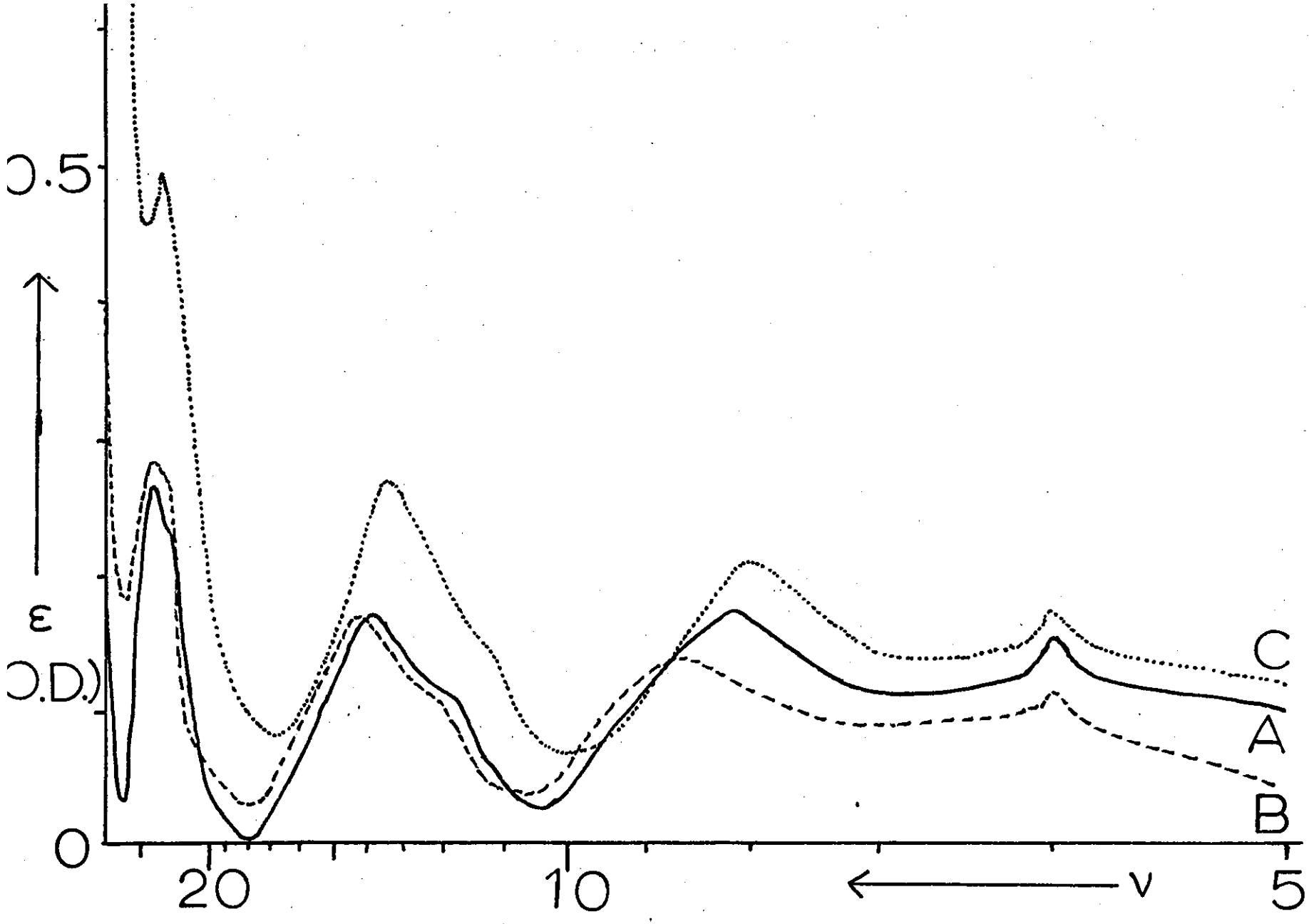

Figure 6.1

The octahedral nature of these complexes is confirmed by the similarity of their spectra to that[463] of $NiCl_2(Th)_4$[464] which has been assigned by Hare and Ballhausen. By analogy, the bands at 24.2kK, 13.8kK and 8.2kK in $NiCl_2py_2$ may be assigned to the ν_3, ν_2 and ν_1 transitions in octahedral symmetry. This agrees with the assignment of König and Schläfer,[188] Brown et al,[275], Nelson and Shepherd[152,183], Goodgame et al,[197,380] and Walton[335]. However, Hare and Ballhausen have observed tetragonal splittings of the bands, and also the occurrence of a spin-forbidden transition (between 10.3 and 12.8kK) in the spectra of $NiCl_2(Th)_4$[463] and $Ni(NH_3)_4(NO_2)_2$[465,466]. The assignment of the weaker bands in the spectra has created some controversy. Goodgame, et al,[197,380] have assigned the 6kK band, the 12kK shoulder and shoulder near 23kK to components of the ν_1, ν_2 and ν_3 transition in tetragonal symmetry. Using weighted mean frequencies, ν_1 can then be predicted (see Chapter II) from ν_3 and ν_2 as 7.9kK for $NiCl_2py_2$ in reasonable agreement with the baricentre (7.5kK) of the two lowest bands. This assumes that the main peak is the doubly degenerate ^3E_g component of the $^3T_{1g}$ and $^3T_{2g}$ states. However, the data cannot be fitted to Maki's diagram[113] for D_{4h} symmetry, since this shows that the best fit of bands is obtained with the 6kK band as the ^3E_g component of the $^3T_{2g}$ state. Further, Goodgame, et al, found[380] difficulty in obtaining the parameters D_s and D_t of the tetragonal field.

The work of Liehr and Ballhausen[118], Tanabe and Sugano[114], Jørgensen[121] and Hare and Ballhausen[463,465] reveals that the spectra of Nickel (II) complexes may exhibit a weak spin-forbidden band, due to the $^3A_{2g} \rightarrow {}^1E_g$ (D) transition, between 10kK and 13kK. A further band near 20kK may arise from the $^1T_{1g}$ (D) state. In agreement with this, the 12kK and 23kK shoulders in the spectrum of $NiCl_2py_2$ have been assigned to the ^1E_g(D) and $^1T_{1g}$(D) excited states by many workers[152,183,275,335]. The diagram[118] of Liehr and Ballhausen shows a spin forbidden transition at 12.2kK, in good agreement with the observed 11.9kK shoulder, at the position of best fit (Dq=0.82kK) for the spin-allowed bands. Such a reasonable agreement would be expected because the diagram was calculated for a B' value (0.81kK) close to those observed in these complexes (see table 6.2).

Using this assignment of ν_3 and ν_2 to the main peaks, with any tetragonal splitting unresolved, the parameters of table 6.2 were calculated (see Chapter II). The predicted values of ν_1 in all cases are in good agreement with the position of the 8kK band, but not with the baricentre of the two lowest bands. The agreement with both possible ν_1 values was worse if the 20kK shoulder was included as a component of ν_3. Some improvement of agreement with the baricentre resulted (ν_1 was predicted at 8.0kK) if both ν_1 and ν_2 were corrected (see Appendix A4) for the interaction[121] of the ^1E_g(D) state with the

Table 6.2

Calculated ligand field parameters (kK) for octahedral nickel(II) complexes with halopyridines.

Complex	Observed Frequencies			Calculated parameters		
	ν_1	ν_2	ν_3	D_q	B'	λ'
$NiCl_2(3Brpy)_2$	8.5	14.1	24.1	.86	.83	-.24
$NiBr_2(3Brpy)_2$	8.0	13.3	23.0	.81	.80	-.20
$NiCl_2(4Clpy)_2$	8.5	14.1	24.1	.86	.83	-.33
$NiBr_2(4Clpy)_2$	8.2	13.7	23.8	.83	.84	-.21
$NiCl_2py_2$	8.2	13.8	24.2	.83	.87	-.33
$NiBr_2py_2$	8.0	13.7	23.4	.83	.81	-.26
$NiBr_2py_4$	9.8	15.5	25.2	.97	.77	-.32

$^3T_{2g}$ and $^3T_{1g}(F)$ states, via spin-orbit coupling. The origin of the 6kK band is unclear. It could be a spin-forbidden transition, such as Maki's diagrams[113] show at some values of her parameters ($\mathcal{N}$, p, Z and R), though the Liehr-Ballhausen[118] diagram does not support this. Alternatively, it could be a component of ν_1, in which case the parameters given in table 6.2 are suspect, due to the inaccuracies introduced into the calculation by tetragonal splitting[380].

The assignment of the spectrum of $NiBr_2py_4$ is more straightforward. The 20.4kK and 13.3kK shoulders are again taken as spin-forbidden bands, and the main bands at 25.2kK and 15.5kK as ν_3 and ν_2. ν_1 is then predicted at 9.7kK, in good agreement with the baricentre of the two lowest bands (9.8kK). This follows from the assignment of Hare and Balhausen[463] for the spectrum of $NiCl_2(Th)_4$, in which the ν_1 band is also split, far more than ν_2 or ν_3, by the tetragonal perturbation. Rowley and Drago have[387] resolved a shoulder on ν_2 at low temperature.

In spite of the uncertainties in the assignment of the spectra of the halopyridine complexes of Nickel (II), tables 6.2 and 5.2 reveal good agreement between the Dq and B' values of analogous Nickel (II) and Cobalt (II) complexes. This is expected from the proximity of the two metal ions in the spectrochemical and nephelauxetic series (see Chapter II). Further, for the same organic ligand, the anions

follow the spectrochemical series,

Magnetic Susceptibilities

The room temperature magnetic moments of the complexes, listed in table 6.1, are all close to 3.3 B.M. Such moments are typical of high-spin nickel (II) complexes. Moments greater than 3.3B.M. have often been attributed to tetrahedral Nickel (II) species. However, Lever has pointed out that many tetragonally distorted octahedral nickel (II) complexes have moments as high as 3.5 B.M., and this certainly includes all the halopyridine complexes. Further, the moments will be lower by about 0.09 B.M. after a correction has been applied for the temperature-independent-term . All the moments are, therefore, consistent with the octahedral structures, suggested for these complexes on the basis of their electronic spectra . The moments are given by equation 1.14 for a $^3A_{2g}$ ground-state.

Infrared Spectra

The frequencies of the complexes in the infrared region have again been assigned by comparison with the work of Green, et al, and are listed in table 6.3. No splitting of the bands is observed, in agreement with the proposed octahedral structures (see Chapter V).

The average magnitudes of the frequency shifts due to co-ordination

Table 6.3

Infrared spectra (375 - 1700 cm^{-1}) for the halopyridine complexes of Nickel (II)

Vib$^{n.}$ No.	3Brpy	$NiCl_2(3Brpy)_2$	$NiBr_2(3Brpy)_2$
16a	410ms	415m	408mw
11	430ms		
2 x 15	499s		516mw
6b	591ms	638ms	637m
12	690s	676s	682m
4		713m,b	732ms
			762m
10b	787ms	784s	787m
10a		900mw	891mw
5	946mw		938sh
17a		975w	970m
1	1005s	1028ms	1031m
18a	1022m	1044sh	
13	1083 ms	1090sh	1087 mw
18b	1093 ms	1100ms	1100 mw
10b+6a	1117m	1122mw	1154 m
9a	1189mw	1194mw	1169 m
14	1320m	1322mw	1307sh
	1388mw	1380mw	
19b	1411s	1422ms	1418ms
19a	1452s	1471ms,b	1456mw
8b	1558m	1560mw	1559m
8a	1564ms	1591m	1592m

Table 6.3 cont....

Vib^{n}.No.	4Clpy	$NiCl_2(4Clpy)_2$	$NiBr_2(4Clpy)_2$
11	492m	494vs,b	↑ Not recorded ↓
6b		659mw	660m
12	708ms	710sh	716sh
4		727s,b	724vs
10b	807ms	802s	804vs
		826mw	828mw
	984w	1002w	1000mw
1	999w	1021m	1018m
18a	1060mw	1058m	1053ms-
18b		1091sh	1090sh
13	1102m	1110ms,b	1103s
12 + 16a	1130w	1159mw,b	1158m,b
4 + 11	1213 } mw	1208m,b	1202ms
9a	1220 }	1229mw	
3	1318w	1312mw,b	1312mw
19b	1407ms	1412ms	1410vs
19a	1482ms	1483ms	1485s
8b		1562m	1560mw
8a	1573ms,b	1594ms,b	1586vs
5 + 10b	1642m,vb	1654w,b	1638m,b

were calculated for the complexes of Cu(II), Co(II) and Ni(II). It was found that for analogous complexes they followed the Irving-Williams[86] order, Cu > Ni > Co; in agreement with the work of El-Sayed and Sheline[432] on the cyanide ligand. They found that as the electronegativity of the metal ion decreased (Cu(II)> Ni(II) > Co(II) as given by second ionisation potentials[86], which are 12.55ev, 10.59ev and 9.47 ev respectively[467]) the metal-ligand σ-bond strength decreased (as measured by stability constant data, thermal stability[80], or far-infrared frequencies[270]), but metal-ligand π-bonding increased. Both the decrease of σ-bond strength and the increase of metal-ligand π-bonding (which results in more occupancy of the ligand π^*orbitals) will lower the ligand vibration frequencies. A correlation between ligand ring vibrations and the Irving-Williams order has also been observed by other workers[213,90,59,272].

Without structural data it is not possible to interpret the lower ligand frequencies in the bromide complexes, relative to the chlorides.

Discussion

On the basis of their reflectance spectra, an octahedral stereochemistry has been proposed for the complexes. This is in agreement with the infrared and magnetic data. The stoicheiometry of

the complexes requires that they are polymeric, and the low electronic intensities, and lack of infrared band splittings, suggest a trans-configuration like that of $NiCl_2py_2$.

These structures are similar to those very recently suggested[335] by Walton for the bis-complexes of Nickel (II) with the weak bases 3CNpy and 4CNpy. It appears (as proposed in Chapter V) that if steric effects are absent then octahedral structures predominate, unless very basic ligands or very polarisable anions are co-ordinated.

Table 3.1 compares the bond lengths in the known Cobalt (II) and Nickel (II) complexes of this type. Such a comparison is valid, since neither ion exhibits a large Jahn-Teller distortion, and indicates that the bond lengths in $NiCl_2py_2$ may be nearly the same as those[186] in α-$CoCl_2py_2$. Steric hindrance may, therefore, be expected to be important for the nickel (II) complexes, and this is confirmed by the absence of octahedral complexes of the 2-halopyridines. The non-existence of octahedral polymeric, bis-complexes of nickel halides with 2CNpy[335] and all the sterically hindered ligands (with the exception of Quin[79,192] - see table 3.5) offers more extensive confirmation of this principle.

The absence of four-co-ordinate complexes of the 2-halopyridines may be due to the inability of these weak bases to form sufficiently strong bonds to overcome the unfavourable tetrahedral C.F.S.E. or square-

planar spin pairing energy (see Chapter 1).

The high octahedral C.F.S.E. for Nickel (II) might be expected to yield more stable NiX_2L_4 complexes than their cobalt (II) analogues. Studies of equilibria in solution have confirmed[370,334] this. It is not, therefore, surprising that weak bases form tetrakis-complexes with Nickel(II) but not with Cobalt (II). Under forcing conditions $Ni(ClO_4)_2(3Brpy)_4$[176] and NiX_2L_4 ($X^-=Br^-,I^-$; L=3CNpy,4CNpy)[335] have been prepared.

Experimental

Nickel was determined gravimetrically as the dimethylglyoxime[444] complex. Other details have been described in Chapter 4.

Dichloro bis (3-bromopyridine) Nickel(II)

3-bromopyridine (1.3g. 2 mols) was added to a stirred solution of Nickel (II) chloride hexahydrate (1g. 1 mol) in ethanol (10 ml). The product (1.7g.91%) formed as a yellow-green precipitate and was filtered off and washed with ethanol and ether. (Found: Ni, 13.1; Cl,15.9. $C_{10}H_8Br_2Cl_2NiN_2$ requires Ni,13.2; Cl,15.9%).

Dibromo bis (3-bromopyridine) Nickel (II) was similarly prepared as a yellow precipitate on allowing the solution to stand. (Found: Ni,10.6; Br', 28.6. $C_{10}H_8Br_2Br_2'NiN_2$ requires Ni,10.6; Br'28.8%); as was Dichlorobis (4-chloropyridine) Nickel (II), as a yellow precipitate.

(Found: C,33.7; H,2.4; Ni,16.2; Cl'_2,19.7. $C_{10}H_8Cl'_2NiN_2$ requires C,33.7; H,2.3; Ni,16.5; Cl'_2,19.9%); and crude (12.4%Ni) yellow-green Dibromobis (4-chloropyridine) Nickel (II) which, on heating at 70°C overnight, gave the pure yellow product. (Found: Br,36.6; Ni,13.1. $C_{10}H_8Cl_2Br_2NiN_2$ requires Br,35.9; Ni,13.2%).